CRYOGENICS

An International Journal of Low Temperature Engineering and Research

VOL. 2 NO. 1 SEPTEMBER 1961

Superconducting Magnets

R. H. Kropschot and V. Arp *National Bureau of Standards, Boulder, Colorado*

Received 13 June 1961

THE abrupt and total disappearance of electrical resistivity of certain metals at low temperatures was discovered by H. Kamerlingh Onnes in 1911[1] not long after he first succeeded in liquefying helium. This phenomenon very quickly became known as superconductivity. Since then a great number of experiments have elucidated the basic properties of superconductors, and fairly satisfactory theoretical explanations have been given. Up to the last several years, however, superconductivity has remained a laboratory phenomenon with essentially no practical application having been made. The comparatively recent expansion of cryogenics as an engineering science has resulted in a number of suggestions for the engineering use of this unique phenomenon.[2]

The first suggestion to use superconductors for electromagnet windings was made by Onnes in 1913.[3] Soon afterwards it was found that applied magnetic fields greater than a certain rather low critical value restore the electrical resistance characteristic of a normal metal.[4] In 1931 de Haas and Voogd[5] found a lead–bismuth alloy with a critical field of about 15 kgauss. Attempts to use this alloy for superconducting magnets[6,7] did not succeed, for reasons which were never clearly stated. The subject then rested until 1960 when Autler[8] reported a 4·3 kgauss superconducting air core solenoid, using niobium wire. Since then Autler and others, in unpublished work, have reached 10 kgauss in niobium solenoids, and Kunzler et al. have reported a 15 kgauss superconducting alloy solenoid.[9] Very recently (February, 1961) a superconducting alloy wire of niobium stannide has been produced which remains superconducting in a field of 88 kgauss.[10] The use of this wire to construct a magnet seems certain. It is not too optimistic to expect that it will be used to wind solenoids which will produce fields in excess of 100 kgauss.

The advantages of a superconducting magnet over a normal magnet derive from the zero power dissipation in the former compared with the totally wasted Joule heating in the latter. For relatively small low field laboratory installations this is an unimportant economic consideration, but in some instances it permits smaller and more convenient experimental arrangements. For large magnets, in terms of either large volume of field or very high fields or both, the economic advantage of superconducting magnets is an important consideration.

The problems of building superconducting magnets are centred around the quenching of superconductivity of the magnet windings by the field of the magnet. There are three avenues of approach toward increasing the maximum field obtainable. The first involves a selection and fabrication of superconducting alloys with very high critical fields. The second involves the possible use of the enhanced critical fields of thin superconducting films. The third involves enhancement by means of ferromagnetic cores.

In this paper, the authors hope to give a coherent treatment of the problem of attaining high fields with superconducting magnets, and to illustrate some of their advantages and possible uses.

Fundamentals of superconductivity

The electrical resistivity of a superconducting sample carrying a direct current has been experimentally determined to be less than 8×10^{-23} Ω cm,[11] and a detailed quantum-mechanical theory[12,13] predicts that it is identically zero. It is also found that the superconducting state is perfectly diamagnetic ($\chi = -1/4\pi$ in Gaussian units) or, in other terms, that magnetic fields not not penetrate into a superconducting volume. This is known as the Meissner effect and is distinct from zero resistivity in that neither effect can be derived from the other by classical electromagnetic theory. The magnetic field which represses or quenches superconductivity is known as the critical field H_c.

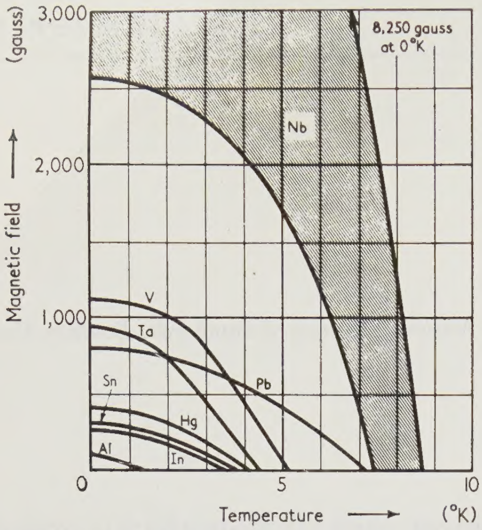

Figure 1. The critical field as a function of temperature for some selected elemental superconductors. The shaded area shown for niobium illustrates the variation in reported values

Figure 1 is the phase diagram for some elemental superconductors in the H–T plane. The transition temperature in zero field is denoted T_c and the critical field at $T = 0$ is denoted H_0. As a general rule, a high critical field accompanies a high critical temperature. An approximate empirical relation for $H_c(T)$ is

$$H_c(T) = H_0\left(1 - \frac{T^2}{T_c^2}\right)^{1/2} \qquad \ldots (1)$$

It is usually found that in pure and unstrained samples the transition between superconducting and normal states is very sharp, as illustrated in Figure 2; this does assume, however, that in the case of magnetic field induced transitions the sample geometry is so arranged that all the surface of the sample experiences the same field. Magnetic field induced transitions can be observed in a sample in three ways: (1) the self-generated field of a large measuring current may be used to induce resistive transitions; (2) the magnetic susceptibility can be measured as a function of applied field; and (3) a very small measuring current can be used to detect electrical resistance in the presence of an applied field. In ideal superconductors, all three methods give the same critical field, and the equality of critical fields determined by methods (1) and (3) is, in fact, known as Silsbee's rule.

Very broad and smeared-out transitions between superconducting and normal states are found in some samples, usually as a result of strains, impurities, or inhomogeneities in the sample. This transition region is commonly called the intermediate state, and is qualitatively described in terms of coexisting regions or domains of superconductor and non-superconductor.[14–17] Most theoretical treatments of this state are no more than semi-quantitative. Abrikosov[18] has developed a complicated quantitative theory which seems to account for some, but not all, of the observed effects. Magnetic field induced transitions usually exhibit considerable hysteresis, both in resistivity and susceptibility, and upon reducing the applied field to zero, a residual 'frozen in' magnetic moment is often found. The critical magnetic fields found by the three methods are far from equal. In the absence of hysteresis, the area under the magnetization curve (M vs H) is $H_c^2/8\pi$. When hystersis is present, this determination of H_c, i.e. method 2, is somewhat ambiguous.

An important contribution to the understanding of superconductivity was given by F. and H. London in 1935.[19] They added two terms to Maxwell's equations to account for the observed electrodynamics of superconductors, and in doing so predicted the existence of a fundamental parameter, now known as the penetration depth λ, which was later measured in thin film experiments. Though essentially a phenomenological theory, it formed the basis for all further studies of superconductivity until fairly recently when detailed quantum-mechanical theories were developed.

The first satisfactory theoretical derivation of the existence of the superconducting state was given by Bardeen, Cooper, and Schrieffer[12] (BCS) in 1957. A short while later Bogoliubov[13] presented an alternative treatment which bypassed some of BCS's mathematical difficulties and explicitly included the current-carrying superconducting state. Hardly a single paper on superconductivity has been written since that time without giving reference to one or the other of these works. At the heart of the theories is a temperature dependent gap in the spectrum of allowed energies between the superconducting ground state and all excited states. In the ground state, pairs of electrons of equal but opposite momentum remain correlated even at large spatial separations by means of an electron-virtual phonon–electron interaction. The single particle excited

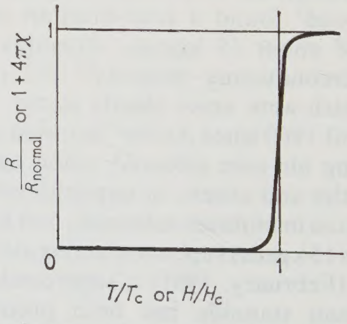

Figure 2. The qualitative variation of resistance and magnetic susceptibility with either temperature or magnetic field observed in superconductors. The sharp transitions in an applied field are observed only when all the surface of the sample experiences the same field

states are similar to those normally considered in the theory of metals. With a single modification (that of requiring a non-local rather than local relation between the superconducting current density J and vector potential A), the London equations are found valid. A wealth of experiments has demonstrated that the theory is essentially correct.

It is the common practice in books and papers on superconductivity to denote magnetic fields as H and give their magnitudes in gauss. We shall use this convention, and unless otherwise stated, units of amperes, centimetres, and gauss (1 gauss = 1 oersted) shall be used.

Basic types of superconducting magnets

Air core solenoids

The maximum magnetic field obtainable in an air core superconducting solenoid is equal to the externally applied critical magnetic field of the superconducting windings. Actually, this limit is never quite reached, because of the decrease in critical field when the superconductor is carrying a non-negligible current. Figure 3 shows a hypothetical curve which can be used to illustrate this fact. H and I are, respectively, the externally applied field and the current through a given sample or wire. If the maximum field of a solenoid wound from this wire is to be H_m, the maximum current is then I_m. For a long solenoid of length l, the required number of turns n, and hence the radial thickness of the magnet windings is determined by the familiar relation

$$\frac{n}{l} = \frac{H_m}{0{\cdot}4\pi I_m} \qquad \ldots (2)$$

As H_m approaches H_c, I_m approaches zero and the magnet size becomes very large. An obvious means of reducing the required magnet size is to use more than one set of concentric windings, running a large current through the outer windings which are subject to a lower applied field. If a large number of such sets of windings is used, the radial thickness is determined from

$$\frac{n}{l} \simeq \int_0^{H_m} \frac{\mathrm{d}H}{0{\cdot}4\pi I(H)} \qquad \ldots (3)$$

As an example, if $H_m/H_c = 0{\cdot}95$ and $I(H)$ (Figure 3) is linear with H, the radial thickness of the magnet is reduced from that of a single coil magnet by a factor of about six. This may be an important consideration when wires of small critical current are used.

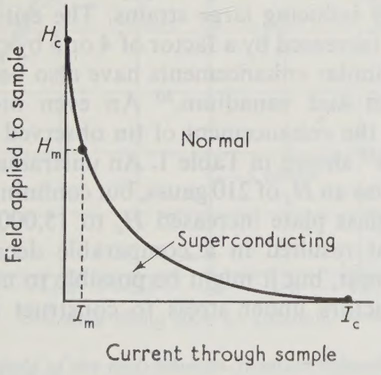

Figure 3. An arbitrary curve showing the dependence of the critical field upon the measuring current. H_m and I_m are, respectively, the field of and the current through the superconducting magnet wound with this wire

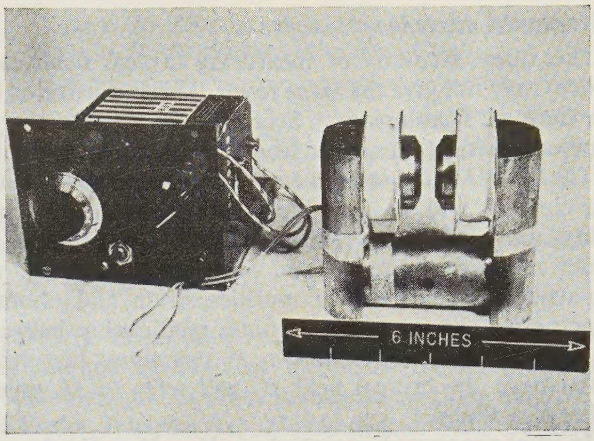

By courtesy S. H. Autler, Lincoln Laboratory

Figure 4. An iron core magnet with superconducting windings

Ferromagnetic cores

Ferromagnetic cores can be designed to yield very homogeneous fields and they require fewer ampere turns to produce a given field up to the saturation magnetization of the metal. The critical field of the superconducting windings can be much less than the saturation magnetization of the metal. Figure 4 shows an iron core magnet reported by Autler[8] which will produce 14 kgauss. In a subsequent design he has obtained 25 kgauss, using niobium windings which have a critical field of about 9 kgauss.[20] A variation of ferromagnetic enhancement which maintains air core solenoid geometry while attaining fields near the saturation of iron has been given by Mills.[21]

When the core is cooled to the temperature of the superconducting windings, room temperature ferromagnetism is no longer a requirement. For example, dysprosium[22, 23] and holmium[24] are ferromagnetic below about 85 and 20° K, respectively, and both have magnetic moments of about 10·6 Bohr magnetons per atom, corresponding to saturation magnetizations of about 39 kgauss. This is almost double that of iron. However, these elements are magnetically very hard, and their full saturation magnetization may not be attainable. Other elements, or alloys, may be equally or more desirable. Throughout the remainder of this paper, only air-core solenoids are considered.

Wire-wound solenoids

The three methods of measuring critical fields (see above) may not give the same result. This is illustrated by the data of Rjabinin and Schubnikow[7] for the 'hard' superconducting compound lead thallide shown in Figure 5. The fields H_1 (the self-generated field of a large measuring current) and H_2 (determined by magnetic susceptibility) are usually less than the field H_3 (determined by small measuring current and large external field). H_3 is particularly sensitive to impurities, strain, and inhomogeneities in the sample. A definite relationship between H_1, H_2, and H_3 is not known at this time. In further discussion, the critical field H_c will refer to H_3 unless otherwise stated.

In ideal superconductors (where $H_1 = H_2 = H_3$) the current flows only within a very small distance of the surface of the wire and, therefore, the critical current is proportional to the wire circumference. In hard superconductors the current is usually assumed to flow along connected superconducting filaments throughout the wire volume, since the critical currents are found to be approximately proportional to the cross-sectional area of the wire. Behaviour intermediate between these two examples can also occur so that, in general, it is necessary to specify both critical current and wire diameter, rather than just a critical current density.

Elemental superconductors

Figure 1 shows the H_c–T curves for some of the 'elemental' superconductors. Of these, niobium appears to be one of the best materials for the construction of an electromagnet. With the exception of technetium, it has the highest critical field (H_c), highest critical temperature (T_c), and it has good mechanical properties and is commercially available in wire or sheet. In addition, the critical field is enhanced appreciably with cold working.[25, 26] Autler,[8] LeBlanc and Little,[27] and others[28] have constructed niobium solenoids which will produce 4 to 10 kgauss, depending upon the amount of cold work of the wire used in the windings. Figure 6 shows Autler's[29] data of the quenching field as a function of current for a sample of niobium wire oriented transverse to the magnetic field. The data of LeBlanc and Little[27] are less regular. Adequate leads can be made from niobium to copper by heliarc welding, spot welding, copper plating, or ultrasonic soldering.

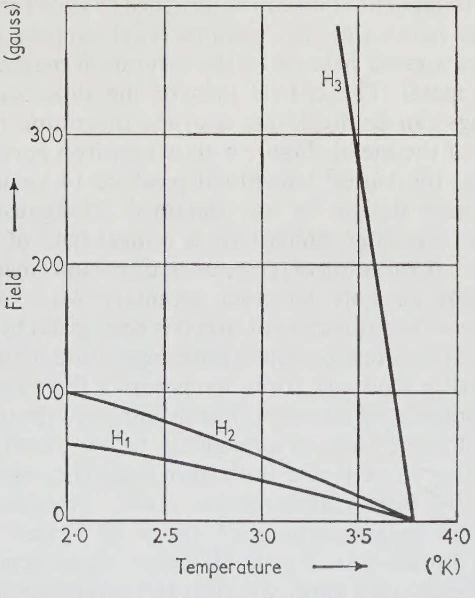

Figure 5. The three critical fields of the alloy lead thallide, as reported by Rjabinin and Schubnikow.[7] H_1 is determined from resistance measurements using a large current and zero external field. H_2 is determined by susceptibility measurements in an applied field. H_3 is determined from resistance measurements using a small current and large external field

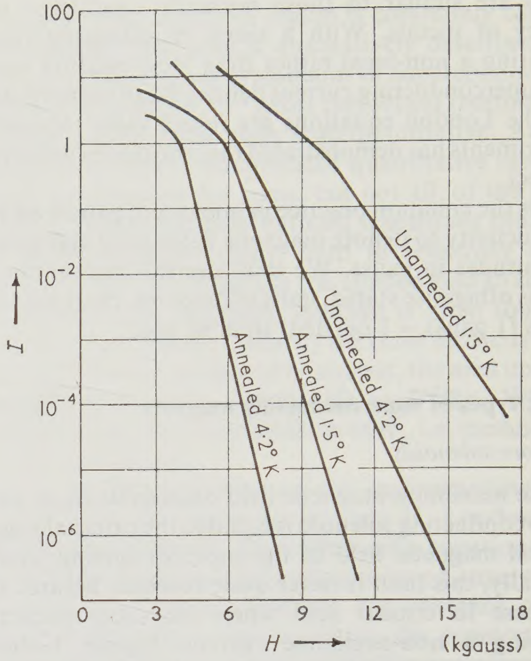

Figure 6. The critical field of 0·004 in. niobium wire as a function of measuring current. From unpublished data

It may be possible to greatly enhance H_c of selected elements by inducing large strains. The critical field for niobium is increased by a factor of 4 or 5 by cold drawing the wire. Similar enhancements have also been observed in tantalum and vanadium.[30] An even more striking example is the enhancement of tin observed by Lasarew and Galkin[31] shown in Table 1. An unstrained sample of tin at 2° K has an H_c of 210 gauss, but confining the sample against a glass plate increased H_c to 15,000 gauss. The confinement resulted in a comparable decrease in the critical current, but it might be possible to use elemental superconductors under stress to construct a high field magnet.

Alloy superconductors

The superconducting properties of a metal can be changed radically by the addition (metallurgically) of another metal or metals. Significant for our application are

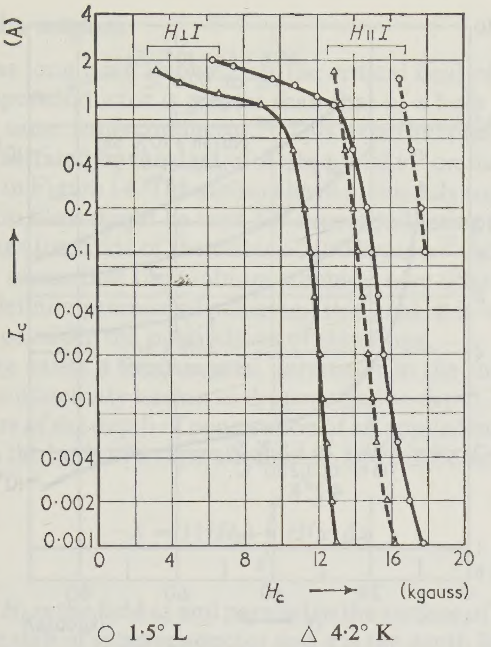

Figure 7. The critical current of 0·007 cm molybdenum–rhenium wire as a function of applied field. From Kunzler, Buehler, Hsu, Matthias, and Wahl[9]

the large increases in H_c and T_c of certain alloys and intermetallic compounds. In 1931 de Haas and Voogd[5] reported that a lead–bismuth alloy exhibited zero resistance in a field of 15 kgauss. The current–field characteristics were then measured by Keesom[6] in 1935, who found that Silsbee's rule was not obeyed, and that an appreciable current reduced the value of H_c to approximately that of lead. His project of building a lead–bismuth magnet was apparently abandoned without further investigation. Rjabinin and Schubnikow[7] also measured the properties of lead–bismuth but never reported a working magnet.

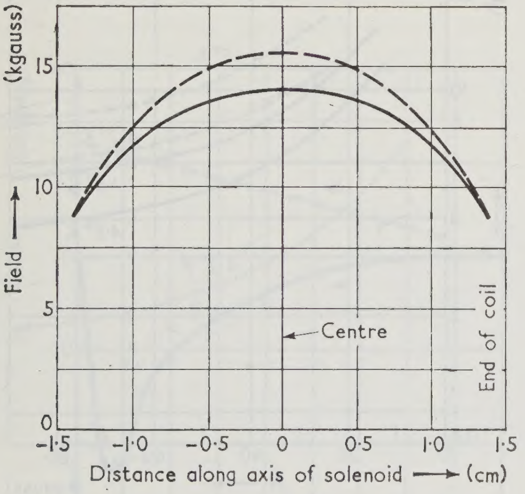

Figure 8. The field of the molybdenum–rhenium solenoid reported by Kunzler, Buehler, Hsu, Matthias, and Wahl.[9] *The solid curve was obtained with two sets of windings in series, resulting in a uniform current density. The dashed curve was obtained with the two sets of windings in parallel, resulting in a lower current density in the inner coil and a higher current density in the outer coil*

Table 1. The Effect of Inhomogeneous Strain on the Superconducting Properties of Tin

Specimen	$R_{4 \cdot 2}/R_{room}$	T_c(°*K*)	H_c *at* 2° *K*	dH_c/dT *at* 2° *K*	I_c *at* 2° *K* (*A*)
Unstrained	$1 \cdot 5 \times 10^{-3}$	3·72	210	100	3
Strained	0·1	~9	15,000	1,750	0·067

Kunzler, Buehler, Hsu, Matthias, and Wahl[9] have used a molybdenum–rhenium alloy and attained 15·5 kgauss inside a solenoid at 1·5° K. Figure 7 shows their results of the current–field characteristics of this alloy. Figure 8 shows a field plot of their solenoid. Note that the maximum field is obtained by using parallel windings with a lower current density in the inner coil. The molybdenum–rhenium alloy is the first material having a critical field higher than niobium which has been produced in sufficient quantities to construct a magnet. In this alloy (as well as most other superconductors) the metallurgical condition greatly determines the maximum critical field.

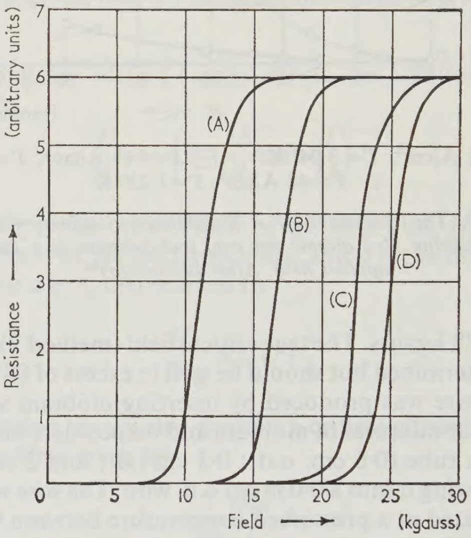

A. $J = 4 \cdot 4$ A/cm², $T = 1 \cdot 519$° K B. $J = 4 \cdot 4$ A/cm², $T = 1 \cdot 367$° K
C. $J = 21 \cdot 9$ A/cm², $T = 1 \cdot 144$° K D. $J = 4 \cdot 4$ A/cm², $T = 1 \cdot 144$° K

Figure 9. The resistance of a gamma phase uranium–molybdenum alloy containing 11·6 atomic per cent molybdenum as a function of field, applied perpendicular to the current. After Berlincourt[32]

Berlincourt has investigated the current quenching characteristics of uranium–molybdenum[32] and titanium–molybdenum[33] alloys. These results are shown in Figures 9 and 10. One sample (18·3 atomic per cent molybdenum in titanium) exhibited zero resistance at 1·2° K in a magnetic field of 30 kgauss for a measuring current density of

34 A/cm². The critical temperature T_c of titanium–molybdenum alloys increases with increase in molybdenum content. A corresponding increase in H_c should be associated with this increase in T_c.

The recent successes by Kunzler, Buehler, Hsu, and Wernick[10] of producing niobium clad niobium stannide wire having a critical field in excess of 88 kgauss has tremendous practical importance. Figure 11 shows the current–field characteristics of this material. One specimen 0·038 cm o.d. shows the amazing property of sustaining a super current of greater than 10^5 A/cm² in an external field of 88 kgauss. The true critical field (method 3) has yet to be determined but should be well in excess of 88 kgauss.

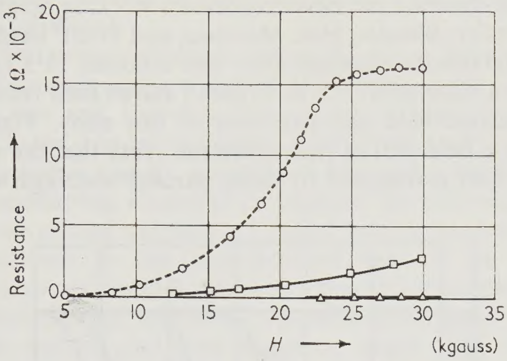

○ $J = 48$ A/cm², $T = 3·04°$ K ☐ $J = 144$ A/cm², $T = 1·23°$ K
△ $J = 48$ A/cm², $T = 1·23°$ K

Figure 10. The resistance of a β-stabilized titanium–molybdenum alloy containing 16·3 atomic per cent molybdenum as a function of applied field. After Berlincourt[33]

The wire was produced by inserting niobium stannide powder or mixtures of niobium and tin powders inside of a niobium tube (0·6 cm. o.d.; 0·3 cm i.d.; and 2 cm long) and drawing it into a 0·038 cm o.d. wire. The wire was then heat treated at a prescribed temperature between 970 and 1,400° C for a predetermined time to sinter the niobium stannide core.

In a given field, the clad niobium stannide has a much higher critical current density than the unclad material. The current–field characteristics of several samples of unclad material are shown in Figure 12.[10] However, all of the samples are superconducting in a field of 88 kgauss whereas the data of Bozorth[34] shown in Figure 13 indicate a final transition field of 70 kgauss (method 2).

The current density of the clad niobium stannide does not scale with the perimeter as expected for 'soft' superconductors nor with cross-sectional area as observed for some 'hard' superconductors. In addition, the critical field–temperature relation (equation (1)) is not valid for this material. The critical temperature is approximately 18° K and the critical current increases over 50 per cent when the temperature is decreased from 4·2 to 1·5° K.

If the niobium clad niobium stannide wire can be produced in sufficient quantities, superconducting solenoids can be built to produce fields in excess of 88 kgauss. With the expected current densities possible with this material, a winding thickness of 5 to 10 cm will be sufficient.

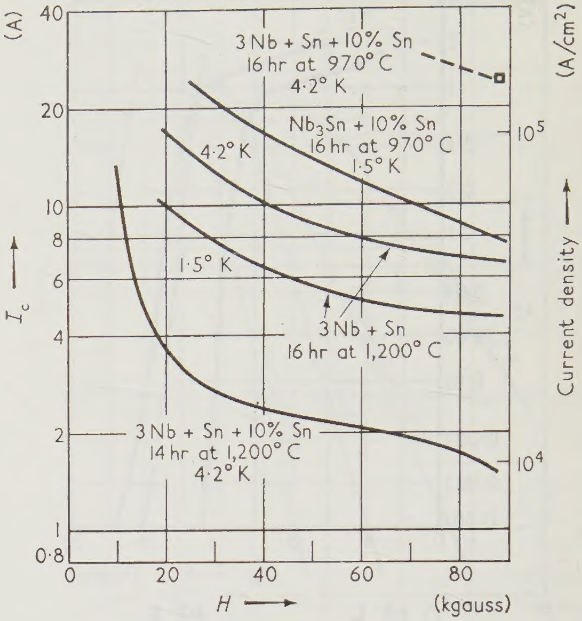

Figure 11. Critical currents of several niobium clad niobium stannide wires as a function of field applied perpendicular to the current. After Kunzler, Buehler, Hsu, and Wernick[10]

There is a distinct possibility that other alloys or intermetallic compounds, yet to be determined, can also be used to wind high field magnets. At the present time the most promising materials appear to be systems which include one of the refractory metals.

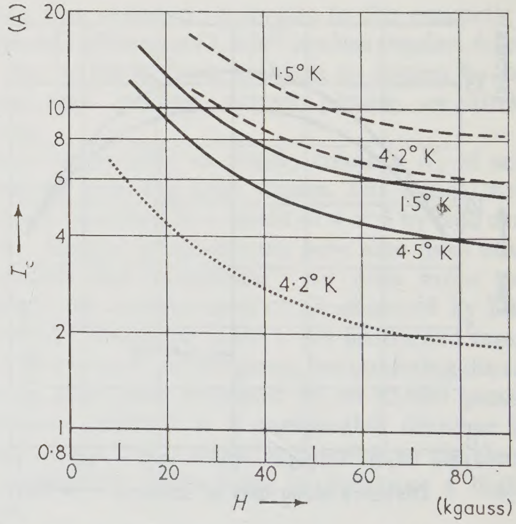

——— 0·030 cm × 0·053 cm – – – – 0·050 cm × 0·063 cm
. . . . 0·025 cm × 0·025 cm

Figure 12. Critical currents of several niobium stannide samples as a function of field, applied perpendicular to the current. After Kunzler, Buehler, Hsu, and Wernick[10]

Thin film magnets

It has long been known that the critical field of a thin film superconductor is greater than that of a bulk sample of the same superconductor.[35] This experimental fact is well illustrated by the data of Alekseyevsky[36] on thin films shown in Figure 14. The authors have previously suggested that thin films might be used for superconducting magnet windings for fields of the order of 100 kgauss.[37] Although it now seems that the niobium stannide wire offers much more definite promise of achieving this goal, it is interesting to consider the possibilities of thin films.

There exists a fundamental parameter in the theory of superconductivity known as the penetration depth λ. It is a measure of the depth of penetration of an applied magnetic field in the body of a superconductor, and can be defined as

$$\lambda = (1/H_0) \int_0^\infty H(x)\,\mathrm{d}x \qquad \ldots (4)$$

where H_0 is the field at and parallel to the surface of a semi-infinite slab of superconductor and x is the depth from the surface. This parameter was first introduced by F. and H. London in their modification of Maxwell's equations to account for the observed electrodynamics of superconductors.[38] It is typically of the order of 500 Å at $T = 0$; its approximate temperature dependence is given by

$$\lambda = \lambda_0 \left[1 - \left(\frac{T}{T_c}\right)^4\right]^{-1/2} \qquad \ldots (5)$$

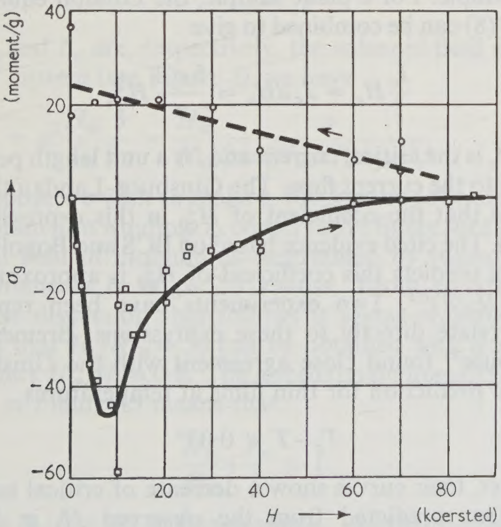

Figure 13. The magnetization of niobium stannide. After Bozorth, Williams, and Davis[34]

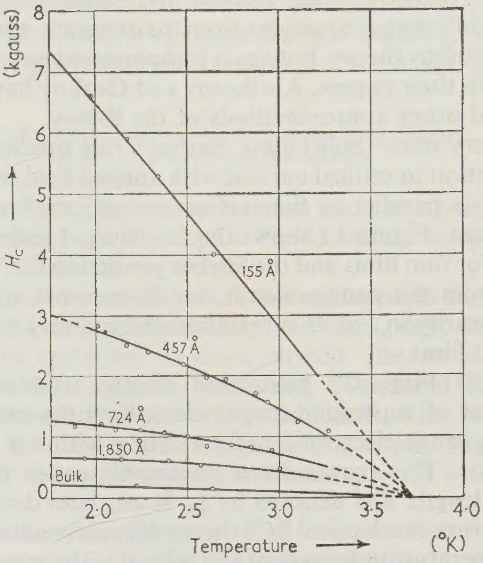

Figure 14. The critical fields of thin tin films. Thicknesses in Angström units are indicated. After Alekseyevsky[36]

It is observed that critical temperatures of carefully prepared and annealed thin films differ negligibly from those of the corresponding bulk superconductors. This implies that in zero field the (Helmholtz) free energy is independent of film thickness. Using this assumption, and neglecting any surface energy effects, the London theory predicts

$$\frac{H_c}{H_{cB}} = \left(1 - \frac{2\lambda}{d}\tanh\frac{d}{2\lambda}\right)^{-1/2} \qquad \ldots (6)$$

where H_c is the critical field of the thin film, H_{cB} is the critical field of the bulk specimen, and d is the film thickness. For $d \ll \lambda$, this reduces to

$$\frac{H_c}{H_{cB}} \simeq 2\sqrt{3}\frac{\lambda}{d} \qquad \ldots (7)$$

The London theory also predicts a critical current density for thin films given by

$$J_c = \frac{5}{2\pi}\frac{H_{cB}}{\lambda}\ \mathrm{A/cm^2} \qquad \ldots (8)$$

or about 10^7 A/cm². Shoenberg[35] gives a qualitative thermodynamic argument that this critical current density may in fact increase for very thin films.

Ginsburg and Landau[39] have modified the London equations to account for the positive surface energies of superconductors required by the existence of the Meissner effect. For very thin films their theory agrees with the London equations (7) and (8), except that the coefficients $2\sqrt{3}$ and $5/(2\pi)$ become $2\sqrt{6}$ and $10/(3\pi\sqrt{6})$, respectively. Their theory also gives the variation in critical current with applied magnetic field (Figure 15) as

$$\frac{J}{J_c} = \left(1 - \frac{H^2}{H_c^2}\right)^{3/2} \qquad \ldots (9)$$

The original derivation involves an approximation valid for $T \simeq T_c$, but later work of Abrikosov[40] and of Ginsburg[41] indicates that the conclusions should be valid for all T.

Recently Gorkov[42] has derived the basic Ginsburg–Landau differential equations from the quantum-mechanical Bogoliubov theory, but again in the approximation that $T \simeq T_c$. In their papers, Abrikosov and Gorkov have also discussed other approximations of the theory.

For very thick (bulk) films, Silsbee's rule predicts that the variation in critical current with applied field is linear when H is parallel to the surface and perpendicular to the current. Figure 15 shows the Ginsburg–Landau prediction for thin films and the Silsbee prediction for 'thick' films. From this comparison it can be seen that approximate linearity in I vs H is maintained from very thick to very thin films.

In 1953 Pippard[43] postulated another fundamental parameter of superconductivity describing the extent of the long range electronic order existing within a superconductor. This parameter is commonly called the coherence length, and denoted by ξ_0. It was later derived in the quantum-mechanical BCS theory of superconductivity. It is temperature independent and related to the speed of an electron at the Fermi surface v_F and the critical temperature by the equation

$$\xi_0 = 0{\cdot}18\frac{\hbar v_F}{kT_c} \qquad \ldots(10)$$

where $\hbar$ and k are, respectively, Planck's constant divided by 2π and Boltzman's constant. It turns out that ξ_0 lies in the range 1,000 to 10,000 Å.

Ittner[44] has investigated the critical fields of thin film superconductors on the basis of BCS theory. He finds that the enhancement H_c/H_{cB} predicted by the London theory (equation (6)) is close to being correct provided an effective penetration depth λ_{eff} is used rather than the λ determined from experiments on bulk samples. From the work of Miller,[45] Ittner shows that when the electron mean free path or film thickness becomes less than ξ_0, λ_{eff} becomes greater than λ. The asymptotic expression for λ_{eff}/λ given by Miller for $d \ll \xi_0$ is

$$\frac{\lambda_{eff}}{\lambda} \simeq \left(\frac{\xi_0}{d}\right)^{1/2} \qquad \ldots(11)$$

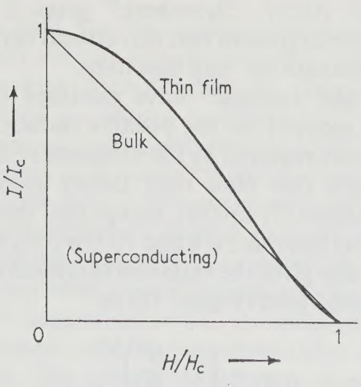

Figure 15. Theoretical variation of critical current with applied field for planar samples. The field is parallel to the surface and perpendicular to the current flow. The straight line (bulk) is the Silsbee prediction for thick samples. The thin film curve is the prediction of the Ginsburg–Landau theory

where we have made the assumption that the electron mean free path equals the film thickness d. This is the same result obtained earlier by Tinkham[46] from comparatively simple arguments.

Parmenter[47] has given some consideration to critical currents on the basis of BCS and Bogoliubov theories. His work is in reality concerned with the possible reappearance of superconductivity when the current density is increased to about 10^9 A/cm^2. It is suggested that this new superconducting state might even occur at room temperature, and in metals which are not 'ordinary' superconductors. This is a most intriguing possibility, but the experimental problems of ever reaching and utilizing this state, should it even exist, seem very difficult. He does give arguments, however, showing that the 'ordinary' thin film critical current density should be $\sqrt{(2/3)}$ times that given by the London theory (equation (8)).

Experimental evidence

Data from several experiments can be checked against these predictions. Alekseyevsky's data (Figure 14) show about $2\frac{1}{2}$ times greater enhancement, H_c/H_{cB}, for a given d than equation (7) predicts. Ginsburg and Shal'nikov[48] observe a greater enhancement than predicted by equation (7). Glover[49] has reported critical currents for plane indium and lead films estimated to be about 50 Å thick. The figures he gives correspond to critical current densities of the order of $0{\cdot}0025H_{cB}/\lambda$ A/cm^2. Crittenden et al.[50] have reported the critical currents of indium films to be proportional to the square root of the thickness in the range 400 to 5,000 Å. For their thinnest film the critical current density is about $0{\cdot}1\ H_{cB}/\lambda$.

The difficulty in comparing observed critical fields or critical currents with theoretical predictions lies in making accurate determinations of film thickness. A perhaps more direct verification of theory can be obtained by direct comparison of critical currents and critical fields in the same sample. For a plane sample, the London equations (7) and (8) can be combined to give

$$\frac{I_c}{l}H_c = J_c d H_c = \frac{5\sqrt{3}}{\pi}H_{cB}^2 \qquad \ldots(12)$$

where I_c is the critical current and l is a unit length perpendicular to the current flow. The Ginsburg–Landau theory predicts that the coefficient of H_{cB}^2 in this expression is $20/(3\pi)$. The cited evidence based on BCS and Bogoliubov theories predicts this coefficient of H_{cB}^2 is approximately $(5/\pi)\ (2\xi_0/d)^{1/2}$. Two experiments have been reported which relate directly to these expressions. Bremer and Newhouse[51] found close agreement with the Ginsburg–Landau prediction for thin films at temperatures

$$T_c - T < 0{\cdot}03°$$

However, their curves show a decrease of critical current from that predicted from the observed H_c at lower temperatures. Ginsburg and Shal'nikov[48] used thin cylindrical tin films in a transverse magnetic field; as explained in their paper, an extra factor of 2 appears in the predicted coefficient of H_{cB}^2 for this geometry. Their measured critical currents were about 0·22 times the value predicted by Ginsburg–Landau theory from the observed H_c.

It should be noted that for very thick (bulk) films there is negligible enhancement and $H_c \simeq H_{\mathrm{cB}}$. Assuming that such a film also obeys Silsbee's rule, the predicted coefficient of H_{cB}^2 (equation (12)) is just $5/\pi$. Comparing this with the above predictions for very thin films, it seems that the coefficient of H_{cB}^2 should be a very slowly varying function of thickness down to, perhaps, all but the very thinnest films. However, no experimental investigation has measured this coefficient over a wide range of film thicknesses. In addition no experimental investigation of thin film critical currents as a function of applied field has been made.

Thin film magnet size

The apparent feasibility of 100 kgauss superconducting solenoids follows from the above theories. Consider a 'wire' of a cylindrical thin film of thickness d deposited on a non-superconducting fibre of diameter a ($a \gg d$) which is then used to wind a solenoid. Though the first trace of resistance is restored in a bulk wire by a transverse field of 0·5 H_{cB}, it will not be restored in the thin film wire until the transverse field very nearly reaches the H_c of a plane film because of the very small thin film susceptibility. It is convenient to rewrite equation (12) in the form

$$\frac{\pi}{5} J_c d H_c = \frac{\pi}{5} \frac{I_c}{\pi a} H_c = \alpha H_{\mathrm{cB}}^2 \qquad \ldots (13)$$

where α is a dimensionless quantity to be determined by experiment. Neglecting insulation thickness and assuming a tight-packed winding, the radial winding thickness ΔR for a given number of turns per centimetre n/l is approximately

$$\Delta R = a^2 \frac{n}{l}$$

If H_m and I_m are, respectively, the solenoid field and the 'wire' current (see Figure 3), we have

$$\Delta R = a^2 \frac{H_m}{I_m} \frac{5}{2\pi} = \frac{H_m^2}{H_{\mathrm{cB}}} \frac{a}{2\pi\alpha (H_m/H_c)(I_m/I_c)} \qquad \ldots (14)$$

Suppose we wish to make a 100 kgauss solenoid using a niobium film winding. A conservative figure for the bulk critical field of niobium as determined by susceptibility measurements is $H_{\mathrm{cB}} = 2{\cdot}5$ kgauss. From equation (7) and the discussion that follows it seems reasonable to expect that $H_c/H_{\mathrm{cB}} = 50$ can be obtained with $d \simeq 50$ Å. This puts $H_m/H_c = 0{\cdot}8$. The approximate linearity of the curve in Figure 15 means that

$$\frac{H_m}{H_c} + \frac{I_m}{I_c} \simeq 1 \qquad \ldots (15)$$

so that $I_m/I_c \simeq 0{\cdot}2$ in this example. The theories indicate that α should be 1·3 or greater, but it is probably more realistic to (arbitrarily) put $\alpha = 0{\cdot}1$ in view of the smaller than theoretical critical current densities which have been reported. Finally we assume that $a = 0{\cdot}0005$ in. $= 0{\cdot}0013$ cm. The predicted radial thickness of the windings is then

$$\Delta R = \frac{100^2}{2{\cdot}5} \times \frac{1{\cdot}3 \times 10^{-3}}{2\pi \times 0{\cdot}1 \times 0{\cdot}8 \times 0{\cdot}2} \simeq 20\,\mathrm{cm} \qquad \ldots (16)$$

This is not of unreasonable size, and the cryogenics of maintaining the windings at liquid helium temperatures would be modest.

It should be noted that in their earlier paper the authors specifically considered thin plane films, deposited on a dielectric and rolled up like a jellyroll. The resulting magnet size is comparable with that considered here, but the problems of attaching electrical leads to the inside end of the film, and of current quenching at film edges seem to make this geometry more difficult to work with.

Discussion of thin films

It is important to realize that the thin film theories have neglected possible surface energy effects. These effects become relatively more important as film thickness is decreased. It seems probable that they will quench superconductivity at fields smaller than those given by the above formulae. No experimental work on high field thin film superconductivity has been reported, so that this remains an open question.

Assuming that the stated theories correctly describe thin film superconductivity, the maximum magnetic field which could possibly be generated by thin film superconducting magnets is limited by the minimum film thickness at which superconductivity can be established. Ginsburg and Tinkham[52] have reported a 20 Å superconducting lead film, the critical current of which was reduced only 2 per cent by an applied field of 8 kgauss. Assuming a linear variation in critical current with applied field, this extrapolates to $H_c \simeq 400$ kgauss or $H_c/H_{\mathrm{cB}} \simeq 500$.

Androes and Knight[53] have obtained tin 'films' of 50 Å thickness with a critical field of about 25 kgauss, or $H_c/H_{\mathrm{cB}} \simeq 80$. Zavaritskii[54] has reported a 35 Å superconducting thallium film and a 10 Å superconducting tin film. Khukhareva and Shal'nikov[55] reported that a 1,200 Å niobium film evaporated 'in a vacuum' was not superconducting above 2° K. In a rather lengthy paper, van Gerven and Heremans[56] reported on superconductivity of niobium, tin, and lead films. In all cases their transitions are smeared out, and occur at temperatures considerably below the bulk transition temperature, indicating probably poor vacuum during the evaporation. Unfortunately they do not attempt any very good estimates of film thickness. A rough estimate places their thinnest niobium film at which some evidence of superconductivity was seen at 300 Å. Marchand and Venema[57] reported that tantalum films prepared in a vacuum of 10^{-5} mm never show correct transition properties, but that those prepared in vacua of 10^{-11} mm exhibit sharp transitions at the bulk transition temperature. Their film thicknesses are not stated. Levenstein[58] has studied the growth and structure of thin metallic films. He finds that films of high melting point metals (including tantalum and niobium) form in crystallites less than 15 Å in size, with lattice spacings equal to that of the bulk metals. Films of lower melting point metals show a greater tendency toward aggregation and granular structure. It seems reasonable that 50 Å films of predictable superconducting properties could be obtained if sufficient care is taken in the evaporation process and that such a film would have a critical field enhancement H_c/H_{cB} of the order of 50.

It is doubtful that the anomalously high critical fields H_3 of Figure 5 found in bulk samples of various alloys could be similarly utilized in thin films. In the limit of very large film thicknesses, the thin film theories do not distinguish between the critical fields measured by the three different methods, i.e. the film is 'well behaved'. A bulk sample is 'well behaved' only below the critical field H_2 determined by susceptibility measurements, since only when $\chi = -1/(4\pi)$ is all of the sample volume superconducting. It follows that the H_{cB} in the thin film theories must be approximately equal to the critical field H_2, and it is this field which is enhanced by going to thin films.

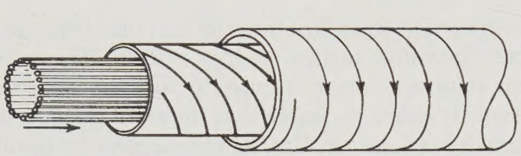

Figure 16. Schematic diagram of current flow in force free cylindrical windings

It is possible that the increased critical field observed in partially oxidized films and films evaporated in an inert gas atmosphere might be used to advantage. The increased critical field probably follows from the decreased electron mean free path due to scattering by impurity atoms in the same way the decreased electron mean free path of thin films increases the critical field. The effect of the decreased electron mean free path on the critical current has not been investigated, but the critical current is certain to decrease. The transition curves for such films are similar to those of most superconducting alloys in that they are considerably broadened and smeared out. For very thin films, superconductivity may be quenched entirely.

The material on to which the superconducting film is evaporated probably must be a non-conductor. Meissner[59] has shown that thin tin films plated on gold or copper substrates are not superconducting at thicknesses less than 6,000 and 2,000 Å, respectively. He suggests that this is about the range of order of the superconducting electrons, and that in thinner films superconductivity is inhibited by electrons which drift in from the normal base metal.

Special design considerations

Forces on magnets

The electromagnetic forces experienced by the windings of high field solenoids can be extremely large. In some instances these forces can result in catastrophic failure of the magnet. With a current density at any point in the windings of $\mathbf{J}(r, \theta, z)$, the force of the magnetic field on a current carrying element $r\,dr\,d\theta\,dz$ is

$$d\mathbf{F} = 0{\cdot}1\mathbf{J}\times\mathbf{H}r\,dr\,d\theta\,dz \qquad \ldots(17)$$

in units of dynes, centimetres, amperes, and gauss. An additional contribution to the current density **J** will come from any induced diamagnetic currents which screen the body of the windings from the central field of the magnet. The mechanical stresses experienced by magnet windings are not related to the magnetic forces in a simple manner.

The force on the windings may be reduced appreciably by using so-called force free winding techniques.[60–64] The individual turns are adjusted so that **J** and **H** are not perpendicular, as illustrated in Figure 16. A design of this type can result in a significant reduction in the maximum stress experienced by the individual windings. For a normal magnet the reduced stress is obtained at the expense of increased Joule heating for a given field, but the superconducting magnet does not have to pay this penalty. In addition it may be possible to obtain higher fields with a given material since the critical field of a superconducting wire is higher in longitudinal fields than in transverse fields.

It is possible that the mechanical stresses due to high fields may be advantageous, provided the magnet does not blow apart. As mentioned above, the critical fields are often increased and critical currents decreased by mechanical strain. However, in the case of the niobium stannide 'wire' the strains may actually rupture the continuity of the brittle niobium stannide core.

Time constants

The very long time constant L/R of a superconducting magnet is an advantage if noise free magnetic fields are desired. In this case the most desirable arrangement is to set up a current in a closed superconducting circuit; since $R = 0$, the current will persist indefinitely. By Faraday's law, the total flux through the magnet cannot change, so the persistent current always adjusts itself to cancel out any externally applied flux. Therefore, the initial current in the magnet must be such that the total (initial plus induced) current will always be less than the critical value.

When external control of the magnetic field is used, the resistance of the electrical leads connecting the power supply to the superconducting windings reduces the magnet time constant to a finite but large value, possibly on the order of many minutes or hours. This is long enough to attenuate a given percentage ripple voltage in the circuit to a much lower percentage ripple current. If rapid time variation of field is desired, it would be necessary to put a large power-absorbing resistance in series with the magnet. The use of persistent fields of superconducting magnets for energy storage might be limited by the very slow delivery of power into all but very high resistance circuits.

Three methods of setting up a persistent current are illustrated in Figure 17. In method (a), superconductivity of the loop is destroyed in region R, either by an applied

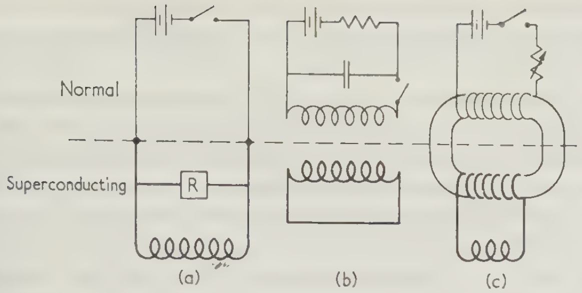

Figure 17. Schematic diagrams of the three methods described in the text for setting up persistent currents

field greater than critical or by heat, and a current is established by the external source. When superconductivity is restored in region R, a persistent current flows in the closed loop of superconductor, and the external source may be removed. In method (b), an external pulsed field, at its peak greater than critical field, quenches the superconductivity of the closed loop. As the external field decays, the closed loop becomes superconducting, and a persistent current builds up in order to enclose a constant flux. The magnitude of the persistent field is determined by the temperature of the superconductor. However, this method does not work well with the 'hard' superconductors because of hysteresis effects and frozen-in flux. In method (c), a d.c. transformer is used. The circuit is cooled to below T_c with a fixed primary current I_p. When I_p is turned off, a persistent current builds up in order to keep the total flux linked into the superconducting circuit constant. Alternately, the magnetic field can be easily controlled by controlling I_p. This method was first suggested by Mendelssohn in 1933.[65] It is not practical with large volume or high field magnets since the required size of the transformer becomes prohibitive.

Field distribution

In principle, the field inside an air core superconducting solenoid should be more uniform than that inside a conventional (copper) one, due to the perfect diamagnetism of the superconductor.[66] At the same time, the maximum field experienced by the windings should occur at the inner winding near the ends of the solenoid where the (trapped) lines of flux are diverging as they leave the interior. In practice this condition probably occurs only when operating below the critical field as determined by susceptibility measurement (the middle curve of Figure 5). Since superconducting alloy solenoids generally would operate at fields much greater than this, their field distribution is probably closer to that of the conventional magnet. This is in fact observed in the molybdenum–rhenium solenoid shown in Figure 8. The same conclusion would apply to thin film solenoids, since the flux penetration through very thin films is practically complete. Frozen-in flux in the windings of a superconducting magnet which has previously been driven normal by too high a current may influence the field configuration, and possibly even reduce the critical current of the magnet. This can be eliminated by warming the magnet above its transition temperature and recooling it in zero field.

Operational precautions

An important consideration in the testing and operation of a superconducting magnet is the heating and possible destruction of the magnet should it go normal while containing high fields. The energy of the collapsing field will be dissipated as Joule heating of the magnet windings, liquid helium refrigerant, and, perhaps, other metal parts. The energy per unit volume $H^2/8\pi$ stored in a 100 kgauss field is 40 J/cm^3. This is about ten times the latent heat of evaporation per cubic centimetre of liquid helium, but is roughly ten times less than the energy required to raise the temperature of 1 cm^3 of either liquid helium or an average metal from 4 to 300° K. A superconducting magnet may easily contain a field volume considerably greater than the volume of its refrigerated windings. Should the energy of the collapsed field be distributed uniformly over the refrigerated volume, the temperature rise would be significant, but probably not enough to cause damage provided a large gaseous pressure rise were avoided. Should any local hot-spots occur, however, the windings would probably be burned out.

A room temperature resistance in parallel with the magnet will alleviate this problem, in the case that an external current source is used to power the magnet. If this resistance is large compared with the normal state resistance of the windings, and if the low impedance current source can be safely removed from the circuit at the first appearance of resistance across the superconducting circuit, most of the field energy will be dissipated in this resistance, and minimum damage will occur. Protection of the magnet in the case that a persistent current is being used presents a greater problem. Probably this persistent current circuit would have to be mechanically severed in such a manner and place as to dissipate most of the power in an external resistance bridging the broken circuit.

Another possible means of alleviating this problem is to use a second passive circuit coupled to the magnetic field to absorb the field energy. This could be just a large copper pipe enclosing the solenoid. When the magnetic field collapses, the fraction of the total field energy dissipated in the 'copper pipe' is

$$\frac{\int_0^\infty I_2^2 R_2\,\mathrm{d}t}{\frac{1}{2}L_{11} I_0^2} = k\frac{\tau_2}{\tau_1+\tau_2} \qquad \ldots(18)$$

provided R_1 is constant during the time the flux is changing. We have defined:

L_{11} and R_1 = self inductance and (normal) resistance of the magnet windings and their external circuitry;

L_{22} and R_2 = self inductance and resistance of the 'copper pipe';

L_{12} = mutual inductance of the two circuits; and

$$k = \frac{(L_{12})^2}{L_{11}L_{22}}, \quad \tau_1 = \frac{L_{11}}{R_1}, \quad \tau_2 = \frac{L_{22}}{R_2} \qquad \ldots(19)$$

If R_l can be made very large and approximately constant, this fraction can approach one, and most of the field energy will be harmlessly dissipated in the 'copper pipe'.

Economic considerations

It is of practical interest to compare capital investment and operating costs of normal and superconducting magnets. The power required to operate a conventional solenoid can be determined from the equation[67]

$$H = G\left(\frac{P\lambda}{r_i \rho}\right)^{1/2} \qquad \ldots (20)$$

where H is the magnetic field in gauss, P is the power dissipation in watts, λ is the space factor (volume of winding filled with conductor/total volume of coil), r_i is the inside radius of the coil in centimetres, ρ is the resistivity of the coil in ohm-centimetres, and G is a function of the coil geometry and current distribution in the windings.

The maximum value of G for windings of rectangular cross-section containing a uniform current density is $G = 0{\cdot}18$. Using this value for G and assuming appropriate values of $\lambda = 0{\cdot}7$ and $\rho = 2{\cdot}0 \times 10^{-6}$ for a copper solenoid just above room temperature the calculated room temperature power dissipation as a function of internal radius for fields of 30 and 100 kgauss is shown in the top two curves of Figure 18.

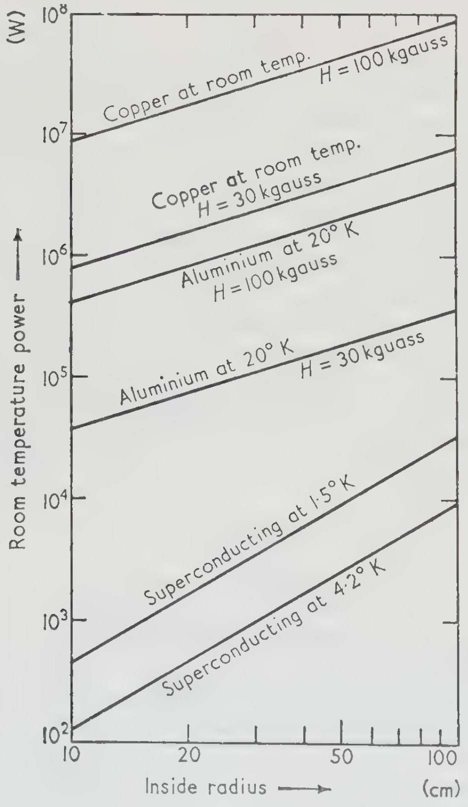

Figure 18. Total power required to operate room temperature, liquid hydrogen cooled, and superconducting magnets with length equal to twice the inside diameter

Reducing the temperature of pure metals results in a significant reduction in the electrical resistivity and can under certain circumstances reduce the total power required to operate a magnet. Cryogenic magnets using sodium or aluminium windings maintained at 10 to 20° K have been suggested.[68, 69] A high field aluminium magnet designed to operate at 20° K is presently being assembled at the National Bureau of Standards, Boulder Laboratories. For this magnet $\lambda = 0{\cdot}95$ and $\rho = 3 \times 10^{-9}$ including the effect of magnetoresistance. The resistivity is based on data for very high purity aluminium in the unstressed condition.

A refrigerator system to remove the Joule heat generated in a magnet operating at 20° K will require about 42 W of room temperature power to remove 1 W at 20° K. The middle two curves of Figure 18 show the calculated power requirement for these conditions. For these calculations the refrigeration required for electrical lead conduction and insulation inefficiencies have neen neglected.

For a superconducting magnet only the heat leaks through the insulation, supports, and electrical leads need be considered. For direct comparison with the normal conducting magnets the superconducting solenoid is chosen to have a length l given by $l/2r_i = 2$. This is the length required for a normal solenoid having $G = 0{\cdot}18$. However, using niobium stannide wire the radial winding thickness $r_o - r_i$ required to produce 100 kgauss is 5 to 10 cm. For large magnets this is much less than the $r_o/r_i \simeq 3$ required for a conventional solenoid.

The lower two curves in Figure 18 show the power required to operate the superconducting magnet. These curves will be approximately independent of the magnetic field. The limiting magnetic field will be determined by the superconducting quenching characteristics of the wire used to wind the solenoid. In the calculations we have arbitrarily considered the solenoid to be insulated inside and out with 2·5 cm of an available insulation having a mean thermal conductivity of $0{\cdot}3 \times 10^{-6}$ W/cm° K.[70] The heat leak through the supports and electrical leads has been assumed equal to the contribution from the insulation. A refrigerator maintaining the magnet at 4·2° K will require about 230 W of room temperature power to remove 1 W of heat, while operation at 1·5° K requires about 800 W of room temperature power for each watt removed. The numbers used for refrigeration cycle calculations are based on results of present day cycle technology.

Even with this comparatively simple insulation the operating cost of the superconducting magnet is significantly less than for either of the normal magnets considered. More sophisticated insulation schemes, probably using an intervening temperature shield at 77° K, would reduce this further.

This analysis assumes that the superconducting magnet is maintained at helium temperatures; if often allowed to warm up, the consequent cool-down costs will sharply increase the overall operating cost. Also if liquid helium is purchased from an outside source and then allowed to evaporate from the Dewar containing the magnet without being recaptured, as is the common laboratory practice in the United States, the operating cost will be markedly increased.

A comparison of the capital costs of normal superconducting magnets is difficult since the cost of production of large quantities of molybdenum–rhenium, niobium stannide, or other desirable wire is unknown at this date. The cost of a small 10 kgauss niobium solenoid for use inside a conventional glass helium Dewar will be of the order of \$100.

The power source required for a superconducting magnet has to supply only the power loss in the (normal) electrical leads and therefore would be only a few watts. This in turn can be reduced to zero by using persistent currents. The cost of this unit would be completely negligible in comparison with the cost of kilowatts or megawatts of power required by conventional power supplies. This is especially true if the large power supplies are required to have a very low ripple. The capital cost of a refrigerator to maintain a cryogenic magnet at 20° K is roughly \$75,000 per kilowatt of power dissipation at 20° K. The capital cost of a helium refrigerator to maintain a superconducting magnet at 4° K in the presence of a few watts heat leak may be in the order of \$50,000. To maintain the superconducting magnet at 1·5° K in the presence of the same heat leak should increase the capital cost by a factor of about two.

Applications

Small size high field superconducting magnets will undoubtedly find their place as general laboratory equipment. The estimated capital investment and operating cost of small high field superconducting magnets make them attractive instruments for experimental laboratories. Numerous physical experiments involve cooling a sample of interest to liquid helium temperature and subjecting it to magnetic fields. This commonly involves fitting the experiment into the narrow tail of a glass Dewar system which is nested between the pole faces of a large iron-core magnet. Often the experimental arrangement can be simplified and improved by using a superconducting magnet located in the same helium bath that is used to cool the sample. At the modest cost of perhaps using more helium, the inside solenoid diameter can be enlarged to any convenient size without decreasing the field strength, thus relaxing the restrictions on sample size or obtaining more homogeneous fields over a given volume. In this category are included solid state maser, cyclotron resonance, de Haas–van Alphen, and adiabatic demagnetization experiments. A description of a simple adiabatic demagnetization apparatus using a superconducting solenoid has been given.[71]

Resonance experiments usually require very ripple-free magnetic fields. These can be obtained quite easily using superconducting magnets. In the optimum case the field of a persistent current would be used, while in the practical case the additional ripple due to an externally controlled current source should be negligible. These low noise fields should be particularly important in maser applications.

Large power consuming iron-core magnets are the backbone of many high energy physics programmes. Besides the synchrotrons and cyclotrons themselves, this category includes bending magnets, focusing magnets, bubble chamber magnets, etc. The Bevatron, for example, has a continuous power dissipation of 8 MW due to Joule heating. The task of making a superconducting synchrotron or cyclotron would be extremely formidable. However, the advantages of a marked reduction in power cost and (with 100 kgauss magnets) an appreciable increase in beam energy are appealing. The power saving obtained using superconducting bending, focusing, or bubble chamber magnets may exceed 1 MW in some instances. The additional track curvature due to 100 kgauss superconducting bubble chamber magnets will decrease the required bubble chamber size or, with a given size, increase the range of particle momentum which can be measured.

High field and large aperture magnets are used for plasma containment and other magnetohydrodynamic applications. An important parameter in plasma physics is

$$\beta \equiv \frac{nkT}{(H^2/8\pi)} = \frac{\text{thermal plasma pressure}}{\text{magnetic field pressure}} \qquad \ldots (21)$$

where n is the number of particles, k is Boltzman's constant, and T the temperature. A low β is required for stable confinement, but when a conventional magnet is used to produce the required high fields, its cost of operation becomes extremely high. A superconducting magnet removes much of this economic difficulty. Some proposed ion and plasma propulsion systems for rockets[72] will utilize magnetohydrodynamic devices. The use of superconducting magnets in this application will result in a tremendous saving in weight of equipment to be sent aloft. An additional application for space flight may be its use in magnetic screening of equipment and personnel from Van Allen radiation.

Conclusion

The old suggestion of H. Kammerlingh Onnes to eliminate the totally wasted Joule heating of magnet coils by using superconducting windings has been followed to produce fields of 15 kgauss in air core solenoids and 25 kgauss in iron core magnets. It seems probable that titanium–molybdenum, lead–bismuth, or some other moderately malleable alloy can be used to wind 20 to 30 kgauss solenoids. Possibly dysprosium or some other metal which is ferromagnetic at 4° K can be used to reach or shape fields of the order of 40 kgauss. However, the most exciting possibility is that of reaching fields of the order of 100 kgauss in superconducting solenoids wound with niobium stannide wire, which at this date is available only in small experimental quantities. Theory predicts that this last goal might also be reached using thin superconducting films, but the lack of experimental evidence and apparent technical difficulties make this much less attractive than the niobium stannide wire.

The design of small low field superconducting magnets presents no unusual difficulties. For large aperture installations, care must be taken to protect the magnet should the wire go normal during operation. For high field installations the effect of the pressure of the magnetic field on the windings must be carefully considered. The long time constant of a superconducting magnet attenuates field ripple to very low values.

Small low field superconducting magnets may make possible more convenient experimental arrangements in studies where liquid helium temperatures are available for other reasons. Small high field (100 kgauss) superconducting magnets should make fields of this magnitude much more generally available than at present. Large superconducting magnets can be very useful for applications where the cost of power for a normal magnet dominates the investment in the magnet. This might well be true for application in large accelerators, bending magnets, bubble chamber magnets, magnetohydrodynamic generators, and plasma applications.

Latest developments

The development of new materials and new techniques for the production of high field superconducting magnets is progressing at a rapid rate. Even before this paper is published many new developments will undoubtedly be available.

Recent results by Kunzler[73] on niobium stannide indicate that the zero current critical field extrapolates to between 200 and 300 kilogauss as T approaches absolute zero. Figure 19 shows the critical current–critical field characteristics of one sample of niobium stannide obtained by the authors using pulsed field of 185 kgauss. Other pulsed field data have also been reported by Arp,[74] Betterton,[75] and Hart.[76]

Other materials which may be even more useful than the niobium stannide include alloys of niobium–zirconium, and molybdenum–technetium. The results of Kunzler[77] indicate that niobium plus 33 atomic per cent zirconium when cold drawn approximately 95 per cent will carry a current density of 10^4 A/cm^2 in a field of 80 kgauss. Another possibility is an alloy of molybdenum plus about 30 atomic per cent technetium. It has a critical temperature in excess of 17° K and Matthias[78] has indicated that it may have a critical field far in excess of niobium stannide.

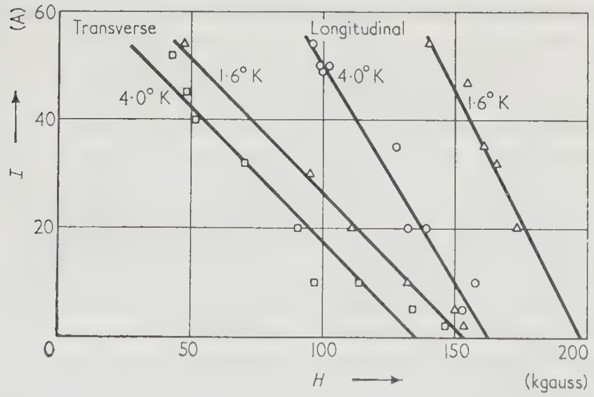

Figure 19. Current–field characteristics of niobium clad niobium stannide wire of diameter 0·063 cm, heat treated for 16 hr at 900° C

The authors wish to thank R. G. Mills and D. H. Wells of Princeton University, S. H. Autler of Lincoln Laboratory, P. Aron and H. C. Hitchcock of Lawrence Radiation Laboratory, and R. J. Corruccini of the National Bureau of Standards for permission to use their unpublished results. (It has been called to the authors' attention that G. B. Yntema reported a 7 kgauss superconducting magnet at the 1955 New York meeting of the American Physical Society.)

REFERENCES

1. Onnes, H. K. *Commun. phys. Lab. Univ. Leiden* No. 122b (1911)
2. Buchhold, T. A. *Sci. Amer.* **203,** 74 (March, 1960)
3. Onnes, H. K. *Commun. phys. Lab. Univ. Leiden* No. 133d (1913)
4. Onnes, H. K. *Commun. phys. Lab. Univ. Leiden* No. 139f (1914)
5. de Haas, W. J., and Voogd, J. *Commun. phys. Lab. Univ. Leiden* No. 214b (1931)
6. Keesom, W. H. *Commun. phys. Lab. Univ. Leiden* No. 234f (1935)
7. Rjabinin, J. N., and Schubnikow, L. W. *Phys. Z. Sowjet.* **7,** 122 (1935); *Nature, Lond.* **135,** 581 (1935)
8. Autler, S. H. *Rev. sci. Instrum.* **31,** 369 (1960)
9. Kunzler, J. E., Buehler, E., Hsu, F. S. L., Matthias, B. T., and Wahl, C. *J. appl. Phys.* **32,** 325 (1961)
10. Kunzler, J. E., Buehler, E., Hsu, F. S. L., and Wernick, J. H. *Phys. Rev. Lett.* **6,** 89 (1961)
11. Hildebrandt, A. F., and Elleman, D. D. *Bull. Amer. phys. Soc.* **5,** 111 (1960)
12. Bardeen, J., Cooper, L. N., and Schrieffer, J. R. *Phys. Rev.* **108,** 1175 (1958)
13. Bogoliubov, N. N. *J. exp. theor. Phys.* **34,** 58 (1958), *Soviet Phys. JETP* **7,** 41 (1958)
14. DeSorbo, W. *Proceedings of the VIIth International Conference on Low Temperature Physics*, p. 367 (University of Toronto Press, Toronto, 1961)
15. Sharvin, Y. V., and Gantmacher, V. F. Reference 14, p. 370
16. Shiffman, C. A. Reference 14, p. 373
17. Haenssler, F., and Rinderer, L. Reference 14, p. 375
18. Abrikosov, A. A. *J. exp. theor. Phys.* **32,** 1442 (1957), *Soviet Phys. JETP* **5,** 1174 (1957)
19. London, F., and London, H. *Physica* **2,** 341 (1935)
20. Comment by Autler, S. H., in paper by Arp, V., and Kropschot, R. H. *Advances in Cryogenic Engineering*, Vol. 6, p. 166 (Plenum, New York, 1961)
21. Mills, R. G. Unpublished data (Princeton University)
22. Trombe, F. *C.R. Acad. Sci., Paris* **221,** 19 (1945)
23. Behrendt, D. R., Legvold, S., and Spedding, F. H. *Phys. Rev.* **109,** 1544 (1958)
24. Rhodes, B. L., Legvold, S., and Spedding, F. H. *Phys Rev.* **109,** 1547 (1958)
25. Cook, D. B., Zemansky, M. W., and Boorse, H. A. *Phys. Rev.* **80,** 737 (1950)
26. Berlincourt, T. G. *Phys. Rev.* **114,** 969 (1959)
27. LeBlanc, M. A. R., and Little, W. A. Reference 14, p. 362
28. Unpublished data obtained at Massachusetts Institute of Technology, Stanford University, and National Bureau of Standards
29. Autler, S. H. Data presented at 1961 New York meeting of the American Physical Society, reported in *Bull. Amer. phys. Soc.* **6,** 64 (1961)
30. Aron, P., and Hitchcock, H. C. Unpublished data
31. Lasarew, B., and Galkin, A. *J. Phys., Moscow* **8,** 371 (1944)
32. Berlincourt, T. G. *J. Phys. Chem. Solids* **11,** 12 (1959)
33. Berlincourt, T. G. *J. Phys. Chem. Solids.* In press
34. Bozorth, R. M., Williams, A. J., and Davis, D. D. *Phys. Rev. Lett.* **5,** 148 (1960)

35. Shoenberg, D. *Superconductivity*, Vol. 2, p. 166 (Cambridge University Press, London, 1960)
36. Alekseyevsky, N. E. *J. Phys., Moscow* **4,** 401 (1941)
37. Arp, V., and Kropschot, R. H. *Advances in Cryogenic Engineering*, Vol. 6, p. 166 (Plenum, New York, 1961)
38. London, F. *Superfluids*, Vol. 1 (Wiley, New York, 1950)
39. Ginsburg, V. L., and Landau, L. D., *J. exp. theor. Phys.* **12,** 1064 (1950)
40. Abrikosov, A. A. *C. R. Acad. Sci. U.R.S.S.* **86,** 498 (1952)
41. Ginsburg, V. L. *J. exp. theor. Phys.* **30,** 593 (1956)
42. Gorkov, L. P. *J. exp. theor. Phys.* **36,** 1918 (1959), *Soviet Phys. JETP* **9,** 1364 (1959)
43. Pippard, A. B. *Proc. roy. Soc.* **A216,** 547 (1953)
44. Ittner, W. B., III. *Phys. Rev.* **119,** 5 (1960)
45. Miller, P. B. *Phys. Rev.* **113,** 1209 (1959)
46. Tinkham, M. *Phys. Rev.* **110,** 26 (1958)
47. Parmenter, R. H. *Phys. Rev.* **116,** 1390 (1959)
48. Ginsburg, N. I., and Shal'nikov, A. I. *J. exp. theor. Phys.* **37,** 399 (1959), *Soviet Phys. JETP* **10,** 285 (1960)
49. Glover, R., III. *Low Temperature Physics and Chemistry*, p. 330 (University of Wisconsin Press, Madison, 1958)
50. Crittenden, E. C., Jr., Cooper, J. N., Schmidlin, F. W., and Learn, A. J. *Structure and Properties of Thin Films*, p. 282 (Wiley, New York, 1959)
51. Bremer, J. W., and Newhouse, V. L. *Phys. Rev.* **116,** 309 (1959)
52. Ginsburg, D. M., and Tinkham, M. *Bull. Amer. phys. Soc.* **3,** 338 (1958)
53. Andhoes, G. M., and Knight, W. D. *Phys. Rev.* **121,** 779 (1961)
54. Zavaritskii, N. V. *C. R. Acad. Sci. U.R.S.S.* **87,** 229 (1952)
55. Khukhareva, E. S., and Shal'nikov, A. I. *C. R. Acad. Sci. U.R.S.S.* **99,** 735 (1954)
56. van Gerven, L., and Heremans, F. *Verh. Kon. vlaams. Acad. Wet.* 42 (1953)
57. Marchand, J. F., and Venema, A. *Philips Res. Rep.* **14,** 427 (1959)
58. Levenstein, H. *J. appl. Phys.* **20,** 306 (1949)
59. Meissner, H. *Phys. Rev. Lett.* **2,** 458 (1959)
60. Chandrasekhar, S., and Fermi, E. *Astrophys. J.* **118,** No. 1 (1953)
61. Lundquist, S. *Ark. Fys.* **2,** 363 (1950)
62. Chandrasekhar, S., and Woltjer, L. *Proc. nat. Acad. Sci., Wash.* **44,** 285 (1958)
63. Furth, H. P., Levine, M. A., and Waniek, R. W. *Rev. sci. Instrum.* **28,** 949 (1957)
64. Wells, D. R. Unpublished results
65. Mendelssohn, K. *Nature, Lond.* **132,** 602 (1933)
66. Jet Propulsion Laboratories *Research Report* No. 36-4, p. 6
67. Cockroft, J. D. *Phil. Trans.* **227,** 317 (1928)
68. Post, R. F., and Taylor, C. E. *Advances in Cryogenic Engineering*, Vol. 5, p. 13 (Plenum, New York, 1960)
69. Corruccini, R. J. Unpublished results (Cryogenic Engineering Laboratory, National Bureau of Standards)
70. Kropschot, R. H. *Cryogenics* **1,** 171 (1961)
71. Arp, V., and Kropschot, R. H. *Rev. sci. Instrum.* **32,** 217 (1961)
72. Hendel, F. J. *Chem. Engr* **68,** 99, 131 (1961)
73. Kunzler, J. E. *Bull. Amer. phys. Soc.* **6** (Post deadline paper given at American Physical Society meeting in Monterey, California, March 1961)
74. Arp, V., Kropschot, R. H., Wilson, J. H., Love, W. F., and Phelan, R. *Phys. Rev. Lett.* **6,** 452 (1961)
75. Betterton, J. O., Boom, R. W., Kneip, G. D., Worsham, R. E., and Roos, C. E. *Phys. Rev. Lett.* **6,** 532 (1961)
76. Hart, H. R. *Bull. Amer. phys. Soc.* **6,** 308 (1961)
77. Kunzler, J. E. *Bull. Amer. phys. Soc.* **6,** 298 (1961)
78. Matthias, B. T. *Bull. Amer. phys. Soc.* **6,** 298 (1961)

(This work is supported in part by the U.S. Atomic Energy Commission.)

Abstracts

MEASUREMENTS OF THE PRESSURE DEPENDENCE OF LIQUID NORMAL HYDROGEN

A. VAN ITTERBEEK O. VERBEKE

MEASUREMENTS of the dependence of the density ρ of liquid normal hydrogen on pressure are carried out below 20° K and up to near the melting curve (150 kg cm^{-2}). We compare our measurements with the existing ones on liquid normal hydrogen by Bartholomé and Johnston. The former were carried out below 20° K and the latter above 20° K. Very good agreement is found for our results at the normal boiling point, especially with those of Johnston. However, at the lower temperatures, a large difference appears against the data of Bartholomé. Comparing the velocity of sound calculated from our results or from those of Bartholomé with the experimental values determined directly in our laboratory, we found a good agreement except for Bartholomé's values at the lower temperatures. Another conclusion following from these measurements is that Eucken's equation for the density as a function of pressure has to be reconsidered.

THE CALCULATION OF TEMPERATURE DIFFERENCES FROM RESISTANCE THERMOMETER MEASUREMENTS USING A DIGITAL COMPUTER

L. J. CHALLIS

A DIGITAL computer has been used to calculate the magnitudes of temperature differences from carbon resistance thermometer measurements in the helium range. The method is being applied to differences produced in the measurement of thermal conductivities and Kapitza resistances below 2·2° K but has also been checked with measurements made in temperature ranges up to 4·2° K. A description is given of how the data are fitted to empirical formulae and of how these are used in the computer programme. An estimate is made of the errors involved in this method and these are thought to be of a similar magnitude to those obtained by the more laborious conventional methods.

SOME THERMAL AND MAGNETIC PROPERTIES OF TANTALUM, NIOBIUM, AND VANADIUM AT HELIUM TEMPERATURES

A. CALVERLEY P. M. ROWELL
K. MENDELSSOHN

MEASUREMENTS of the thermal conductivity of tantalum, niobium, and vanadium in the normal and superconducting states have been made using specimens of various chemical purities and crystalline states. The difference between annealed monocrystals and strained polycrystals is discussed and the contribution in the superconductive state of the lattice waves at temperatures below one-sixth of the transition temperature is clearly shown. The thermal resistance in the intermediate state has been measured for the purest monocrystals of tantalum and niobium, and the critical field curve for a monocrystal of tantalum has been determined.

ISOTHERMAL FLOW OF LIQUID HELIUM-II IN WIDE CAPILLARIES

S. M. BHAGAT K. MENDELSSOHN

THE isothermal flow of liquid helium-II under gravity has been investigated in capillaries varying from 8×10^{-3} to 7×10^{-2} cm diameter between 1·3 and 2·1° K. Except for the narrowest long tube, the flow velocity was found to depend in all cases on the *initial* pressure difference. This effect has been explained in terms of an eddy viscosity due to turbulence in the superfluid component.

THERMOMECHANICAL PRESSURE MEASUREMENTS IN LIQUID HELIUM-II

S. M. BHAGAT P. R. CRITCHLOW

MEASUREMENTS of the thermomechanical pressure have been carried out on capillaries of 0·01–0·08 cm diameter between 1·3 and 1·8° K. In all cases the behaviour showed a marked change at a critical heat current. Below this value the only process of dissipation is the viscosity of the normal fluid. While above the critical heat current mutual friction can explain the observed temperature differences it is insufficient to account for the pressure differences. An attempt has been made to explain this discrepancy by the existence of an eddy viscosity in the superfluid.

NEW REFRIGERATION CYCLE FOR THE PRODUCTION OF LIQUID NITROGEN

S. C. COLLINS R. W. HUGHES

A NOVEL arrangement of reversing exchangers which are cooled by expanded nitrogen makes possible unattended operation of a liquid nitrogen plant for long periods of time. Air for use in the distillation column is compressed to 5 atm and purified by refrigeration.

Unlike procedures in earlier cycles employing reversing exchangers, the functions of refrigeration and rectification are separate. The refrigerant stream is composed of pure nitrogen except for the starting period when air is used. The pressure range is from about 4·5 to 37 atm. Compression takes place in two stages, expansion in one stage.

Several small liquid nitrogen plants based on this cycle have been in service for more than a year.

THE THERMOSIPHON AS A NITROGEN CRYOSTAT FOR OPERATION IN THE HORIZONTAL REACTOR CHANNEL

L. BEWILOGUA R. KNÖNER

A TWO-PHASE closed circuit according to the thermosiphon principle allows cooling of samples which are arranged at a large distance or are located at points of difficult access, even in cases of considerable heat supply. With the model described here, a temperature of 80° K was attained at a distance of 2 m using nitrogen. This temperature could be maintained for a long period even under unfavourable conditions, such as heat supply of up to 500 W, poor insulation, and partial evaporation of the external cooling liquid.

AN APPARATUS FOR STUDYING ULTRASONIC ABSORPTION IN METALS AT LOW TEMPERATURES

A. A. GALKIN A. P. KOROLYUK

AN apparatus is described for measuring the ultrasonic absorption coefficient in metals at low temperatures. The absorption in the frequency range 50–250 Mc/s can be determined, recorded on a two-dimensional plotter.

Résumés

MESURES DE L'INFLUENCE DE LA PRESSION SUR L'HYDROGENE LIQUIDE NORMAL

A. VAN ITTERBEEK O. VERBEKE

Nous avons mesuré l'influence de la pression sur la densité ρ de l'hydrogène liquide normal à des températures inférieures à 20° K et jusque près de la courbe de fusion (150 kg cm^{-2}). Nous comparons nos mesures avec celles qui ont été réalisées sur l'hydrogène liquide normal Bartholomé et Johnston. Les premières mesures ont été faites à moins de 20° K, les autres au dessus de 20° K. Nous avons constaté que nos résultats s'accordent très bien, au point d'ébullition normale, avec ceux de Johnston en particulier. Toutefois, aux températures plus basses, nous avons observé une forte différence avec les données de Bartholomé. En comparant la vitesse du son, calculée d'après nos résultats et ceux de Bartholomé avec les valeurs expérimentales obtenues directement dans notre laboratoire, nous avons constaté un accord satisfaisant, excepté pour les valeurs de Bartholomé aux températures les plus basses. Nous avons conclu, également, de ces mesures que l'équation d'Eucken donnant la densité en fonction de la pression doit être reconsidérée.

LE CALCUL DES DIFFERENCES DE TEMPERATURE OBTENUES AVEC UN THERMOMETRE A RESISTANCE, AU MOYEN D'UNE MACHINE A CALCULE DIGITALE

L. J. CHALLIS

L'auteur s'est servi d'une machine digitale pour déterminer la grandeur des différences de température obtenues avec un thermomètre à résistance au carbone, dans le domaine de l'hélium. La méthode est appliquée aux différences déterminées dans la mesure des conductivités thermiques et des résistances Kapitza au dessous de 2,2° K, mais elle a été vérifiée, également, pour des mesures réalisées dans une zone de températures allant jusqu'à 4,2° K. L'article décrit la manière dont les valeurs numériques sont adaptés à des formules empiriques et l'emploi de ces dernières dans la programmation. On evalue les erreurs de cette méthode; on pense qu'elles sont de l'ordre de grandeur de celles faites au moyen de méthodes conventionnelles beaucoup plus laborieuses.

QUELQUES PROPRIETES THERMIQUES ET MAGNETIQUES DU TANTALE, DU NIOBIUM ET DU VANADIUM AUX TEMPERATURES DE L'HELIUM

A. CALVERLEY K. MENDELSSOHN
P. M. ROWELL

On a mesuré la conductivité du tantale, du niobium et du vanadium, à l'état normal et à l'état supraconducteur, en utilisant divers échantillons de pureté chimique et de constitution cristalline différentes. On a étudié la différence entre les monocristaux recuits et les polycristaux tendus, et on a montré clairement la contribution, à l'état supraconducteur, des ondes à réseau aux températures inférieures à un-sixième de la température de transition. On a mesuré la résistance thermique, dans l'état intermédiaire, des monocristaux de tantale et de niobium les plus purs, et déterminé la courbe de champ critique d'un monocristal de tantale.

ECOULEMENT ISOTHERMIQUE DE L'HELIUM-II LIQUIDE DANS DES CAPILLAIRES LARGES

S. M. BHAGAT K. MENDELSSOHN

L'écoulement isotherme de l'hélium-II liquide sous l'influence de la pesanteur a été étudié dans des capillaires dont le diamètre est compris entre 8×10^{-3} et 7×10^{-2}, à des températures allant de 1,3 à 2,1° K. Sauf dans le cas des tubes longs les plus fins, on a constaté que la vitesse de l'écoulement dépend, dans tous les cas, de la différence de pression *initiale*. On a expliqué cet effet en invoquant une viscosité additionelle due à une turbulence dans la fraction superfluide.

MESURES DE LA PRESSION THERMOMECHANIQUE DANS L'HELIUM-II LIQUIDE

S. M. BHAGAT P. R. CRITCHLOW

Les auteurs ont mesuré la pression thermomécanique avec des capillaires de 0,01–0,08 cm de diamètre, entre 1,3 et 1,8° K. Dans tous les cas, le comportement change nettement pour un certain flux de chaleur critique. Au dessous de cette valeur, la viscosité du liquide normal est à l'oufine du seul processus de dissipation. Alors qu'au dessus du flux de chaleur critique, la friction mutuelle peut expliquer les différences de température observées, ce phénomène ne suffit pas pour expliquer les différences de pression. Les auteurs ont essayé d'expliquer cette différence en invoquant la presence d'une viscosité de turbulence dans le superfluide.

NOUVEAU CYCLE DE REFRIGERATION POUR LA PRODUCTION D'AZOTE LIQUIDE

S. C. COLLINS R. W. HUGHES

Une nouvelle disposition d'échangeurs reversibles refroidis par de l'azote detendu, rend possible le fonctionnement prolongé sans surveillance d'une installation d'azote liquide. L'air utilisé dans la colonne de distillation est comprimé à 5 atmosphères et purifié par réfrigération. Contrairement aux procédés des cycles antérieurs utilisant des échangeurs reversibles, les fonctions de réfrigération et de rectification sont indépendantes. Le courant réfrigérant est constitué d'azote pur sauf au démarrage, au cours duquel on utilise, alors, de l'air. La gamme des pressions va de 4,5 à 37 atmosphères. La compression a lieu en deux étages, la détente en un seul. Plusieurs petites installations d'azote liquide basées sur ce cycle sont en service depuis plus d'un an.

LE THERMOSIPHON UTILISÉ COMME CRYOSTAT AZOTIQUE DANS LE CANAL HORIZONTAL D'UN RÉACTEUR

L. BEWILOGUA R. KNÖNER

Grâce à un circuit fermé deux phases disposé d'après le principe du thermosiphon, on peut refroidir des échantillons placés à de grandes distances ou situés en des endroits d'accès malaisé, même

lorsque la source de chaleur est considérable. Avec le modèle décrit dans l'article, on a atteint une température de 80° K à une distance de 2 mètres en se servant d'azote. On a pu maintenir cette température pendant une longue période même dans des conditions défavorables: source de chaleur jusqu'à 500 W, mauvais isolement et évaporation partielle du liquide de refroidissement externe.

UN APPAREIL POUR L'ETUDE DE L'ABSORPTION ULTRASONIQUE DANS LES METAUX A BASSES TEMPERATURES

A. A. GALKIN A. P. KOROLYUK

Les auteurs décrivent un appareil pour la mesure du coefficient d'absorption ultrasonique dans les métaux à basses températures. On peut déterminer, enregistrée sur un cartographe à deux dimensions, l'absorption dans la gamme de fréquence de 50 à 250 Mc/s.

Auszüge

MESSUNG DER ABHÄNGIGKEIT DES DRUCKES VON DER DICHTE BEI FLÜSSIGEM NORMALWASSERSTOFF

A. VAN ITTERBEEK O. VERBEKE

Die Messung des Einflusses der Dichte ρ von flüssigem Normalwasserstoff auf den Druck wurde bei Temperaturen unter 20° K bis zur Nähe der Schmelzkurve (120 kg cm^{-2}) durchgeführt. Wir vergleichen unsere Messungen mit denen von Bartholomé und Johnston. Diese Messungen wurden unter 20° K und später auch über 20 K durchgeführt. Unsere Messungen stimmen bein normalen Siedepunkt besonders mit den Messungen Johnston's ausserordentlich gut überein. Bei niedrigeren Temperaturen zeigt sich jedoch ein bedeutender Unterschied von den Daten, die von Bartholomé errechtnet wurden. Ein Vergleich der Schallgeschwindigkeit, berechnet aus unseren oder aus Bartholomés Resultaten mit den im Laboratorium unmittelbar bestimmten Werten, zeigt gute Ubereinstimmung mit Bartholomé, mit Ausnahme der niedrigen Temperaturen. Ein weiterer aus diesen Messungen folgender Schluss ist, dass Euckens Gleichung für die Dichte als Funktion des Drucks einer Überprüfung bedarf.

DIE BERECHNUNG VON TEMPERATURUNTERSCHIEDEN AUS WIDERSTANDSTHERMOMETERMESSUNGEN UNTER EINSATZ EINER DIGITALRECHENMASCHINE

L. J. CHALLIS

Eine Digitalrechenmaschine wurde dazu benützt, die Grösse der Temperaturunterschiede zu berechnen, die sich aus Kohlewiderstandsthermometermessungen im Heliumbereich eragben. Das Verfahren wurde auf Differenzen in der Messung der Wärmeleitfähigkeiten und Kapitza-Widerständen unter 2,2° K angewendet, wurde jedoch auch durch Messungen im Temperaturbereich bis zu 4,2° K überprüft. Es folgt eine Beschreibung über das Angleichen dieser Daten an empirische Formeln und ihren Einsatz in der Programmierung der Rechenmaschine. Eine Schätzung der Fehler dieses Verfahrens zeigt, dass ihre Grössenordnung wahrscheinlich der des komplizierteren Verfahrens entspricht.

EINIGE THERMISCHE UND MAGNETISCHE EIGENSCHAFTEN VON TANTAL, NIOB UND VANADIUM BEI HELIUM-TEMPERATUREN

A. CALVERLEY K. MENDELSSOHN
P. M. ROWELL

Messungen der Wärmeleitfähigkeit von Tantal, Niob und Vanadium in normalem und supraleitendem Zustand wurden unter Verwendung von Mustern verschiedenen chemischen Reinheitszustands und verschiedener Kristallstrukturen vorgenommen. Der Unterschied zwischen entspannten Monokristallen und verspannten Polykristallen wird besprochen und der Beitrag der Gitterwellen im Supraleitzustand bei Temperaturen unter einem Sechstel der Übergangstemperatur wird klar dargestellt. Der Thermalwiderstand im Zwischenzustand wurde für die reinsten Monokristalle von Tantal und Niob gemessen und die kritische Feldkurve für ein Tantal-Monokristall wurde bestimmt.

DER ISOTHERME FLUSS VON FLÜSSIGEM HELIUM-II IN BREITEN KAPILLARROHREN

S. M. BHAGAT K. MENDELSSOHN

Der isotherme Fluss von flüssigem Helium-II unter dem Einfluss der Schwerkraft wurde in Kapillarrohren mit Durchmessern von 8×10^{-3} bis 7×10^{-2} cm bei 1,3 – 2,1° K gemessen. Mit Ausnahme des dünnsten Rohres wurde festgestellt, dass die Strömungsgeschwindigkeit in allen Fällen von der anfänglichen Druckdifferenz abhing. Diese Wirkung wurde durch eine Wirbelviskosität erklärt, welche auf das Suprafluidum zurückzuführen war.

THERMOMECHANISCHE DRUCKMESSUNGEN IN FLÜSSIGEM HELIUM-II

S. M. BHAGAT P. R. CRITCHLOW

Messungen des thermomechanischen Drucks in Kapillarrohren von 0,01–0,08 cm Durchmesser wurden bei 1,3 – 1,8° K durchgeführt. In allen Fällen zeigte das Verhalten eine ausgeprägte Änderung bei einem kritischen Heizstrom. Unter disem Wert ist der einzige Streuungsvorgang die Viskosität der normalen Flüssigkeit. Obwohl der beobachtete Temperaturunterschied oberhalb des kritischen Heizstroms durch Reibung erklärt werden kann, ist dies ungenügend für die Druckunterschiede. Es wird versucht, den Unterschied durch die Existenz einer Wirbelviskosität im Suprafluidum zu erklären.

NEUER KÄLTEKREISLAUF FUR DIE HERSTELLUNG VON FLUSSIGEM STICKSTOFF

S. C. COLLINS R. W. HUGHES

Eine neue Ausführung eines Umkehrwärmeaustauschers, welcher durch sich ausdehnenden Stickstoff gekühlt wird, gestattet den Betrieb einer flüssigen Stickstoffanlage ohne Aufsicht für längere Zeiträume. Die Luft in der Destillationssäule wird auf 5 at komprimiert und durch Kühlung gereinigt. Im Gegensatz zu bisherigen Kreisläufen sind hier die Kühlung und Rektifikation getrennt. Der

Kühlstrom besteht aus reinem Stickstoff, mit Ausnahme der Anlaufzeit, während welcher Luft verwendet wird. Der Druckbereich liegt zwischen 4,5 und 37 at. Die Verdichtung findet in zwei Stufen statt, die Expansion in einer Stufe. Kleinere Anlagen dieser Art sind seit über einem Jahr in Betrieb.

THERMOSIPHON ALS STICKSTOFFKRYOSTAT FÜR ARBEITEN IM HORIZONTALEN KANAL DES REAKTORS

L. BEWILOGUA R. KNÖNER

Ein nach dem Thermosiphonprinzip arbeitender geschlossener zweiphasiger Kreislauf ermöglicht die Abkühlung von Proben, die sich in relativ großem Abstand oder an schwer zugänglichen Stellen befinden, auch bei beträchtlichen thermischen Belastungen. In dem beschriebenen Modell wurde mit Stickstoff in 2 m Abstand eine Temperatur von etwa 80°K erreicht. Sie liess sich auch unter ungünstigen Bedingungen, wie Belastung bis zu 500 Watt, schlechter Wärmeisolation, teilweisem Verdampfen des äußeren Kältemittels über beliebige Zeit aufrecht erhalten.

APPARAT ZUM STUDIUM DER UKTRASCHALLABSORPTION IN METALLEN BEI NIEDRIGEN TEMPERATUREN

A. A. GALKIN A. P. KOROLYUK

Der Artikel beschreibt einen Apparat zum Messen des Ultraschallabsorptionskoeffizienten in Metallen bei niedrigen Temperaturen. Die Absorption im Frequenzgebiet von 50–250 MHz kannmit einem zweidimensional aufzeichnenden Kurvenschreiber bestimmt werden.

Резюме

ИЗМЕРЕНИЯ ЗАВИСИМОСТИ ДАВЛЕНИЯ НА ПЛОТНОСТЬ ЖИДКОГО НОРМАЛЬНОГО ВОДОРОДА

A. VAN ITTERBEEK O. VERBEKE

Выполняются измерения зависимости плотности с жидкого нормального водорода на давление ниже 20° K и почти до кривой плавления (150 кг см$^{-2}$). Мы сравниваем наши измерения со существующимися измерениями для жидкого нормального водорода Бартоломэ и Джонстона. Первые выполнились при температуре ниже 20° K и последние сверх 20° K. Находится очень хорошее согласие для наших результатов при нормальной точке кипения, особенно с теми Джонстона. Однако при более низких температурах большая разность находится между нашими данными и теми Бартоломэ. Сравняя скорость звука вычисленную по нашим результатам или по данным Бартоломэ с опытными величинами определенными непосредственно в нашей лаборатории, мы нашли хорошее согласие за исключением величин Бартоломэ при более низких температурах. Другим заключением найденным из этих измерений является то, что уравнение Эукена для плотности как функция давления должно быть пересчитано.

ВЫЧИСЛЕНИЕ РАЗНОСТЕЙ ТЕМПЕРАТУР ОТ ИЗМЕРЕНИЙ С ТЕРМОМЕТРОМ СОПРОТИВЛЕНИЯ ПРИМЕНЯЯ ЦИФРОВУЮ ВЫЧИСЛИТЕЛЬНУЮ МАШИНУ

L. J. CHALLIS

Цифровая вычислительная машина применилась для вычисления величин разностей температур от измерений с термометром угольного сопротивления в зоне гелия. Метод применяется для определения разностей произведенных в измерении термических проводностей и сопротивлений Капитза ниже 2,2° K а также проверился с измерениями сделанными при температурах до 4,2° K. Описывается то как данные применяются к эмпирическим формулам и как эти употребляются в программе вычислительной машины. Вычисляются ошибки вовлеченные в этом способе и эти считаются подобной величины как ошибки добываемые по более трудным нормальным методам.

НЕКОТОРЫЕ ТЕРМИЧЕСКИЯ И МАГНИТНЫЕ СВОЙСТВА ТАНТАЛА, НИОБИЯ И ВАНАДИЯ ПРИ ТЕМПЕРАТУРАХ ГЕЛИЯ

A. CALVERLEY K. MENDELSSOHN P. M. ROWELL

Термическая проводимость тантала, ниобия и ванадия в нормальном и сверхпроводящем состояниях измерилась применяя пробы различных химических чистотей и кристаллических состояний. Разница между прокаленными монокристаллами и напряженными поликристаллами обсуждается и содействие в сверхпроводящем состоянии волн решетки при температурах ниже одной шестой переходной температуры ясно показано. Измерилось термическое сопротивление в переходном состоянии при наичистых монокристаллах тантала и ниобия, и определилась кривая критической величины поля при монокристалле тантала.

ИЗОТЕРМИЧЕСКОЕ ТЕЧЕНИЕ ЖИДКОГО ГЕЛИЯ II в ШИРОКИХ КАПИЛЛЯРНЫХ ТРУБКАХ

S. M. BHAGAT K. MENDELSSOHN

Изотермический самотек жидкого гелия-II исследовалось в капилляных трубках диаметром от 8×10^{-3} до 7×10^{-2} см при температурах между 1,3 и 2,1° K. За исключением самой узкой длинной трубки, нашли что скорость течения во всех случаях зависит от исходной разности давления. Этот эффект объясняется в терминах вихревой вязкости благодаря турбулентности в верхжидком компоненте.

ТЕРМОМЕХАНИЧЕСКИЕ ИЗМЕРЕНИЯ ДАВЛЕНИЯ В ЖИДКОМ ГЕЛИИ-II

S. M. BHAGAT P. R. CRITCHLOW

Выполнились измерения термомеханического давления на капиллярных трубках диаметром 0,01–0,08 см между 1,3 и 1,8° K. Во всех случаях поведение подвергалось четному изменению при критическом токе теплоты. Ниже этой величины единственным процессом рассеяния является вязкость нормальной жидкости. Пока сверх критического тока теплоты взаимное трение является причиной наблюденной разностей температуры, это недостаточно объясняет разности давления. Сделана попытка приписывать различие это наличию вихровой вязкости в верхжидкости.

НОВЫЙ ХОЛОДИЛЬНЫЙ ЦИКЛ ДЛЯ ПРОИЗВОДСТВА ЖИДКОГО ВОДОРОДА

S. C. COLLINS **R. W. HUGHES**

Новое устройство реверсирующхся теплообмеников, которые охлаждаются расширенным водородом позволяет долговременную работу установки для жидкого водорода без обслуживающего персонала. Воздух примененный в дистиляционной колонне сжимается до 5 атм, и чистится рефрижерацией. В отличие от процессов в презних циклах применяющих реверсирующиеся теплообменики. функции рефрижерации и ректификации самостоятельны. Поток охдалителя состоит из чистого водорода за исключением начального периода когда применен воздух. Пределы давления — от приближительно 4,5 до 37 атм. Сжатие имеет место в двух степенях, а расширение в одной степени. Несколько маленьких установок для жидкого водорода основанных на этот цикл работает уже более одного года.

КРИОСТАТ — ТЕРМОСИФОН ДЛЯ РАБОТ В ГОРИЗОНТАЛЬНОМ КАНАЛЕ РЕАКТОРА

L. BEWILOGUA **R. KNÖNER**

Замкнутый двухфазный цикл, работающий по принципу термосифона, обеспечивает охлаждение образцов, находящихся в некотором отдалении или в трудно доступных местах, даже при условии значительных термических нагрузок. В описанной модели, на расстоянии 2 метров, посредством азота была достигнута температура примерно 80° K. Поддержка этой температуры оказалась возможной на неограниченное время, и при неблагоприятных условиях, как-то нагрузке до 500 ватт, недостаточной изоляции и частичном испарении внешнего хладоагента.

ПРИБОР ДЛЯ ИЗУЧЕНИЯ ПОГЛОЩЕНИЯ УЛЬТРАЗВУКА МЕТАЛЛАМИ ПРИ НИЗКИХ ТЕМПЕРАТУРАХ

A. A. GALKIN **A. P. KOROLYUK**

Описана установка для изучения коэффициентов поглощения ультразвука металлами при низких температурах. Прибор позволяет производить измерения поглощения в области частот 50÷250 *Мгц* с записью на двухкоординатном самописце.

Measurements of the Pressure Dependence of Liquid Normal Hydrogen

A. Van Itterbeek and O. Verbeke

Institut voor Lage Temperaturen en Technische Fysica, Louvain, Belgium

Received 24 April 1961

A DETAILED description of the apparatus used in this experiment has been given in earlier publications.[1,2] It should be noticed that only the density variation $\Delta\rho = \rho - \rho(P=0)$ is determined in this experiment. $\rho(P=0)$ is obtained by extrapolating the density ρ down to zero pressure using density data at the vapour pressure curve.[3,4]

The experimental results are given in Table 1, and presented graphically in Figure 1 together with the results of Bartholomé[5] and Johnston.[6]

It should be noticed that at the lowest temperatures a large discrepancy appears for $(\partial\rho/\partial P)_T$ between our measurements and those of Bartholomé.

From these measurements we calculated by means of equation (1) the velocity of sound, and then compared the results with experimental values measured directly in our laboratory[7]

$$W^2 = 1:\left\{\left(\frac{\partial\rho}{\partial P}\right)_T - \frac{\left[\frac{1}{\rho}\left(\frac{\partial\rho}{\partial T}\right)_P\right]^2 \times T}{C_P}\right\} \qquad \ldots(1)$$

The value of C_P is calculated from values of the specific heats at the vapour tension curve[8] and by means of the equation

$$C_S = C_P - T\left(\frac{\partial V}{\partial T}\right)_P\left(\frac{\partial P}{\partial T}\right)_{\text{sat}} \qquad \ldots(2)$$

In Figure 2 we have given graphically the values obtained for the velocity of sound. We can conclude from this that the agreement with the results of Bartholomé is poor.

Finally, we compared our measurements with the Eucken equation[9]

$$\rho^3 = \frac{1}{2}\rho_0^3\left[1+\sqrt{\left(1+\frac{A_P}{\rho_0^6}\right)}\right]$$

In this equation A is expected to be constant, but at the normal boiling temperature we found that this is not exactly the case, as can be seen from the values of Table 2 where we have calculated the value of A from the work of the different authors.

Table 1. Pressure Dependence of the Density of Liquid Hydrogen at Six Temperatures

T(°K)	P(kg/cm²)	ρ(g/cm³)
20·396	149·60	0·08262
	110·50	0·08036
	70·80	0·07816
	41·95	0·07526
	13·20	0·07231
	0	0·07079
20·420	149·70	0·08273
	108·45	0·08034
	78·89	0·07840
	47·71	0·07593
	18·40	0·07274
	0	0·07079
20·420	149·42	0·08242
	107·98	0·08002
	76·60	0·07792
	47·62	0·07561
	17·08	0·07254
	0	0·07079
19·051	149·10	0·08324
	108·20	0·08107
	72·60	0·07877
	38·10	0·07606
	11·40	0·07349
	0	0·07230
17·909	110·72	0·08186
	77·40	0·07991
	43·85	0·07758
	12·20	0·07468
	0	0·07350
16·666	82·80	0·08115
	47·15	0·07875
	13·82	0·07595
	0	0·07465

The variation of A as a function of pressure is linear

$$A = A_0 + A_1 P$$

and we obtained at the different temperatures the following values

T (°K)	$A_0 \times 10^{10}$	$A_1 \times 10^{10}$
20·41	28·30	0·0350
19·05	28·25	0·0184
17·91	28·60	0·0000
16·67	28·44	0·0225

We take this opportunity to express our sincere thanks to the Belgian Ministry of Education from whom we obtained the financial support to carry out these measurements.

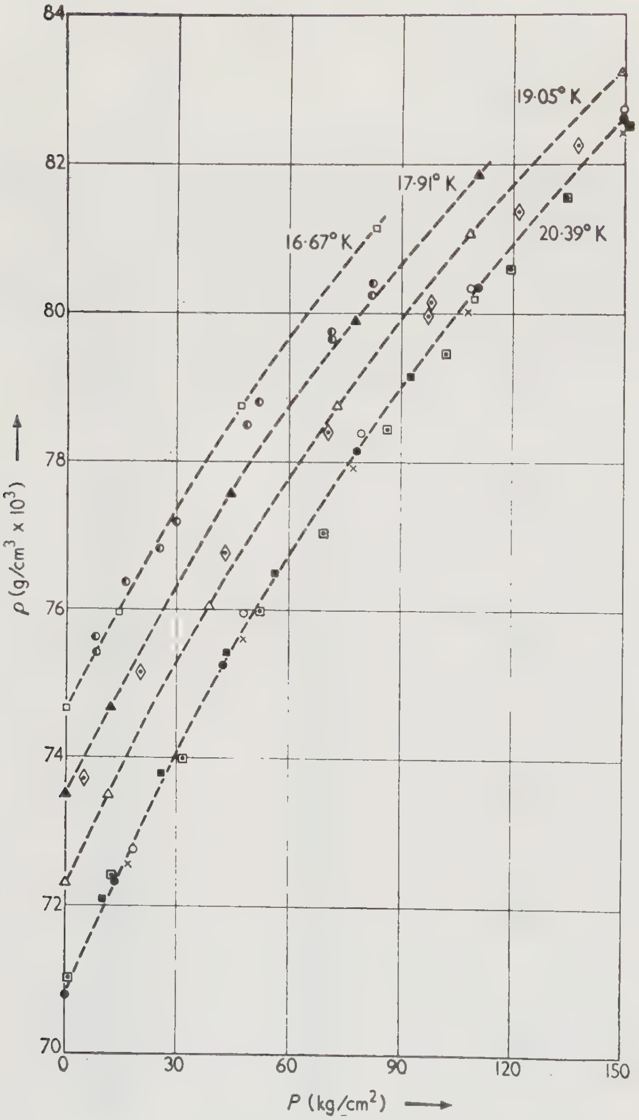

Louvain:[7]
○ 20·39° K, ● 20·42° K, × 20·42° K, △ 19·05° K, ▲ 17·90° K, □ 16·67° K

Johnston:[6]
■ 20·38° K

Bartholomé:[5]
⊡ 20·33° K, ◊ 18·24° K, ◐ 16·43° K

Figure 1. Dependence on pressure of the density of liquid hydrogen

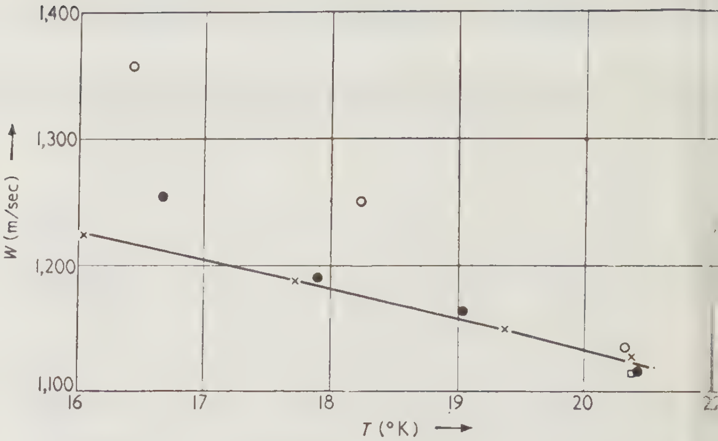

× Measured ○ Bartholomé □ Johnston ● Louvain

Figure 2. Velocity of sound directly measured and calculated from density measurements of Bartholomé, Johnston, and our laboratory

Table 2. Comparison of A from the Work of Different Authors (20·4° K)

Authors	*P(kg/cm²)*	$A \times 10^{10}$
Bartholomé	1	22·71
	12·5	28·14
	31·5	24·92
	52·0	27·72
	69·0	26·65
	86·0	28·31
	102·0	28·57
	119·5	29·37
	134·5	29·92
	151·0	30·57
Johnston	10·300	28·54
	25·554	29·16
	43·005	29·59
	55·859	29·66
	77·105	30·07
	92·391	30·15
	109·704	30·27
Louvain measurements	41·95	29·13
	77·80	30·13
	110·50	30·84
	149·60	31·55

REFERENCES

1. VAN ITTERBEEK, A., and VERBEKE, O. *Cryogenics* **1,** 77 (1960)
2. VAN ITTERBEEK, A., and VERBEKE, O. *Physica* **26,** 931, 936 (1960)
3. MATHIAS, E., CROMMELIN, C. A., and KAMERLINGH ONNES, H. *Comm. phys. Lab. Univ. Leiden* 1546 (1921)
4. SCOTT, R. B., and BRICKWEDDE, F. G. *J. Res. nat. Bur. Stand.* (1937)
5. BARTHOLOMÉ, E. *Z. phys. Chem.* **B33,** 387 (1936)
6. JOHNSTON, H. L., KELLER, W. E., and FRIEDMAN, A. S. *J. Amer. chem. Soc.* **76,** 1482 (1954)
7. VAN ITTERBEEK, A., VAN DAEL, W., and COPS, A. *Physica* **27,** 111 (1961)
8. SIMON, F., and LANGE, F. *Z. Phys.* **15,** 312 (1923)
9. EUCKEN, A. *Nachr. Ges. Wiss. Göttingen*

The Calculation of Temperature Differences from Resistance Thermometer Measurements using a Digital Computer

L. J. Challis *Department of Physics, University of Nottingham*

Received 12 May 1961

CARBON resistance thermometers have been used extensively in the measurement of thermal conductivities in the temperature range below 4·2° K and, more recently, they have been used to measure Kapitza resistances. The calculation from the resistance thermometer data of the differences in temperature involved can be very laborious and in recent experiments carried out in this laboratory in which a large number of measurements of both thermal conductivity and Kapitza resistance were made, the calculations were programmed for a digital computer. The thermometers used were 33 Ω, $\frac{1}{4}$ W, LAB radio resistors with resistances of approximately 160 Ω at 4·2° K and 1,400 Ω at 1·2° K. The programme is being used successfully in the present experiments in which measurements are made in the temperature range 1·2–2·2° K and has also been used to examine the data obtained in previous experiments throughout the range 1·2–4·2° K. In the latter case, in one experiment the programme was applied separately in the ranges 1·2–2·1°, 2·1–4·2° K, and in a second experiment, 1·2–2·5°, 2·5–4·2° K. It seems likely that the programme could be used with these or with similar thermometers in any restricted temperature range below 4·2° K.

In the present work, the temperature differences are determined by measuring the resistance of one thermometer and the difference in resistance between the two. This procedure, which seems to have been first used by Mendelssohn and Renton[1] and Fairbank and Wilks[2] and is now common practice, reduces the error caused by drifts in the mean temperature of the two thermometers which could be appreciable in other methods. The difference in resistance changes rapidly with the difference in temperature while remaining relatively insensitive to changes in the absolute temperatures. It will be seen in the following analysis that the two thermometers should be an approximately 'matched' pair; that is that the rate of change of resistance with temperature should be approximately the same for both thermometers. The thermometers are calibrated against the vapour pressure of a helium bath by making the two measurements when the thermometers are both in thermal equilibrium with the bath.

The expression for the temperature difference between the two thermometers is readily found. We denote quantities characteristic of the first and second thermometers by the suffixes 1 and 2. Measurements of the resistance, R_1, and the difference in resistances, R_{12}, are made when the thermometers are at temperatures T_1 and T_2. We denote the mean temperature by T_0 and the difference in temperature by T_{12}. Hence

$$R_{12} = R_1 - R_2 \qquad \ldots (1)$$

$$T_0 = \tfrac{1}{2}(T_1 + T_2) \qquad \ldots (2)$$

$$T_{12} = T_1 - T_2 \qquad \ldots (3)$$

Now

$$\begin{aligned} R_1(T_1) = {} & R_1(T_0) + (T_1 - T_0)(\mathrm{d}R_1/\mathrm{d}T)_{T_0} + \\ & + \tfrac{1}{2}(T_1 - T_0)^2(\mathrm{d}^2R_1/\mathrm{d}T^2)_{T_0} + \\ & + \tfrac{1}{6}(T_1 - T_0)^3(\mathrm{d}^3R_1/\mathrm{d}T^3)_{T_0} + \\ & + \ldots \end{aligned}$$

$$\begin{aligned} R_2(T_2) = {} & R_2(T_0) + (T_2 - T_0)(\mathrm{d}R_2/\mathrm{d}T)_{T_0} + \\ & + \tfrac{1}{2}(T_2 - T_0)^2(\mathrm{d}^2R_2/\mathrm{d}T^2)_{T_0} + \\ & + \tfrac{1}{6}(T_2 - T_0)^3(\mathrm{d}^3R_2/\mathrm{d}T^3)_{T_0} + \\ & + \ldots \end{aligned}$$

Subtracting and substituting equations (1), (2), and (3) gives

$$\begin{aligned} R_{12} = {} & R^{\circ}_{12} + T_{12}(\mathrm{d}R_1/\mathrm{d}T - \tfrac{1}{2}\mathrm{d}R^{\circ}_{12}/\mathrm{d}T)_{T_0} + \\ & + \tfrac{1}{8}T_{12}^2(\mathrm{d}^2R^{\circ}_{12}/\mathrm{d}T^2)_{T_0} + \\ & + \tfrac{1}{24}T_{12}^3(\mathrm{d}^3R_1/\mathrm{d}T^3 - \tfrac{1}{2}\mathrm{d}^3R^{\circ}_{12}/\mathrm{d}T^3)_{T_0} + \\ & + \ldots \end{aligned}$$

where $R^{\circ}_{12} = R_1(T_0) - R_2(T_0)$

When all but the first three terms are negligible,

$$T_{12} = (R_{12} - R^{\circ}_{12})/(\mathrm{d}R_1/\mathrm{d}T - \tfrac{1}{2}\mathrm{d}R^{\circ}_{12}/\mathrm{d}T)_{T_0} \qquad \ldots (4)$$

For any pair of thermometers, the range of T_{12} may be determined over which expression (4) is an adequate approximation and we shall assume in this treatment that the temperature differences are all within this range. (For one pair used in the present work, the maximum value of T_{12} for which the error is less than 1 per cent is 0·28° K at $T_0 = 2{\cdot}1°$ K and 0·10° K at $T_0 = 1{\cdot}2°$ K.)

It is seen that apart from the measured quantity R_{12}, the mean temperature T_0 is required and then the values of

R°_{12}, dR_1/dT, and dR°_{12}/dT at this temperature. The calibration measurements provide values of R_1 and R°_{12} at temperatures throughout the complete temperature range so that once T_0 is known, R°_{12} may be found by interpolation and the gradients dR_1/dT and dR°_{12}/dT may be determined. The other measured quantity R_1 is used to obtain the temperature T_1 of one thermometer.

The interpolation formulae

The calibration points are used to obtain formulae for R_1 and R°_{12} as functions of temperature. It is known that the expression

$$T = A/(R_1-R_0)+B \qquad \ldots(5)$$

where A, B, and R_0 are constants which vary slightly between experiments, can be made to agree with the calibration data for certain carbon resistances over restricted temperature ranges (Montgomery,[3] Lounasmaa[4]). The expression has the advantage that it can be readily transformed to give $R_1 = f(T)$. In the present work, the agreement at the calibration points has been satisfactory. For example, in the most recent experiment this formula was fitted to eight points in the temperature range 1·35–2·15° K. The root mean square deviation at the calibration points was $2{\cdot}3\times10^{-3}$ °K, of which part may be due to errors in calibration.

A quadratic expression

$$R^\circ_{12} = C+D/T+E/T^2 \qquad \ldots(6)$$

can be made to give reasonable agreement with the calibration data. An error in R°_{12} of δR°_{12} gives rise to an error in the temperature difference of

$$\delta R^\circ_{12}/(dR_1/dT-\tfrac{1}{2}dR^\circ_{12}/dT)_{T_0}$$

and, in the most recent experiment, the root mean square value of this error in temperature difference computed at the calibration temperatures was for one pair of thermometers about 5×10^{-4} °K and for the other pair about 6×10^{-4} °K. The errors due to inaccuracies in the measurement of R°_{12} are in general smaller than these values.

The programme

The first chapter of the programme is concerned with the reading in of the experimental values and with the determination of the best values of the constants in the interpolation formulae. The expression for T is written as

$$T = A_i/(R_1-\Delta-2i)+B_i$$

where Δ is a constant chosen from experience to be less than the smallest value of R_0 expected. The values of A_i and B_i are calculated to give the best fit with the calibration data using the method of least squares for each of the range of integral values of i; $0\leqslant i\leqslant 14$. The optimum value of i and hence of A_i and B_i is found by taking the minimum value of the sum of the squares of the deviations of T at the calibration points. The constants in the expression for R°_{12} are found by the method of least squares; the simultaneous equations are solved by the usual method of evaluating the determinants. The values of the constants in the two expressions and also the calculated values of T and R°_{12} at the calibration points are given in the output to the programme.

The second chapter is used to calculate the value of T_{12} from expression (4). As the mean temperature T_0 is unknown, the method of successive approximations is used. The value of T_1 is obtained from the measured value of R_1 using expression (5), and dR_1/dT, R°_{12}, and dR°_{12}/dT are evaluated at T_1 by substituting in expressions (5) and (6) or their differentials. An approximate value, T'_{12}, is then obtained by substituting these quantities into expression (4). These three quantities are next evaluated at temperature $T_1-\frac{1}{2}T'_{12}$ to give a closer approximation T''_{12}. The procedure is repeated twice further to give the final values which are close approximations to T_{12} and T_0. The final value, T_{12}, is multiplied by the appropriate form factor.

In the present work, simultaneous measurements are made of Kapitza resistance and thermal conductivity. Three thermometers are used and the temperature differences between the middle thermometer, R_1, and the other two, R_2, R_3, are found as described above. The constants in expression (6) are evaluated for both R°_{12} and R°_{13}. The programme is written in 'Autocode' for the Ferranti digital computer 'Mercury'. In a typical experiment in which 120 temperature differences were measured, the total computer time was six minutes of which less than one minute was spent in calculation and the rest in punching the output tape. For each temperature difference, the printed output gives the values of T_{12} obtained at each stage in the calculation so that the rate of convergence on to the final value can be observed. The output also gives the final values of R°_{12}, dR_1/dT, $dR_1/dT-\frac{1}{2}dR^\circ_{12}/dT$, T_0, T_{12}, and fT_{12}, where f is the appropriate form factor.

Accuracy of the method

The accuracy of a temperature difference computed in this way is governed principally by the success of the interpolation formulae provided that the difference is within the range in which expression (4) may be said to apply. In the present experiments, the expression used for R°_{12} gives rise to errors of the order of 5×10^{-4} °K so that if temperature differences of less than 5×10^{-2} °K are to be measured, the errors introduced in this way are not negligible. For these small differences an improvement is obtained by using a value for R°_{12} in expression (4) which has been interpolated graphically. A corrected value of T_{12} can be readily found using the computed value of $dR_1/dT-\frac{1}{2}dR^\circ_{12}/dT$ given in the output to the programme. However, for many purposes, the computed values of T_{12} are of sufficient accuracy if T_{12} is greater than about 2×10^{-2} °K.

For the thermometers used, $\frac{1}{2}dR^\circ_{12}/dT \ll dR_1/dT$ and it can be shown that the errors in the denominator of expression (4) are very nearly equal to those in dR_1/dT. An estimate of these can be made by considering successive calibration points. If we consider two such points T' and

T'' with resistance values R_1' and R_1'' then an average value of $\mathrm{d}R_1/\mathrm{d}T$ in this temperature interval is

$$(R_1' - R_1'')/(T' - T'')$$

The values of temperature calculated from expression (5) corresponding to R_1' and R_1'' may be denoted by T_c' and T_c'' and so the calculated average value is $(R_1' - R_1'')/(T_c' - T_c'')$. The percentage difference between these two is approximately $100[(T' - T'') - (T_c' - T_c'')]/(T' - T'')$. The root mean square value of this quantity in the most recent experiment was 2·8 per cent and this represents a rough estimate of the average error in $\mathrm{d}R_1/\mathrm{d}T$.

This estimate does not take into account the errors in obtaining the calibration points. However, since it is thought that these contribute to the differences between T and T_c, the actual error in the denominator may be less than 2·8 per cent. There is a further cause for error in the values used for both $(\mathrm{d}R_1/\mathrm{d}T)_{T_0}$ and $\overset{\circ}{R}_{12}$ due to the error in T_0 (of the order of $2{\cdot}3 \times 10^{-3}$ °K in the most recent experiment). These errors can, however, be shown to be negligible compared with the errors in these quantities from the other causes discussed above.

These estimates suggest a root mean square error of about 4 per cent in temperature difference provided that it lies within a certain range (e.g. for $T_0 = 1{\cdot}7°$,

$$0{\cdot}05° < T_{12} < 0{\cdot}20°\,\mathrm{K})$$

This figure is comparable with the errors obtained by workers using other methods. The relative errors between two values of T_{12} when T_0 is approximately the same for both is, however, considerably less than this.

Note added in Proof

The authors's attention has been drawn to a paper on this subject by Wyder (Wyder, P. *Z. angew. Math. Phys.* **11,** 530 (1960)). In his treatment the resistance of each thermometer is fitted separately to the Clement and Quinnel formula (Clement, J. R., and Quinnel, E. H. *Nav. Res. Lab. Reprint* No. 68–52 (1952)). The temperature difference is obtained directly from the temperatures of the two thermometers so that the error is proportional to the sum of the errors in each temperature. The method is, therefore, less accurate than the present one for small differences (perhaps $< 0{\cdot}1°$ K) although it becomes more accurate for large differences.

The author wishes to acknowledge with gratitude the assistance given by the Autocode service of the Manchester University Computing Laboratory in providing computing facilities. He would also like to thank Professor L. F. Bates, F.R.S., for the use of the facilities in his laboratory, and Mr. R. M. Bull, Mr. W. K. Griffiths, and Dr. P. M. Rowell for most useful discussions during the writing of the programme. The experimental work is being supported by a grant from the Department of Scientific and Industrial Research.

REFERENCES

1. Mendelssohn, K., and Renton, C. A. *Proc. roy. Soc.* **A230,** 157 (1955)
2. Fairbank, H. A., and Wilks, J. *Proc. roy. Soc.* **A231,** 545 (1955)
3. Montgomery, H. *Thesis* (Oxford, 1956)
4. Lounasmaa, O. V. *Phil. Mag.* **3,** 652 (1958)

Some Thermal and Magnetic Properties of Tantalum, Niobium, and Vanadium at Helium Temperatures

A. Calverley *Services Electronics Research Laboratory, Baldock*

K. Mendelssohn and P. M. Rowell *Clarendon Laboratory, Oxford*

Received 10 March 1961

PREVIOUS measurements of the thermal conductivity of these metals have been made in both the superconductive and normal state between 2 and 4° K by Mendelssohn and Olsen[1] and Rosenberg.[2] Inconsistent results have been reported for the critical field values and this agrees with the conclusions that the superconductive properties of these elements are strongly dependent on the method by which the specimens are prepared. All these metals have high melting points and also rapidly absorb gaseous impurities when heated.

This systematic investigation of these three superconductors was stimulated by the rather surprising difference which had been observed between two tantalum specimens.[3] One of these was polycrystalline while the other was a zone refined single crystal. The zone refining technique has been extended to niobium and vanadium and the same behaviour was then observed for each metal. The underlying mechanisms responsible for this behaviour are comparable with those in similar measurements on lead and a lead alloy reported in another paper.[4] Some of the present results have been summarized earlier.[5]

Preparation of the specimens

The single crystal specimens were obtained by the floating-zone melting[6] of polycrystalline rods of the various metals. This was done in a vacuum of better than 10^{-4} mbars, using electron bombardment heating to produce the molten zone.[7] The apparatus used has been fully described elsewhere.[8]

It was observed that the first specimen, $\mathrm{Nb_I}$, had slip lines on its surface. These were caused by stress in the crystal as it cooled after the final zone melting pass was complete, both ends being held by chucks. Consequently, with $\mathrm{Nb_{II}}$, $\mathrm{V_I}$, and $\mathrm{V_{II}}$, the specimens were deliberately parted at the final molten zone so that they cooled with no restraint other than their own weight. $\mathrm{V_{II}}$ was prepared in an improved zone melting apparatus[9] which became available during the course of this work.

Purity of the specimens

The zone travel speeds used in preparing the specimens were faster than the slow speeds required for the impurity segregation normally obtained with zone refining.[10] The purity of the specimens is therefore attributed to the comparatively high purity of the starting material, to the out-gassing of the molten metal, and to the preferential evaporation of lower melting point impurities.

Complete analyses of the specimens were not obtainable, but Tables 1 and 2 give the major impurities detected by spectrographic and gas analysis. The diamond pyramid hardness number (d.p.n.), Table 3, is a measure of the impurity, particularly of the presence of interstitial impurities such as oxygen, nitrogen, and carbon. The very high hardness figures of the vanadium samples show them to have high carbon and gas content.

Method and results

All the measurements of thermal conductivity to be presented in this section were made using the apparatus described by Montgomery.[11] Critical field measurements on tantalum were also made using the same cryogenic

Table 1. Main Impurities (per cent (wt)) in the Polycrystalline Rods before Zone Melting

Niobium		*Vanadium*		*Tantalum*	
Ta	0·1	Fe	0·09	Nb	0·1
Si	0·02	Y	0·41	C	0·01
Fe	0·01	Si	0·01	Fe	0·01
Sn	0·005	N	0·08	W	0·01
Ni	0·001	O	< 0·01	Mo	0·01
Ca	0·0003	C	0·05	O	0·001
Cu	0·0002			N	0·00075
Mn	0·0001			H	0·00045
Na	0·0001				
Mg	< 0·0001				
K	< 0·0001				

Table 2. Impurity Content (per cent (wt)) in the Zone Melted Single Crystal Specimens

	Nb_I	Nb_{II}		V_I	V_{II}		Ta_I
Cu	0·0003	0·0003	Fe	0·2	0·05	Fe	0·005
Mg	0·0003	0·0003	Si	0·02	0·01	Si	0·003
			Cu	0·005	0·0003	O	0·0003
			Ti	0·002	Not detected	H	0·00025
			Mo	0·002	0·005	N	Not detected
			Mn	0·01	0·0005		

Table 3. Diamond Pyramid Hardness Number of the Single Crystal Specimens

Specimen	*Hardness (d.p.n.)*
Nb_I	75
Nb_{II}	66
V_I	185
V_{II}	160
Ta_I	75

technique, but for niobium a Simon expansion liquefier was used in which a slow expansion of helium produced temperatures between 4 and 10°K.[12]

The method of Keeley and Mendelssohn[13] for the determination of critical fields was used to measure the flux changes in the rod-shaped specimens. A small search coil was wound directly on to the centre of the specimen which was in thermal contact with a constant temperature bath. This search coil was connected to a sensitive galvanometer. A longitudinal external magnetic field is established and when it is removed a deflection is observed which is directly proportional to the change in magnetic flux passing through the search coil. When the specimen is totally superconductive a small deflection is due to the flux in the inevitable air gap between the search coil and the specimen. As the field is increased, a point is reached where the specimen begins to become normal and the deflections rapidly increase until the whole of the specimen is in the normal state. Besides giving a value of the critical field required to destroy superconductivity, this method also gives an indication of the sharpness (or otherwise) of the transition. It further shows the amount of flux (usually termed 'frozen-in flux') which is not expelled from the specimen when a super-critical field is removed. The magnetic fields used in measuring the tantalum critical field curves were obtained using a simple air cooled solenoid. As this was wound on a brass former and the currents used to activate it were small, they could be easily switched off. However, for niobium, fields of up to 5,000 oersteds were required and the geometry of the apparatus was such that the only practicable method was to obtain the field with an iron cored electromagnet which was then pulled away from the apparatus whenever a flux change was required. This eliminated the difficulties of switching off large fields in such a magnet and also any errors due to the remanent magnetism in the iron core of the magnet.

Tantalum

Thermal conductivity. In Figure 1, the results of the measurement of the thermal conductivities of both a polycrystalline and a monocrystalline specimen of tantalum are presented. The polycrystal had already been measured by Rosenberg[2] down to 2°K and the results agree in the common temperature range.

The thermal conductivity in the normal state, K_n, in both cases is a roughly linear function of temperature† as is expected in a metal where the heat is carried by conduction electrons which are scattered predominantly by point imperfections.

The relation between the residual electrical resistance ρ_0 and the thermal conductivity K_n is valid in this range

$$K_n = \frac{L_0 T}{\rho_0}$$

where L_0 is the Lorenz number and T the temperature.

We therefore conclude that the monocrystal is considerably purer than the polycrystal, and it was found that the two specimens had residual resistance ratios (i.e. the ratio of room temperature resistance to the residual resistance) of 63 and 31, respectively.

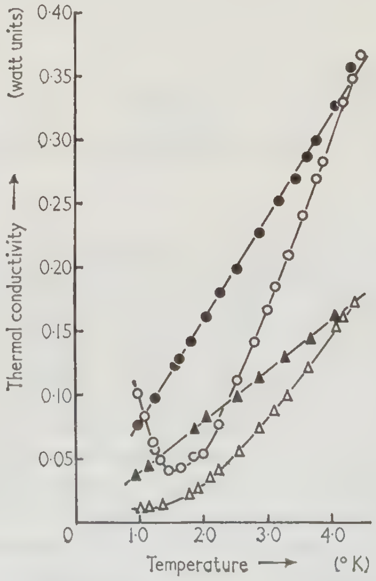

Monocrystal: ● Normal state ○ Superconducting state
Polycrystal: ▲ Normal state △ Superconducting state

Figure 1. Thermal conductivity of tantalum

---

† In these as well as in Rosenberg's results there are small, and unexplained, deviations from linearity which merit further investigation.

In the superconductive state the conductivity, K_s, of the polycrystal drops progressively below its value in the normal state but at the lowest temperatures the curve does not appear to be falling monotonically to zero at $T=0$.

This deviation from the behaviour to be expected from theory[14, 15] is more clearly shown in Figure 2, where the reduced conductivity K_s/K_n is plotted against the reduced temperature T/T_c. The results are compared with the semi-empirical function of Bardeen et al.[15]

It can now be seen that below $T/T_c = 0{\cdot}4$ the behaviour diverges rapidly from approximate agreement with the theoretical predictions.

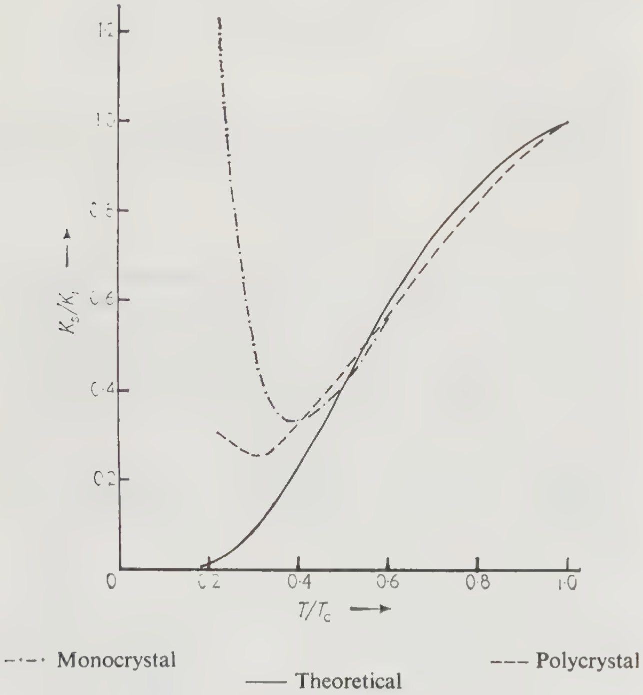

Figure 2. Reduced thermal conductivity of tantalum

On measuring K_s for the monocrystal it was found that again the value fell below K_n at T_c, but at about 1·6° K the curve passes through a minimum and at 1·0° K K_s is greater than the corresponding value of K_n. This behaviour is shown more clearly in Figure 2.

These results can be accounted for by taking into account the effect of thermal conduction by phonons. For a normal metal, conduction of heat by lattice vibrations is only a small fraction, at most, of the total conduction, due to the strong interaction of these waves with the conduction electrons. In a superconductor an increasing density of electrons is found in the superconducting ground state[15] and so they do not interact with phonons. Hence we might expect an increasing fraction of the conduction to be due to the latter. This effect is more noticeable as with decreasing T/T_c conduction of heat by electrons in excited states becomes very small. At the lowest temperatures one would expect heat conduction to be predominantly by phonons giving behaviour similar to that found in dielectric crystals and this is in fact observed.[11, 16, 17]

The main mechanisms for the scattering of lattice waves in this region are crystal boundaries, internal grain boundaries, and dislocations,[18] which can explain the difference in K_s for the two specimens. The first, being an unannealed polycrystal, had large numbers of grain boundaries and dislocations, but the second, being a carefully prepared monocrystal, was comparatively free of grain boundaries and had a much smaller density of dislocations. In this case the magnitude of conduction by lattice waves predominates below $T/T_c = 0{\cdot}4$. Since the theoretical curve referred to above only takes into account electron conduction, additional phonon conductivity must lead to a departure towards higher values of K_s/K_n.

Thermal resistance in the intermediate state. For any situations other than a long cylinder in a longitudinal field the destruction of superconductivity occurs over a range of magnetic fields. In this intermediate region the specimen breaks up into a structure which is a mixture of normal and superconducting regions and which has been explored magnetically by Meshkovsky and Shalnikov[19] and Schawlow et al.[20]

The thermal resistance of cylindrical specimens in the intermediate state at sufficiently low temperatures usually passes through a maximum as a transverse field is increased.[1] In the higher temperature range where conduction is predominantly by excited state electrons the situation resembles that described by Landau[21–23] who predicted a simple linear fall in the electrical resistance to which should correspond a similar fall from W_s (the thermal resistance of the superconductive sample) to W_n (the thermal resistance of the normal sample). At low temperatures, in particular, it seems that the maximum in the thermal resistance is in some way connected with the conduction by lattice waves. In fact, at very low temperatures it is only the lattice conduction which is sufficiently large to suffer appreciable reduction. A systematic investigation of this effect has recently been made on tin–indium alloys by Mendelssohn and Shiffman[24] who have discussed it in detail.

In Figure 3, the variation of thermal resistance in the intermediate state for the tantalum specimen is shown at three temperatures. At 2·0° K the transition from the normal to superconducting resistance is linear with increasing field, the effect of frozen-in flux causing a lag in the return path as the field is reduced. However, as the temperature was reduced below 2·0° K a maximum in resistance is observed which increases in magnitude with decreasing temperature. The curve at 1·1° K is particularly interesting as it is at this temperature that the resistances in the normal and superconducting states are equal.

Critical field measurements. The thermodynamic analysis of the relation between H_c and T_c (the field at which superconductivity is destroyed and the corresponding temperature) predicts a parabolic relation if the specific heat in the superconducting state has a cubic dependence on temperature. Various workers have reported deviations from this parabolic form in most superconductors. This is now ascribed to the fact that the superconducting specific heat has an exponential dependence on temperature.[14]

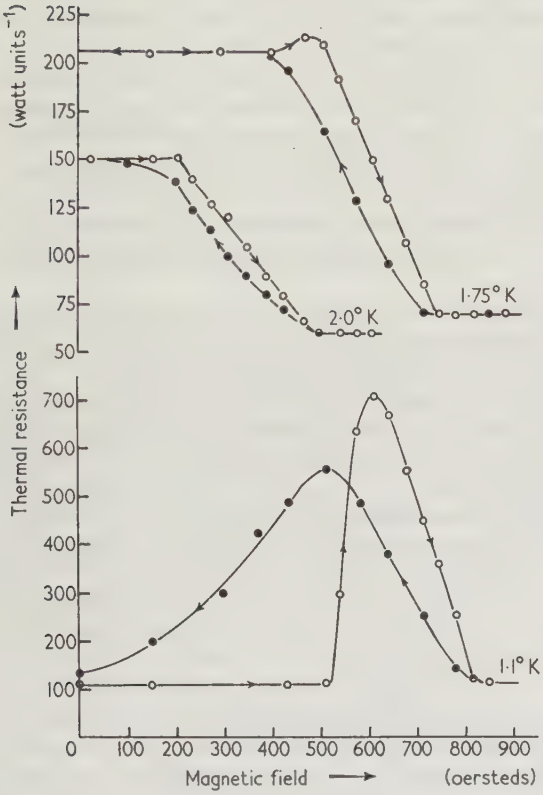

○ Increasing transverse field ● Decreasing transverse field

Figure 3. Thermal resistance of the tantalum monocrystal in the intermediate state

The results obtained for the tantalum monocrystal are presented in Figure 4 from which a critical temperature of 4·32 ± 0·02° K has been determined. The transitions in a magnetic field were found to extend only over a range of about 15 oersteds at the highest fields and the points in Figure 4 correspond to the field at the centre of the transition. The amount of frozen-in flux observed at the highest fields was less than 7 per cent of the total flux.

The value of T_c for this specimen was slightly lower than that reported for their purest sample by Budnick, Ittner, and Seraphim.[25] Deviations from the parabolic form of the curve were found to be almost the same as those observed for the same material, from specific heat data, by Corak and Satterthwaite.[26]

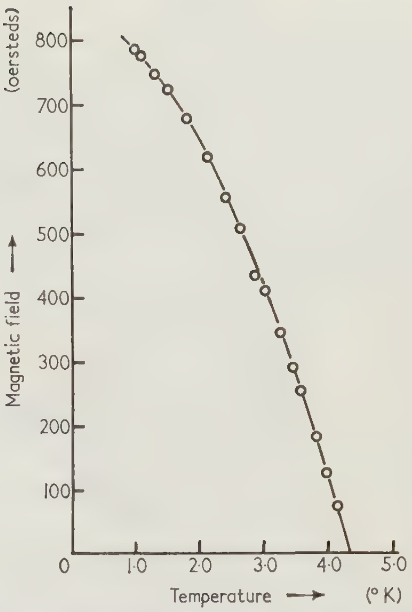

Figure 4. Critical field curve of the tantalum monocrystal

Niobium

Thermal conductivity. The thermal conductivity of the two niobium crystals is shown in Figure 5. In the normal state the conductivity is found to be a linear function of temperature and it can be seen that the second crystal was more free of point defects than the first which was to be expected from a consideration of the method of preparation.

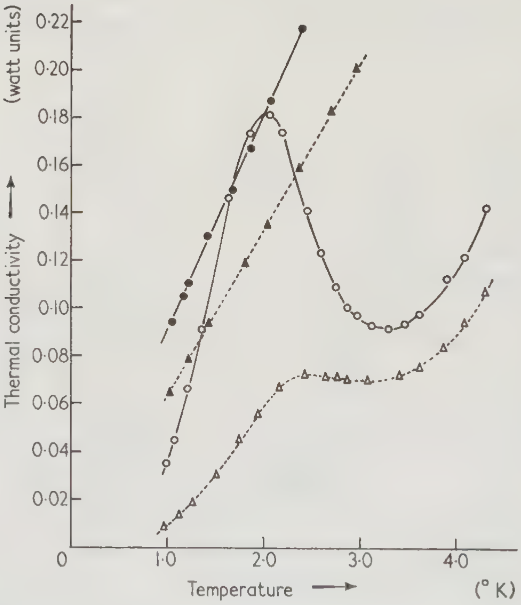

Monocrystal I: ▲ Normal state △ Superconducting state
Monocrystal II: ● Normal state ○ Superconducting state

Figure 5. Thermal conductivity of niobium

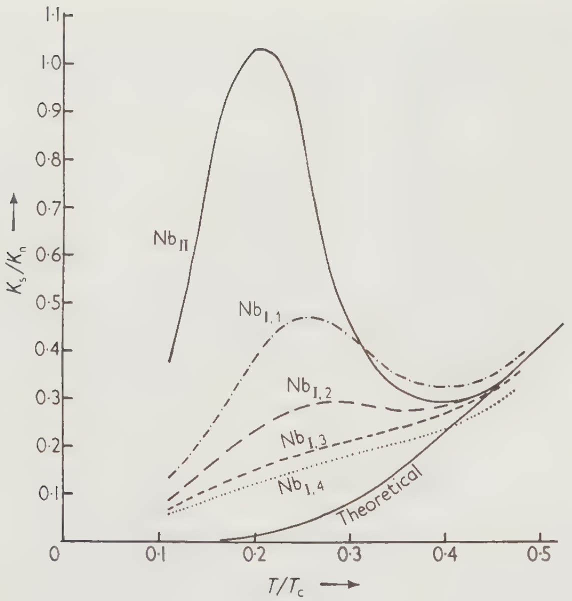

Figure 6. Reduced thermal conductivity of niobium

In the superconductive state the conductivities both have a similar form. At 4°K the conductivity has fallen well below its value in the normal state but it then passes through a minimum at 3·2°K and comes to a maximum near 2°K after which it falls rapidly with decreasing temperature. The first specimen showed these features less distinctly, but the second had a pronounced minimum after which the conductivity rose rapidly to a value just higher than that in the normal state near 2°K. In both cases at the lowest temperatures K_s was proportional to T^3.

Figure 6 shows the reduced conductivity plotted against the reduced temperature for both the specimens and also for the specimen I after it had been strained[4, 5] by increasing amounts ($Nb_{I,1}$–$Nb_{I,4}$). These curves are compared with the semi-empirical function.[15] The most carefully prepared crystal Nb_{II} shows the largest divergence from purely electronic behaviour which is in accordance with the view that this crystal had fewer grain boundaries and dislocations than Nb_I. This latter crystal after being strained shows a variation of reduced conductivity which more nearly approaches the theoretical predictions with increasing strain. These curves give a good illustration of the way in which phonon conduction can be reduced by increasing the density of dislocations in the crystal.

Thermal resistance in the intermediate state. Mendelssohn and Olsen[1] have reported measurements of the thermal resistance of niobium in the intermediate state but their specimen was a polycrystal of relatively poor purity.

In Figure 7 the conductivity of the second specimen is shown at three temperatures as a transverse magnetic field was first applied and then removed.

The general shape of the curves in increasing fields is very similar to that obtained for tantalum with the resistance maximum being more pronounced the lower the temperature. The large resistance observed after removal of the field can be attributed to the effect of a large amount of frozen-in flux which might also explain

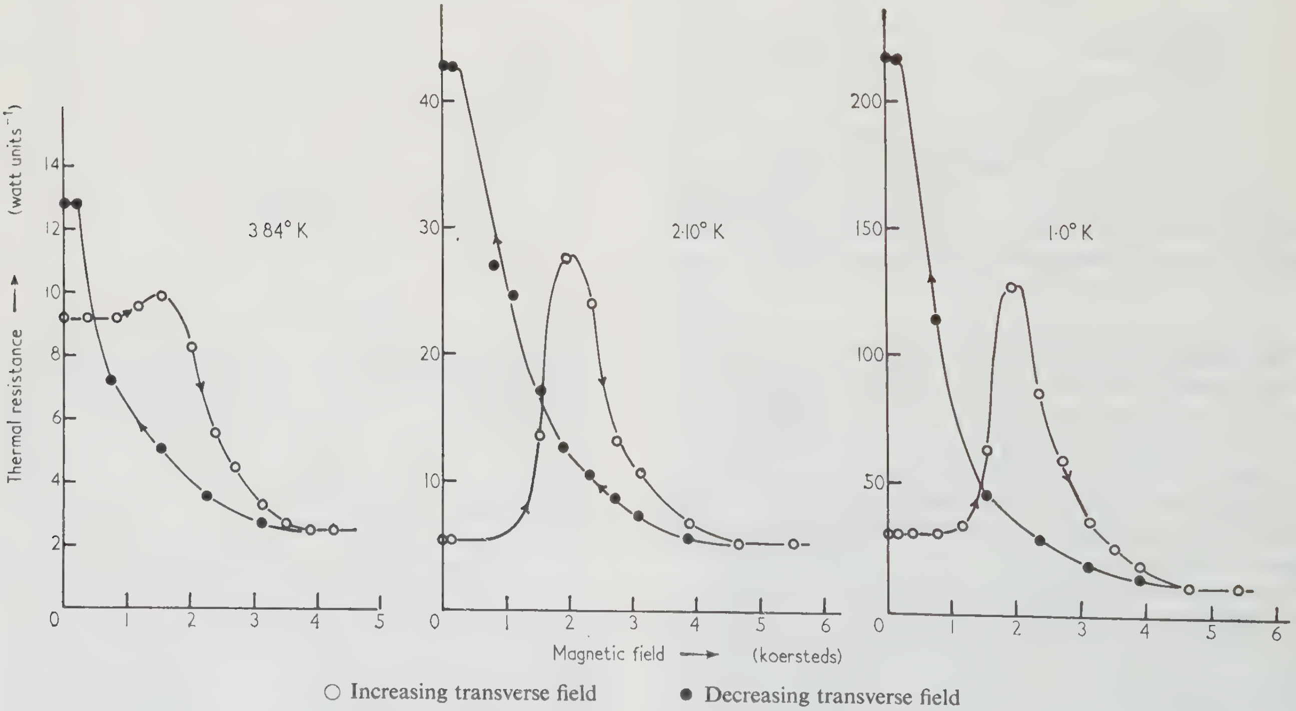

Figure 7. Thermal resistance of Nb_{II} in the intermediate state

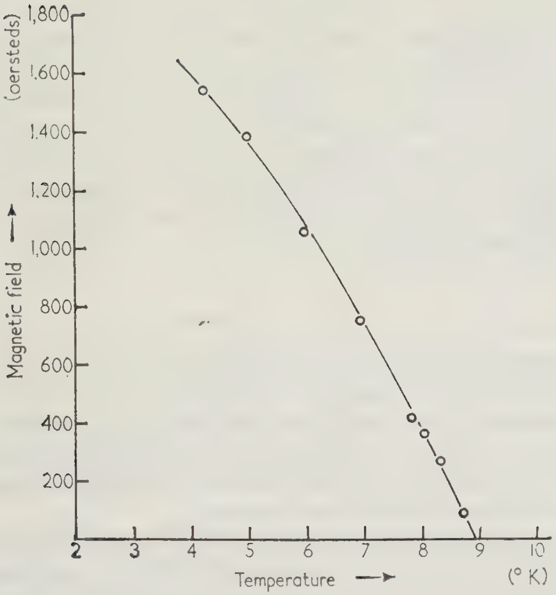

*Figure 8. Critical field curve of Nb*II

why the resistance in decreasing fields at 1° K does not show any suggestion of a maximum similar to that observed in tantalum at 1·1° K. This frozen-in flux causes increased scattering of phonons when the field is removed as indicated by the very high thermal resistance observed after the cycle at 1° K.

Critical field measurements. An attempt was made to obtain the critical field curve for the second niobium specimen, but the results are subject to rather large uncertainties due to difficulty in keeping the temperature constant while using the apparatus referred to above,[12] and also due to the very large range of field over which the transition occurred.

The results were obtained using the same method as for tantalum which showed that as the temperature was reduced the transition became increasingly extended until at 4° K it was still incomplete in fields 2,000 oersteds higher than that required to initiate the transition. For this reason the critical field values plotted in Figure 8 correspond to that field which just penetrates the specimen. Using these results the transition temperature T_c in zero field was found to be $9{\cdot}0 \pm 0{\cdot}1$° K. Table 4 gives a brief summary of the values of H_0, the extrapolated critical field at $T = 0$ and T_c obtained by various workers.

Vanadium

Thermal conductivity. Vanadium was the third and last of these hard superconducting metals to be studied and, as was noted above, it proved to be the most difficult to prepare in a pure monocrystalline state. Two attempts were made which resulted in two monocrystals (in so far as visual inspection could show this) and their thermal conductivities are compared in Figure 9 with that of a severely work-hardened polycrystalline specimen of the same material.

Table 4

Workers	*Method*	*State of sample*	T_c (°*K*)	H_0 (*gauss*)
Daunt and Mendelssohn[30]	Magnetic (a.c. inductance)	As received	8·4	2,600
Jackson and Preston-Thomas[31]	Magnetic (a.c. inductance)	As received	8·85 8·35	
Cook et al.[32]	Magnetic	Vacuum annealed 1,000° C	8·55 transition 0·15° wide	8,050
Brown et al.[33]	Calorimetric	Annealed, strain free	8·7 ± 0·1	2,000
Chou et al.[34]	Calorimetric	Annealed 8 hr 1,200 to 1,600° C	9·07	4,760
		Annealed 20 hr 1,450 to 2,100° C	9·17	3,370
		Annealed 8 hr 2,100° C	9·17	3,370
These measurements	Magnetic	Monocrystal II	9·0 ± 0·1	1,980 ± 60 (wide transitions)

Considering first the results in the normal state it was found that application of a field of 4,600 oersteds (approximately four times the value of the generally accepted critical field at 0° K) gave a straight line relation for K_n down to about 3·5° K for the polycrystal, but below this temperature the results fell increasingly below the expected values. It was found that this could be eliminated by applying a field of 6,200 oersteds which suggests that a field of 4,600 oersteds is not sufficient to maintain the normal state in the polycrystalline specimen. The normal conductivity of the two monocrystals indicates that in the preparation of the monocrystal I the chemical purity has been decreased as the resistance ratio compared with the polycrystal had fallen from 18·2 to 13·8. This result led to an attempt at producing a purer

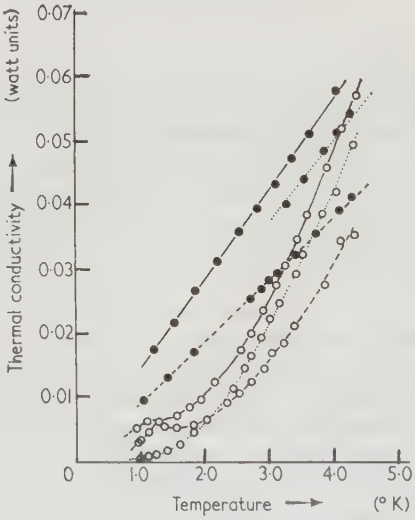

— Monocrystal I --- Monocrystal II .... Polycrystal
● Normal state ○ Superconducting state

Figure 9. Thermal conductivity of vanadium

crystal in a re-designed apparatus, and the monocrystal II was the result. This had a slightly greater purity than the original material, the resistance ratio having risen to 20·2.

In the superconductive state, the results (Figure 9) for the polycrystal are very similar to those obtained for the tantalum polycrystal.

Although K_s for the monocrystal I was lower than that for the polycrystal at 4° K, where the chemical purity governs the conductivity, a maximum was observed when the temperature was lowered to 1·2° K, the conductivity becoming greater than that of the polycrystal.

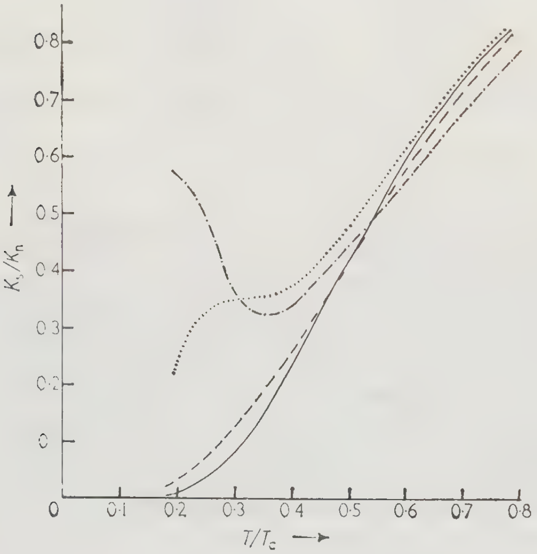

Monocrystal I —·—· Monocrystal II
--- Polycrystal —— Theoretical

Figure 10. Reduced thermal conductivity of vanadium

On plotting the reduced conductivities (Figure 10) the behaviour is more clearly seen and the curves may also be compared with the theoretical one.[15] The cold-worked polycrystal shows the closest agreement with theory and diverges very little from this form even at the low temperature end. However, both the monocrystals show marked divergences below a reduced temperature of 0·5° K.

It came as a disappointment to find that the second monocrystal, which was chemically purer than the first, was not such a good crystal so that, while the conductivity at 4° K was higher than in the other two specimens, at 1° K the conductivity fell below that of the first monocrystal and only showed a slight deviation from a smooth curve instead of a pronounced maximum.

It would seem, therefore, that in the effort to produce a crystal with less absorbed gases and metallic impurities the crystal lattice had been inadvertently strained during cooling.

Due to the fact that both the vanadium monocrystals had either poor chemical purity or a strained lattice, observations in a transverse field and critical field measurements were omitted. Fields much greater than the approximate transition field had to be applied to destroy superconductivity completely, which leads to the conclusion that the transition from normal to superconducting behaviour would be very broad even at temperatures quite close to T_c.

Discussion

Our observations show that measurements of thermal conductivity of superconductors in the normal and superconducting state can be used to indicate the chemical purity and the physical state of the lattice of a metal crystal, and this method has recently been applied to the effects of radiation damage.[27]

In another paper[4] measurements of the thermal conductivities of superconducting lead and a lead–bismuth alloy were reported. It is interesting to note that increase of strain in the pure lead crystal has very little effect on the height or shape of the maximum in the curve at about 3·5° K. However, similar results using a lead alloy crystal show a maximum at a lower temperature (about 2° K) which is greatly reduced by a small strain. We suggest in the light of the present measurements and those in the earlier paper that the maxima in conductivity observed in the lead alloy, tantalum, niobium, and vanadium specimens are all of the same origin. In all these metals, conduction in the region of the maximum is predominantly by phonons, the number of free electrons in excited states being either very small as for tantalum, niobium, and vanadium or their effects reduced by impurities as in the lead alloy. On the other hand, the maximum observed for the pure lead specimen is relatively unaffected by strain and is probably of the same nature as the maximum which is observed in the normal state where scattering of electrons by lattice waves is decreasing and the scattering by impurities is becoming predominant.

The position in the case of pure lead is further obscured by the anomalous way in which K_s departs from the K_n curve. In all the other cases discussed here, T_c lies below the temperature where K_n has a maximum, which means that the scattering of normal electrons below T_c is by impurities. In pure crystals of lead (and mercury) the onset of superconductivity occurs above the maximum in K_n where the normal electrons are scattered by phonons. The former case is that which is adequately covered by the semi-empirical formulae of Heisenberg and Koppe[28, 29] and of Bardeen and his colleagues,[15] and the observed values for K_s/K_n follow this curve reasonably well above $0{\cdot}5T_c$. This is also evident from Figures 2, 6, and 10. The abrupt departure of K_s from K_n at T_c for lead cannot be explained in this manner and it is interesting to plot the values for the unstrained and the strained lead single crystal in the reduced diagram (Figure 11). We

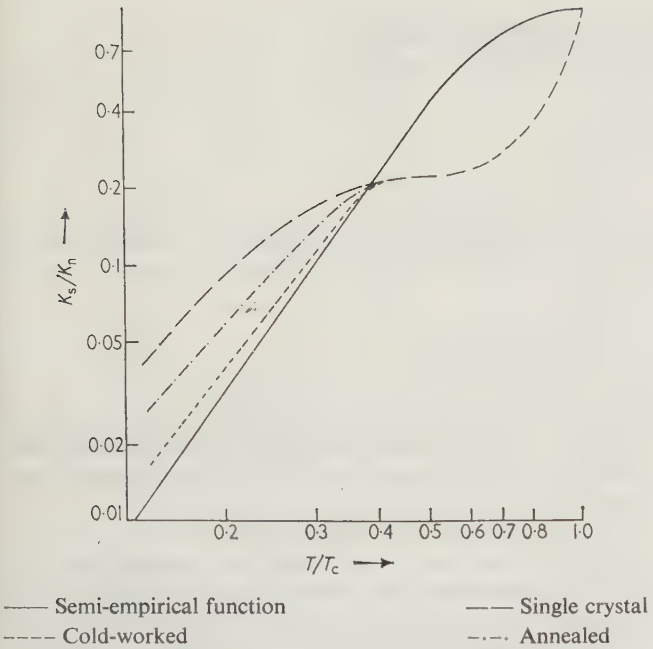

Figure 11. Reduced thermal conductivity of lead

then see that, while there is apparently no agreement in the unstrained case, application of strain brings the experimental and theoretical curves into good agreement below $T/T_c = 0{\cdot}4$. The introduction of strain has reduced the phonon conduction, as could be shown in the case of niobium, and the strained lead specimen is thus behaving below $0{\cdot}4T_c$ as would be expected of a superconductor with electron conduction only. The temperature independent part of the curve between $0{\cdot}4T_c$ and $0{\cdot}6T_c$ evidently corresponds to the region in which the scattering of normal electrons is partly by impurities and partly by phonons. The nature of the maxima in K_s observed in pure lead and mercury is thus quite different from that for the similar looking maxima in tantalum, niobium, and vanadium.

The authors are grateful to Mr. A. R. Powell, F.R.S., of Johnson Matthey and Co. Ltd. for donating the niobium and vanadium. One of us (P.M.R.) wishes to express his thanks to Metropolitan-Vickers Electrical Co. Ltd. for financial support while doing this work.

REFERENCES

1. Mendelssohn, K., and Olsen, J. L. *Proc. phys. Soc. Lond.* **A63,** 2 (1950)
2. Rosenberg, H. M. *Proc. roy. Soc.* **A247,** 441 (1955)
3. Mendelssohn, K. *Canad. J. Phys.* **34,** 1315 (1956)
4. Rowell, P. M. *Proc. roy. Soc.* **A254,** 542 (1960)
5. Mendelssohn, K. *Physica* **24,** 53 (1958)
6. Keck, P., and Golay, M. *Phys. Rev.* **89,** 1297 (1953)
7. Davis, M., Calverley, A., and Lever, R. F. *J. appl. Phys.* **27,** 195 (1956)
8. Calverley, A., Davis, M., and Lever, R. F. *J. sci. Instrum.* **34,** 142 (1957)
9. Birbeck, F. E., and Calverley, A. *J. sci. Instrum.* **36,** 460 (1959)
10. Pfann, W. G. *Trans. Amer. Inst. min. (metall.) Engrs* **194,** 747 (1952)
11. Montgomery, H. *Proc. roy. Soc.* **A245,** 85 (1958)
12. MacDonald, D. K. C., and Mendelssohn, K. *Proc. roy. Soc.* **A202,** 103 (1950)
13. Keeley, T. C., and Mendelssohn, K. *Proc. roy. Soc.* **A154,** 378 (1936)
14. Bardeen, J., Cooper, L. N., and Schrieffer, J. R. *Phys. Rev.* **106,** 162 (1957)
15. Bardeen, J., Rickayzen, G., and Teword, L. *Phys. Rev.* **113,** 982 (1959)
16. Olsen, J. L., and Renton, C. A. *Phil. Mag.* **43,** 946 (1952)
17. Laredo, S. J. *Proc. roy. Soc.* **A229,** 473 (1955)
18. Klemens, P. G. *Solid State Physics,* **7,** 1 (1958)
19. Meshkovsky, A. G., and Shalnikov, A. I. *J. Phys., Moscow* **11,** 1 (1947)
20. Schawlow, A. L., Matthias, B. T., Lewis, H. W., and Devlin, G. E. *Phys. Rev.* **95,** 1344 (1954)
21. Landau, L. D. *Phys. Z. Sowjet.* **11,** 129 (1937)
22. Landau, L. D. *Nature, Lond.* **141,** 688 (1938)
23. Landau, L. D. *J. Phys., Moscow* **7,** 99 (1943)
24. Mendelssohn, K., and Shiffman, C. A. *Proc. roy. Soc.* **A255,** 199 (1960)
25. Budnick, J. I., Ittner, W. B., and Seraphim, D. P. *Physica* **24,** 151 (1958)
26. Corak, W. S., and Satterthwaite, C. B. *Phys. Rev.* **102,** 662 (1956)
27. Chaudhuri, K. D., Mendelssohn, K., and Thompson, M. W. *Cryogenics* **1,** 47 (1960)
28. Heisenberg, W. *Z. Naturf.* **2a,** 185 (1947)
29. Koppe, H. *Ann. Phys., Lpz.* **1,** No. 6, 405 (1947)
30. Daunt, J. G. and Mendelssohn, K. *Proc. roy. Soc.* **A160,** 127 (1937)
31. Jackson, L. C., and Preston-Thomas, H. *Phil. Mag.* **41,** 1284 (1950)
32. Cook, D. B., Zemansky, M. W., and Boorse, H. A. *Phys. Rev.* **78,** 820 (1950)
33. Brown, A., Zemansky, M. W., and Boorse, H. A. *Phys. Rev.* **92,** 52 (1953)
34. Chou, C., White, D., and Johnston, H. L. *Phys. Rev.* **109,** 797 (1958)

Isothermal Flow of Liquid Helium-II in Wide Capillaries

S. M. Bhagat and K. Mendelssohn *Clarendon Laboratory, Oxford*

Received 3 June 1961

THE hydrodynamic properties of liquid helium-II present a complex picture. In thermally induced flow the superfluid exhibits a well defined critical velocity above which non-linear frictional forces appear.[1] These have been explained in terms of turbulence in the superfluid. In isothermal flow the observed behaviour is more complex. In very narrow channels (diameter < 1 micron) the flow rate is only slightly pressure dependent, while in wider channels complex non-linear effects have been reported by Allen and Misener[2] and Atkins.[3] The possibility of turbulence in the superfluid was suggested but no clear demonstration was forthcoming.

About two years ago we made some experiments on gravitational flow in a system consisting of a capillary in series with a 'Vycor' glass filter[4] and found that the flow rates depend upon the 'history' of the experiment in a highly complex manner. The need for a systematic investigation of isothermal flow in wide capillaries thus appeared desirable and the first series of experiments indeed showed that the rates of flow vary with the initial conditions of the experiment.[5]

The present paper is concerned with detailed measurements of gravitational flow in wide capillaries over a wide range of temperatures below the lambda-point. It is shown that, besides the normal viscosity and the mutual friction,[6] it is necessary to introduce a third mechanism involving turbulence in the superfluid in order to explain the observed behaviour.

Method

The experiments were performed in a combined helium liquefier–cryostat.[7] The temperature of the helium bath was controlled manually and measured by a resistance thermometer; it drifted by less than $10^{-4\circ}$ K during a single measurement.

The flow vessel, shown in Figure 1, is suspended in the helium bath. A scale S is mounted on the monitoring tube B which avoids errors due to optical faults in the Dewar walls. The contribution due to film flow is kept small by the constriction O and this was checked by making measurements with the capillary closed.

The observations were made by raising or lowering the flow vessel quickly and then timing the variation in the level in B at intervals of 1 mm. Considering the errors involved in measurement of height and time, the rates of flow could be determined to within 2–3 per cent. In general, some fifty observations were taken at each temperature, bringing the total of flow measurements to about two thousand.

Table 1 gives the details of the capillaries used and their respective reservoirs. The Poiseuille constant ($\pi a^4/8l$), where a is the radius and l the length of the capillary, was determined by measuring the rate of flow of distilled water in Cap. IV and of helium gas in the other capillaries. Comparison of Cap. II with its own segments IIa and IIb indicated that the variation in a^4 along its length amounts to only a few per cent.

The isothermal conditions were well satisfied in all observations. Besides heat transport through the vapour, the copper base of the flow vessel (see Figure 1) provides good thermal contact. The only thermal resistance of importance is the Kapitza[8] boundary resistance at the inner and outer walls of the flow vessel. In the narrowest capillary the normal fluid is more or less immobilized and calculation shows that in our case the mechanocaloric effect will give rise to temperature differences of less than

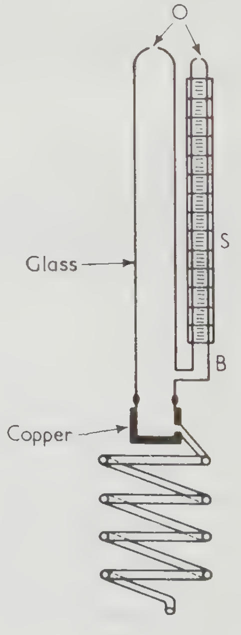

Figure 1. The flow vessel

Table 1

Capillary	*Poiseuille constant (cm³)*	*Length (cm)*	*Approximate internal diameter (microns)*	*Cross-section of flow vessel (cm²)*	*Film correction at 1·3°K (cm/sec)*
Ia	$2{\cdot}156 \times 10^{-12}$	96·6	88	0·0388	0·49
I	$9{\cdot}243 \times 10^{-12}$	33·05	89	0·0785	0·07
II	$1{\cdot}244 \times 10^{-10}$	153·3	297		
IIa	$2{\cdot}686 \times 10^{-10}$	71·0	297	0·2671	0·01
IIb	$1{\cdot}254 \times 10^{-10}$	71·0+ 82·3	297		
III	$1{\cdot}014 \times 10^{-9}$	150·0	499	0·3711	0·003
IV	$3{\cdot}585 \times 10^{-9}$	142·3	676	1·174	0·001

10^{-5}° K. For wider capillaries the mechanocaloric effect is more difficult to estimate but is smaller. The thermomechanical height equivalent of these temperature differences is well below 0·5 mm at the highest temperature at which observations have been taken. This implies an error of about 2 per cent in the velocities for large pressure differences at 2·1° K. At lower temperatures the errors arising from thermal effects are completely negligible.

Some measurements were made to determine whether 'end effects' such as reported by Atkins[3] had any influence on our experiments. Cap. II was cut into two parts. A length of 71·0 cm was used first (Cap. IIa) and later the two pieces were reassembled (Cap. IIb) by joining them together through a short hollow copper cylinder (length and diameter ~ 0·6 cm). There was no difference between the flow rates in Caps. II and IIb although the number of 'ends' had been doubled in the latter case.

Results

Other factors remaining the same, in all experiments the emptying and filling flow rates were identical.

In the long narrow Cap. Ia the mean velocity of flow varies rather slowly with level difference, rising by about 20 per cent as the level difference is increased from 2 mm to 24 mm. Here conditions evidently approach *pure superfluid flow.*

In the other capillaries the observed variation of the level difference h as a function of time can always be expressed by relations of the form

$$\log(h+c) = \gamma t+\beta$$

with c, γ, and β as parameters. It is important to note that all these parameters vary as the initial level difference h_i is altered. The mean velocity of flow can therefore be written as

$$\bar{v} = v_0 - k \operatorname{grad} p \qquad \ldots (1)$$

where both v_0 and k are functions of h_i and $\operatorname{grad} p = (\rho g h/l)$.

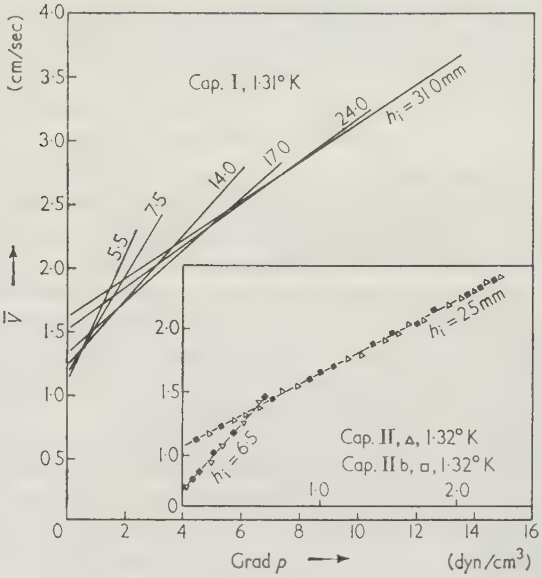

Figure 2. Mean velocity of flow as a function of pressure gradient in Cap. I at 1·32° K, for various values of the initial level difference. Inset, mean velocity of flow in Caps. II and IIb at 1·32° K

Figure 2 shows a typical set of observations (Cap. I, 1·32° K) of the mean velocity $\bar{v}$ as a function of grad p. In addition to the marked dependence of $\bar{v}$ on the initial pressure difference, the results also show a finite intercept on the velocity axis, part of which at least may be due to a critical velocity. The inset in Figure 2 shows two sets of observations in Caps. II and IIb demonstrating that, as mentioned above, end effects do not influence the results.

In classical hydrodynamics the mean velocity of flow of a liquid of viscosity η in a capillary of radius a is given by $(a^2/8\eta)\operatorname{grad} p$. Equation (1) shows that, apart from the

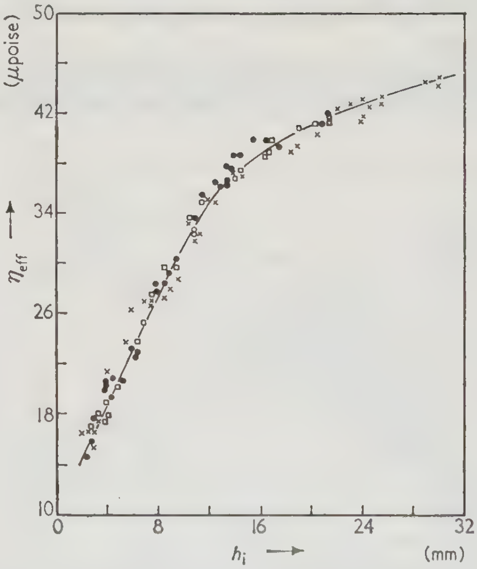

Figure 3. The effective viscosity η_{eff} as a function of h_i for Caps II (●), IIa (×), and IIb (□) at 1·32° K

limiting velocity v_0 and the influence of h_i, the velocity of liquid helium II is also a linear function of grad$p$. It therefore seems useful to define an effective viscosity given by the relation

$$k(h_i) = a^2/8\eta_{\text{eff}} \qquad \ldots (2)$$

with the reservation that the *effective viscosity is not a constant but varies with the initial pressure difference.*

Figure 3 is a plot of η_{eff} as a function of h_i for Caps. II, IIa, and IIb at 1·32° K, Within the limits of experimental error (about 5 per cent) there is no difference between the three sets of results. It may therefore be concluded that firstly h_i, and not h_i/l, is the relevant independent parameter and, secondly, that in this case, η_{eff} is roughly independent of the length of the capillary.

In Figures 4 and 5, values of the effective viscosity are given for the limiting cases of the narrowest and the widest capillaries at a number of temperatures. In all measurements, even in the narrowest tube, η_{eff} is much larger than the value $(\rho_n \eta_n/\rho)$ derived from oscillating disk and viscometer data. For the wide capillaries η_{eff} is, in fact, larger than η_n as measured by Brewer and Edwards.[9] For the narrowest tube η_{eff} increases with rising temperature but this trend is reversed for the other tubes. For all values of h_i, η_{eff} varied in the same manner with tube size, showing a maximum in Cap. III.

Discussion

The features of η_{eff} requiring explanation are, firstly, its magnitude, which is greater than the value $(\rho_n \eta_n/\rho)$ to be expected if the normal fluid alone was contributing, and, secondly, its dependence upon the initial conditions of the experiment. In addition to the normal viscosity the other dissipative process which is known to occur in liquid helium-II is the mutual friction between the normal and superfluid components. However, neither of these can be expected to show any dependence on h_i. Part of the effective viscosity must therefore be attributed to some other mechanism.

The existence of a friction term which is not an intrinsic property of the liquid but depends on the actual conditions of flow is very reminiscent of the eddy viscosity which makes its appearance in classical turbulence.[10] In the range of our experiments there is little possibility of the normal fluid being turbulent because the relevant Reynolds number $(\rho_n v_n a/\eta_n)$ is seldom larger than 500. We therefore conclude that the extra dissipation arises from vorticity in the superfluid.

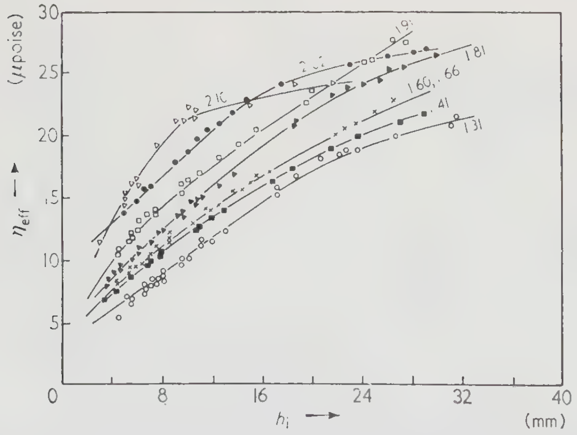

Figure 4. η_{eff} *as a function of* h_i *in Cap. I at various temperatures*

Some indication of such an eddy viscosity has been noted by Vinen[11] in his re-analysis of Mellink's data[12] on the thermomechanical pressure. Recent measurements of this effect carried out in this laboratory[13] also indicate a similar behaviour.

In representing our results as made up of the normal viscosity, mutual friction, and an eddy viscosity, we have approximated by expressing the latter through a single parameter. This may not be entirely justified because the eddy viscosity in classical turbulence varies from place to place in the turbulent field, its nature being that of a distributed parameter. The number η_s must therefore be looked upon as a 'lumped constant' characteristic in some, as yet unspecified, manner of the actual conditions of flow.

With the inclusion of this eddy term the two-fluid equations of motion, for steady isothermal flow, take the form

$$0 = -\frac{\rho_s}{\rho}\operatorname{grad} p + A\rho_s\rho_n|\mathbf{v}_s-\mathbf{v}_n|^2(\mathbf{v}_s-\mathbf{v}_n)+\eta_s\nabla^2\mathbf{v}_s \qquad \ldots (3)$$

$$0 = -\frac{\rho_n}{\rho}\operatorname{grad} p - A\rho_s\rho_n|\mathbf{v}_s-\mathbf{v}_n|^2(\mathbf{v}_s-\mathbf{v}_n)+\eta_n\nabla^2\mathbf{v}_n \qquad \ldots (4)$$

where the symbols have their usual meaning. It must be noted that these equations have application only when the velocity of superflow is larger than the critical velocity, if any.

In considering the solution of these equations there are two cases which it is convenient to distinguish. In the first

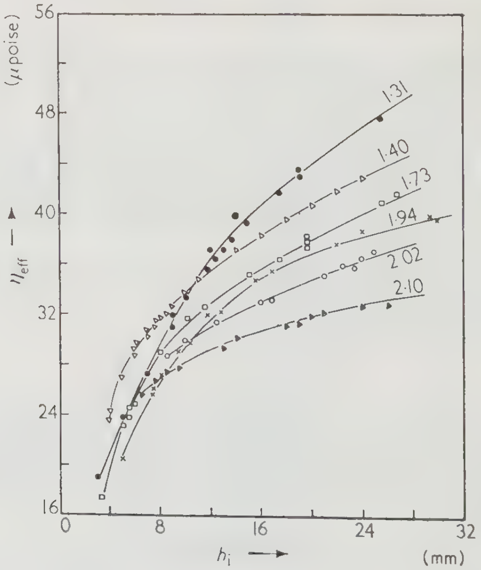

Figure 5. η_{eff} *as a function of* h_i *in Cap. IV at various temperatures*

case, when $(\bar{v}_s - \bar{v}_n)$ is small, the mutual friction terms are negligible. The solution is straightforward and the pressure dependent part of the mean velocity can be written as

$$v_p = -\frac{a^2}{8}\left[\left(\frac{\rho_n}{\rho}\right)^2\left(\frac{1}{\eta_n}\right)+\left(\frac{\rho_s}{\rho}\right)^2\left(\frac{1}{\eta_s}\right)\right]\operatorname{grad} p \quad \ldots (5)$$

Combining equations (2) and (5) the effective viscosity takes the form

$$\eta_{\text{eff}} = \frac{\eta_s \eta_n \rho^2}{\rho_n^2 \eta_s + \rho_s^2 \eta_n} \quad \ldots (6)$$

In deciding to which part of the experimental results this case is applicable, we are helped by some recent measurements made in this laboratory by Critchlow[14] on the thermal resistance of helium in capillaries of the same size. These data show that for Cap. I the mutual friction does not develop to its full value until the relative velocity has reached a value of about 20 cm/sec. This is particularly true at low temperatures. In the present work, even if the normal component were completely immobilized, the values of $(\bar{v}_s - \bar{v}_n)$ seldom exceed 3–4 cm/sec. It therefore seems reasonable to assume that to the case of this tube equation (6) is applicable.

On the other hand, we must expect from Critchlow's work that in our observations on Caps. II, III, and IV the mutual friction was large, which means that solution of equations (3) and (4) becomes much more complicated. An assessment of the importance of the various terms, to be published by one of us elsewhere, suggests, however, that for temperatures above 1·6° K it may be justified to write in the first approximation

$$\eta_{\text{eff}} = \eta_s + \eta_n \quad \ldots (7)$$

provided that h_i is not too small.

The values of η_s computed from equation (6) for Cap. I and from equation (7) for Cap. IV are given in Figures 6 and 7. The graphs are double logarithmic plots and the straight lines show the least-squares fits to the observed data. The data for the intermediate sizes (Caps. II and III) resemble those for Cap. IV. The slopes of the lines have the following mean values: Cap. I, 0·60; Cap. II, 0·74; Caps. III and IV, 0·50.

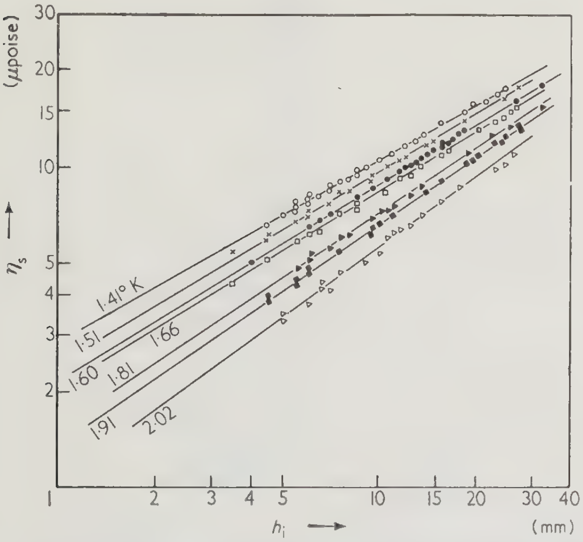

Figure 6. The eddy viscosity η_s as a function of h_i at various temperatures in Cap. I. The straight lines represent least-squares fits

The variation with temperature is too complex to be stressed. A complete explanation would require a more detailed knowledge of the phenomena connected with eddy viscosity.

The fact that in each individual flow experiment the eddy viscosity remains constant suggests that a certain degree of turbulence is created at the beginning and is subsequently maintained. It is not necessary for the density of turbulence to remain entirely unaltered while the flow is proceeding since only very drastic variations of the density will alter η_s. The liquid is accelerated to a supercritical velocity in the beginning and since the level of turbulence is presumably dependent upon how far beyond the critical it is taken, the dependence of the subsequent flow phenomena on h_i seems not unreasonable.

It has already been mentioned, and is clear from Figure 2, that even at zero pressure difference the liquid in the capillaries retains a finite limiting velocity v_0 (equation 1). It is tempting to identify this with the critical velocity of the superfluid observed in heat conductivity experiments by Brewer, Edwards, and Mendelssohn[1] and later work in this laboratory.[13,14] A complication arises through the fact that we have found v_0 to vary with h_i. However, in Cap. I where the flow pattern is relatively simple because $(\bar{v}_n - \bar{v}_s)$ and the mutual friction are small, this variation, too, is small. In Figure 8 we have plotted for this tube the change of v_0 with h_i at various temperatures which shows that this variation is slow at lower temperatures and completely absent at 2·1° K. Moreover, for the limiting case of $h_i = 0$ the values of v_0 agree well with the critical velocity found in heat conductivity experiments on the same capillary.

The close numerical correspondence is lost under the more complex flow conditions in the wider capillaries and,

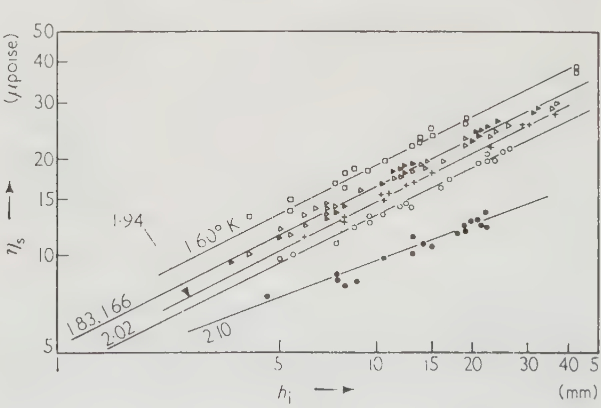

Figure 7. The eddy viscosity η_s as a function of h_i at various temperatures above 1·6° K in Cap. IV. The straight lines show the least-squares fits to the data

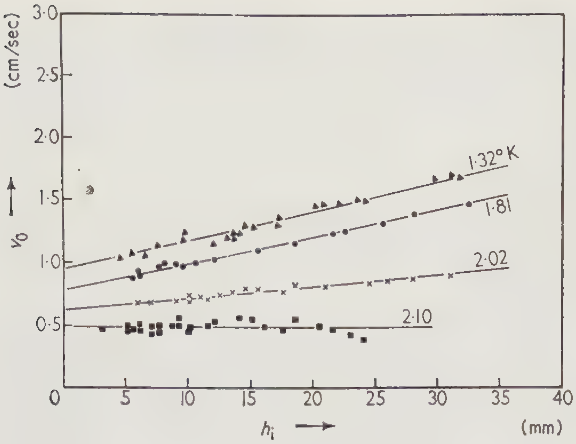

Figure 8. The limiting velocity v_0 as a function of h_i for various temperatures in Cap. I

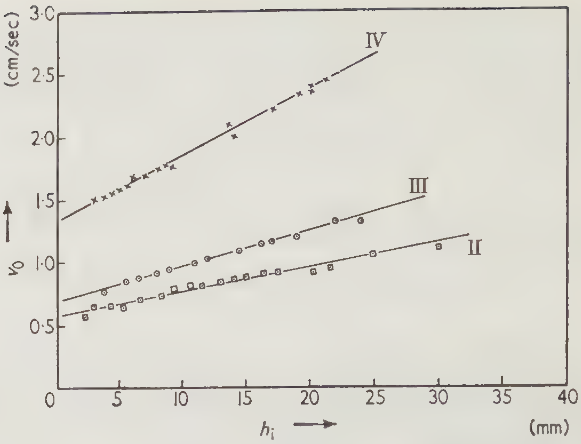

Figure 9. The limiting velocity v_0 as a function of h_i at 1·32° K in Caps. II, III, and IV

as Figure 9 shows, here the variation of v_0 with h_i also grows rapidly with increasing capillary diameter, although it still retains its linear character. Our results thus indicate that simple isothermal flow exhibits a critical velocity which is identical with that observed in thermally induced flow and that this simple relation is only destroyed by the growth of mutual friction.

One of us (S.M.B.) is grateful to the Government of India for financial support. Our thanks are also due to Mr. G. P. Lampel for help with some of the measurements.

REFERENCES

1. Brewer, D. F., Edwards, D. O., and Mendelssohn, K. *Phil. Mag.* **1**, 1130 (1956)
2. Allen, J. F., and Misener, A. D. *Proc. roy. Soc.* **A172,** 467 (1939)
3. Atkins, K. R. *Proc. phys. Soc. Lond.* **A64,** 833 (1951)
4. Bhagat, S. M., and Mendelssohn, K. 'Proceedings of the Kammerlingh-Onnes Conference on Low Temperatures, Leiden.' *Physica* **24,** S147 (1958)
5. Bhagat, S. M., *Proc. phys. Soc. Lond.* **75,** 303 (1960)
6. Gorter, C. J., and Mellink, J. H., *Physica* **15,** 285 (1949)
7. Brewer, D. F., and Edwards, D. O. *J. sci. Instrum.* **33,** 148 (1956)
8. Kapitza, P. L. *J. Phys. Moscow* **4,** 181 (1941)
9. Brewer, D. F., and Edwards, D. O. *Proc. roy. Soc.* **A251,** 247 (1959)
10. Lamb, H. *Hydrodynamics* (6th Ed.), p. 668 (Cambridge University Press, 1959)
11. Vinen, W. F. *Proc. Conf. de Phys. des Bass. Temp.*, p. 60 (Paris, 1955)
12. Mellink, J. H. *Physica* **13,** 180 (1947)
13. Bhagat, S. M., and Critchlow, P. R. *Cryogenics* **2,** 39 (1961)
14. Critchlow, P. R. *Thesis* (Oxford, 1960)

(S. M. Bhagat is now at Carnegie Institute of Technology, Schenley Park, Pittsburgh 13, Penn.)

Thermomechanical Pressure Measurements in Liquid Helium-II

S. M. Bhagat and P. R. Critchlow *Clarendon Laboratory, Oxford*

Received 3 June 1961

THE early experiments on the thermomechanical pressure in liquid helium-II indicated a strict proportionality between this pressure and the heat current. This fact has come to be known as the Allen and Reekie rule.[1] More recently, Vinen[2] as well as Lifshitz and Andronikashvili[3] have re-analysed some of Mellink's data[4] rather carefully and have suggested that the linear relation fails to hold for large heat currents. Similar variations in this range have also been observed by Brewer and Edwards in this laboratory.[5] Vinen has suggested that these deviations may arise from vorticity in the superfluid.

Bhagat and Mendelssohn's experiments[6] on gravitational flow in wide capillaries (diameter > 80 microns) indicate that in addition to the normal viscosity and the mutual friction there is a large eddy viscosity present in the superfluid component.

The present paper deals with measurements of the thermomechanical pressure in similar wide capillaries. These were undertaken in order to establish clearly the existence of deviations from the Allen and Reekie rule and to investigate the connection between such deviations and the appearance of the eddy viscosity.

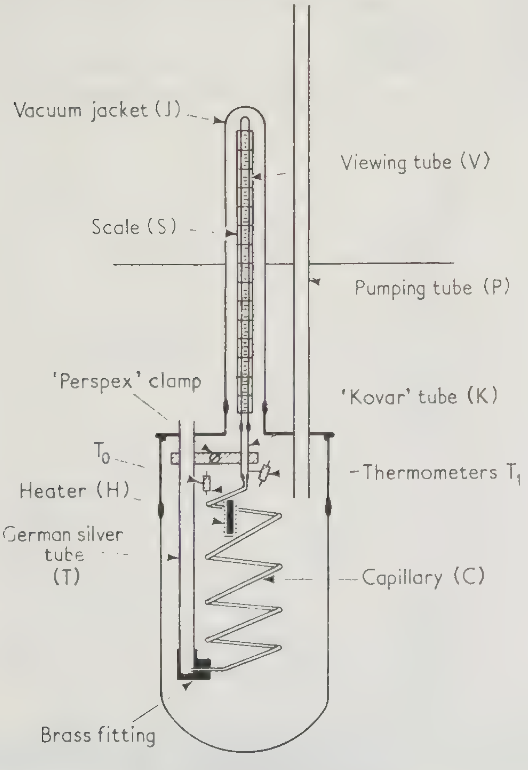

Figure 1. The flow apparatus

Method

The experiments were carried out in a combined helium liquefier–cryostat.[7] The flow apparatus is shown schematically in Figure 1. The capillary C and the viewing tube V are mounted in a vacuum jacket. The temperature of the helium bath was maintained constant to within 10^{-5} ° K during a measurement.[8] The viewing tube V carries a scale S graduated to 0·2 mm. H is a heater, and a dummy heater (not shown in the Figure), matched accurately with H, was placed in the helium bath. Two carbon resistance thermometers T_0 and T_1 were used to measure the temperature differences developed across the capillary. Short lengths of tungsten rod were introduced into the 'Kovar' tube K to reduce the dead volume.

The capillaries used are listed in Table 1. The Poiseuille constant ($\pi a^4/8l$) was measured by the flow of helium gas at room temperature for Caps. I and II, and by the flow of distilled water for Cap. III. The narrowest capillary was made out of glass rod and was straight, its mounting was essentially similar to that shown in Fig 1.

Table 1

Capillary	*I*	*II*	*III*
Length (cm)	10·2	73	150
Poiseuille constant (cm^3)	$3{\cdot}23 \times 10^{-11}$	$2{\cdot}61 \times 10^{-10}$	$6{\cdot}13 \times 10^{-9}$
Approximate internal diameter (microns)	108	297	786

The procedure for the simultaneous measurement of the temperature difference and the accompanying thermomechanical pressure is as follows. A given current is switched into H from the dummy heater. The temperature at one end of the capillary (thermometer T_0) is automatically held constant and the temperature difference across it is measured with an a.c. bridge in which T_0 and T_1 form two adjacent arms. The output from the bridge is displayed on a recording potentiometer so that it is easy to ascertain when thermal equilibrium has been attained.[9] T_1 was calibrated against the 1958 helium vapour pressure scale and the observed points fitted to the Clement and Quinnell formula[10] in order to evaluate (dT/dR).

Figure 2 shows some of the typical traces obtained on the potentiometer when the heat current is switched on.

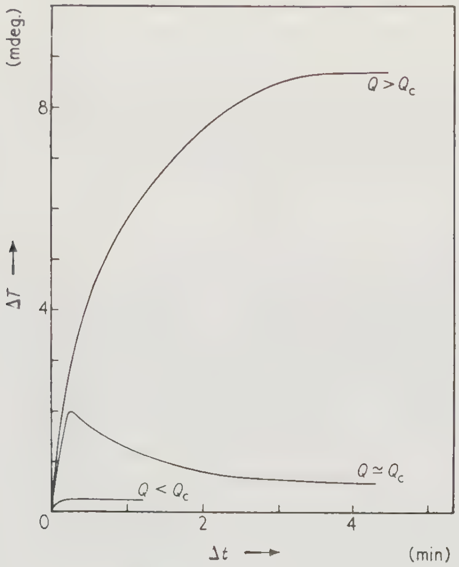

Figure 2. Variation of temperature difference with time for various values of heat current

For low heat currents the temperature difference grows quickly to its equilibrium value. At higher heat currents, ΔT first increases rapidly but then falls slowly to its final value. This happens when Q is in the neighbourhood of its critical value Q_c (see below). Since the thermal time constant of the apparatus is small, this 'overshoot' is probably due to an initial burst of turbulence which either decays away (for $Q \lesssim Q_c$) or settles down (for $Q \gtrsim Q_c$) to a lower value consistent with the flow conditions. For still larger values of Q, ΔT increases more or less exponentially to its equilibrium value. No oscillations were observed but the time constant of the recording potentiometer is presumably too large to resolve any oscillations which may be present.

Figure 3 shows what happens to the position of the meniscus in V when a heat current is applied. For low heat currents the level rises and attains an equilibrium position. With larger heat currents the initial rise is followed by a fall and for large enough heat currents the final position of the meniscus may, in fact, be several millimetres below the main bath level. In some cases, near the critical region, oscillations are superimposed on the initial rise. The negative level difference at high heat currents is due to the increased vapour pressure at the warm end of the capillary and the true thermomechanical pressure ΔH (in mm of He) across the capillary has therefore to be written in the form

$$\Delta H = \Delta H_{\text{obs}} + p(T+\Delta T) - p(T) \qquad \ldots(1)$$

where $p(T)$ and $p(T+\Delta T)$ are the saturated vapour pressures at the 'cold' and 'warm' ends of the capillary, respectively. For small ΔT the second term on the right-hand side can be expanded to give

$$\Delta H = \Delta H_{\text{obs}} + \left(\frac{\delta p}{\delta T}\right)\Delta T + \frac{1}{2}\left(\frac{\delta^2 p}{\delta T^2}\right)(\Delta T)^2 \qquad \ldots(2)$$

In the present analysis the differential coefficients $(\delta p/\delta T)$ and $(\delta^2 p/\delta T^2)$ were evaluated from the 1958 helium vapour pressure scale. The contribution of the second order term amounts to only a few per cent at the largest values of ΔT measured. Higher order terms were therefore neglected. Figure 4 shows the relative importance of the first two terms on the right-hand side of equation (2) for Cap. II at 1·41 °K. Except in the region close to Q_c, the scatter in ΔT and ΔH is well below 5 per cent.

Results and discussion

Measurements of the pressure gradient indicate the presence of a well defined critical heat current Q_c above which non-linear effects begin to appear. This corresponds to the critical heat current observed earlier by Brewer, Edwards, and Mendelssohn[11] in temperature gradient measurements and confirmed by the present investigations. Either set of data leads to the same value of Q_c. The critical velocities $v_{s,c}$ thus obtained vary with channel size roughly as $1/a$. A more detailed discussion of the critical velocities has been given by Critchlow[9] and will be published separately.

For the present discussion it is convenient to describe the results in two different regions separately.

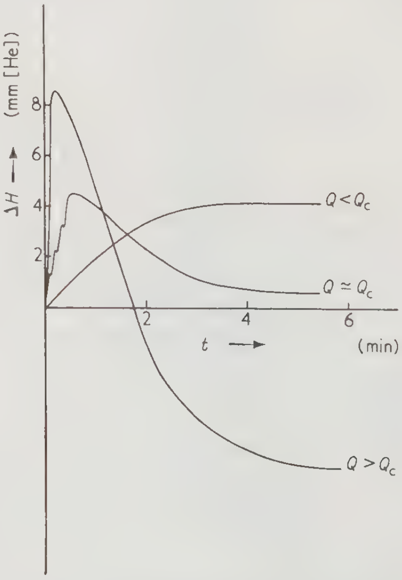

Figure 3. Variation of level difference with time for various values of heat current

The sub-critical region

In this region the present results are in good agreement with those reported previously. The main features may be summarized as follows:

(1) $\Delta T/Q$ is a constant. Using the relation

$$\frac{\Delta T}{Q} = \frac{(\eta_n 8lT)}{[\pi a^4(\rho ST)^2]} \qquad \ldots(3)$$

the values of the normal viscosity were computed and were found to agree reasonably with those reported by Brewer and Edwards[8] and Heikkila and Hallett.[12]

(2) $\Delta H/Q$ is a constant, i.e. the Allen and Reekie rule is obeyed. The values of η_n can also be obtained from $\Delta H/Q$ and agree well with those obtained from $\Delta T/Q$. This means that ΔT is proportional to ΔH, and hence London's equation[13] is obeyed.

The sub-critical region can be described reasonably well in terms of the viscous dissipation in the normal component alone. Generally, no sizeable dissipation is present in the superfluid, but in some cases small deviations occurred when Q approached Q_c.

The super-critical region

(1) *The temperature gradients.* Brewer and Edwards[5] have suggested that the transition through the critical region is related to the appearance of vorticity in the superfluid. Also, Vinen[14] has proposed that if such a mass of vortex line exists in the superfluid then, under some simplifying assumptions, its interaction with the rotons and phonons constituting the normal fluid will give rise to the Gorter and Mellink[15] mutual friction force. With such a mutual friction force present, the temperature gradient across the capillary is made up of two terms

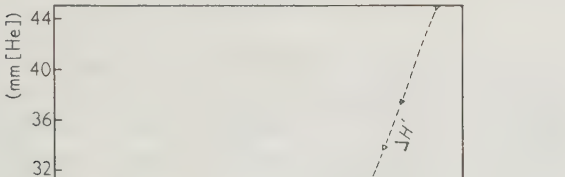

Figure 4. Relative contribution from the observed level difference ΔH_{obs} and the vapour pressure correction $\Delta H'$ to the thermomechanical pressure (Cap. II, 1·41° K)

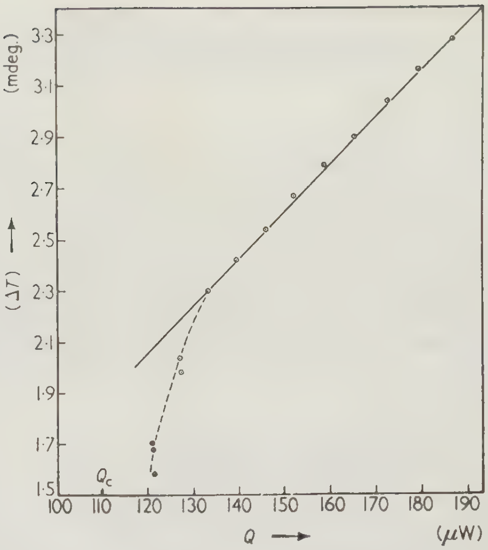

Figure 5. Dependence of the temperature difference due to mutual friction ΔT_{mf} on the heat current (Cap. II, 1·41° K)

$$\Delta T = \Delta T\eta_n + \Delta T_{mf} = \frac{8T\eta_n lQ}{\pi a^4(\rho ST)^2} + \frac{A\rho_n Q^3}{S(\rho_s ST)^3} \qquad \ldots(4)$$

where the first term arises from the normal viscosity only, while the mutual friction term (ΔT_{mf}) leads to dissipation involving the superfluid also. To take account of the variation of temperature along the length of the capillary the second term on the right-hand side of equation (4) has to be modified to read

$$\frac{\Delta T_{mf}}{Q} = \frac{A\rho_n Q^2}{S(\rho_s ST)^3}\left[1+\frac{1}{\Omega}\frac{\delta\Omega}{\delta T}\right] \qquad \ldots(4a)$$

with $\Omega = A\rho_n/[S(\rho_s ST)^3]$. Figure 5 shows a typical result of $(\Delta T_{mf})^{1/3}$ plotted as a function of Q. It shows that, for heat currents not too close to Q_c, the law of Gorter and Mellink is obeyed accurately. From the slopes of this and similar plots, values of A were computed, and although the scatter, particularly at high temperatures, is considerable no systematic variation with channel width was found. Also, the numerical magnitudes and the temperature dependence are consistent with Vinen's data.

However, there is a finite region just above Q_c in which the observed temperature gradients due to mutual friction fall below the values predicted by equation (4). Owing to the complex phenomena at the onset of turbulence the actual width of this transition region is difficult to determine. The present data indicate a width of about $Q_c \rightarrow 1{\cdot}3\, Q_c$. The eddy viscosity considered below is too small to account for the entire discrepancy. The failure of the parameter A to assume its full value may arise from the fact that the density of vortex line becomes relatively small near the critical current and therefore the assumptions underlying the calculation of a uniform volume force are no longer justified.

(2) *The pressure gradients.* In the pressure measurements the critical current was determined by deviations from the Allen and Reekie rule. As mentioned above, the critical velocities obtained in this manner are in close agreement with those found in the temperature gradient measurements. At first sight it may seem that the mutual friction terms might also account for the deviations in the pressure gradients. However, closer examination shows that this is not so. The two-fluid equations of motion for steady flow, i.e.

$$0 = -\frac{\rho_s}{\rho}\,\mathrm{grad}\,p + \rho_s S\,\mathrm{grad}\,T + A\rho_s\rho_n|\mathbf{v}_s-\mathbf{v}_n|^2(\mathbf{v}_s-\mathbf{v}_n) \qquad \ldots(5)$$

$$0 = -\frac{\rho_n}{\rho}\,\mathrm{grad}\,p - \rho_s S\,\mathrm{grad}\,T - A\rho_s\rho_n|\mathbf{v}_s-\mathbf{v}_n|^2(\mathbf{v}_s-\mathbf{v}_n) + \eta_n\nabla^2 v_n \qquad \ldots(6)$$

may be added together to give

$$\mathrm{grad}\,p = \frac{8\eta_n}{\pi a^4(\rho S T)}\,Q \qquad \ldots(7)$$

This relation shows that, whether mutual friction is present or not, the Allen and Reekie rule will continue to hold. The deviations must therefore be caused by some other effect which arises from turbulence in the superfluid. The existence of such an effect has been suggested by other experiments,[6,16] which indicate the presence of an eddy viscosity. Equation (5) must therefore be modified to read

$$0 = -\frac{\rho_s}{\rho}\,\mathrm{grad}\,p + \rho_s S\,\mathrm{grad}\,T + A\rho_s\rho_n|\mathbf{v}_s-\mathbf{v}_n|^2(\mathbf{v}_s-\mathbf{v}_n) + \eta_s\nabla^2 v_s \qquad \ldots(8)$$

On the other hand, Lifshitz and Andronikashvili[3] have suggested that the deviations may be attributed to irreversible effects in the normal fluid. Although this possibility cannot be entirely ruled out, it seems unlikely that irreversible effects appear in the normal component at the same critical current Q_c at which the superfluid begins to develop turbulence. The solution of equations (6) and (8) requires further assumptions and will be published elsewhere together with an estimate of the magnitude of the eddy viscosity in the present experiments.

As long as $Q < Q_c$ and $\eta_s = 0$, the Allen and Reekie rule will be obeyed. On the other hand, for $Q > Q_c$ turbulence appears in the superfluid and η_s has a finite value, the density of turbulence, and hence the eddy viscosity, becoming progressively larger as Q is increased. The observed thermomechanical pressure difference should therefore exceed the value given by equation (7) as Q becomes larger than Q_c. The present observations show that this is in fact the case. Figure 6, which is a typical plot of $\Delta H/Q$ as a function of Q, shows that deviations appear at a fairly sharply defined value of Q_c.

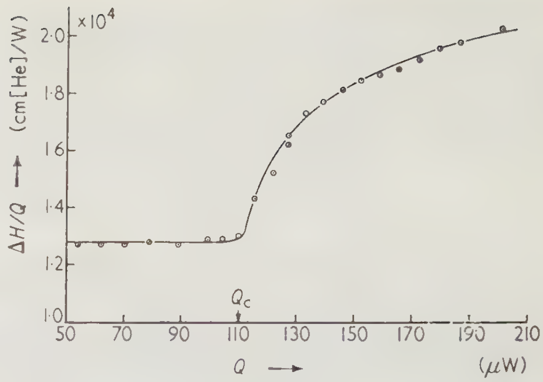

Figure 6. (ΔH/Q) as a function of the heat current (300 microns capillary, 1·41° K)

We are indebted to Dr. K. Mendelssohn, F.R.S., for a number of valuable suggestions and for his constant interest in this work. One of us (P.R.C.) is grateful to the D.S.I.R. for the award of a maintenance grant.

REFERENCES

1. Allen, J. F., and Reekie, J. *Proc. Camb. phil. Soc.* **35,** 114 (1939)
2. Vinen, W. F. *Proc. Conf. de Phys. des Bass. Temp.*, p. 60 (Paris, 1955)
3. Lifshitz, E. M., and Andronikashvili, E. L. *A Supplement to Helium*, p. 121 (Chapman and Hall, London, 1959)
4. Mellink, J. H. *Physica* **13,** 180 (1947)
5. Brewer, D. F., and Edwards, D. O. *Proc. 5th Intern. Conf. Low Temp. Phys. Chem.*, p. 12 (Madison, 1957); *Phil. Mag.* (1961). In press
6. Bhagat, S. M., and Mendelssohn, K. *Cryogenics* **2,** 34 (1961)
7. Brewer, D. F., and Edwards, D. O. *J. sci. Instrum.* **33,** 148 (1956)
8. Brewer, D. F., and Edwards, D. O. *Proc. roy. Soc.* **A251,** 247 (1959)
9. Critchlow, P. R. *D. Phil. Thesis* (Oxford, 1960)
10. Clement, J. R., and Quinnell, E. H. *Rev. sci. Instrum.* **23,** 213 (1952)
11. Brewer, D. F., Edwards, D. O., and Mendelssohn, K. *Phil. Mag.* **1,** 1130 (1956)
12. Heikkila, W. J., and Hallett, A. C. H. *Canad. J. Phys.* **33,** 420 (1955)
13. London, H. *Proc. roy. Soc.* **A171,** 484 (1939)
14. Vinen, W. F. *Progress in Low Temperature Physics*, Vol. III (North-Holland, Amsterdam, 1961)
15. Gorter, C. J., and Mellink, J. H. *Physica* **15,** 285 (1949)
16. Bhagat, S. M. *Proc. phys. Soc. Lond.* **75,** 303 (1960)

(S. M. Bhagat is now at Carnegie Institute of Technology, Schenley Park, Pittsburgh 13, Penn.)

New Refrigeration Cycle for the Production of Liquid Nitrogen

S. C. Collins *M.I.T., Cambridge, Mass.*
R. W. Hughes *Joy Manufacturing Company, Saltsburg, Penn.*

Received 9 June 1961

DURING World War II reversing exchangers were improved to the extent of being useful in the manufacture of oxygen and nitrogen from air. At the present time a significant fraction of the oxygen produced in the United States comes from plants which utilize reversing exchangers in the dual role of purifier and heat exchanger. Compressed air containing normal amounts of water and carbon dioxide is progressively cooled while it flows along one channel in heat exchange relationship with an outgoing stream of cold waste gas flowing in the opposite direction in a similar channel of the reversing exchanger. Periodically the streams swap channels. Water, carbon dioxide, and other condensible impurities carried by the impure air condense upon the channel surfaces. During the next half-cycle these liquid and solid deposits evaporate into the stream of waste gas.

The degree of success of the reversing exchanger as a purifier of air is determined by the operating conditions. Among the common impurities carbon dioxide is the most troublesome. Because of the volatility of solid carbon dioxide its concentration is not sufficiently reduced until the process air is cooled to approximately 112° K. At higher pressures air liquefies while the equilibrium concentration of carbon dioxide is fairly high. Furthermore, the Poynting effect, the displacement of the equilibrium vapour concentration toward higher values with increasing air pressure, becomes important.

Complete evaporation of condensed impurities into the waste gas during the purging half-cycle is just as important as thorough purification of the incoming air. Otherwise blocking of the heat exchanger will eventually occur. The greater the volume of waste gas, other conditions remaining the same, the more thorough the purging. If the purging stream could become saturated with impurities at the temperature of the process air at the time of deposition, the volume rate of flow of the purging stream would need to be no larger than that of the air stream. Unfortunately, the temperature of the purge gas must always be colder at a given site in the heat exchanger than that of the counter current of air in the adjacent channel. The fact that the vapour pressure of all substances falls rapidly as the temperature decreases makes temperature an important factor in the purging of a heat exchanger. Certain factors combine to make the temperature difference between process air and purging gas rather large at the cold end of the heat exchanger. In the most favourable case the desired product is gaseous oxygen or nitrogen. The mass rate of flow of the outgoing cold gases, product plus waste gas, equals that of the incoming process air. Because of the higher specific heat of the compressed air relative to that of the outgoing gases, however, the temperature difference between streams becomes sufficiently great at the zone of carbon dioxide deposition as to make it impossible for the waste gas to carry away during one half-cycle all of the carbon dioxide which was deposited during the previous half-cycle. If the product is removed from the system as liquid, conditions become even more unfavourable. The temperatures spread wider apart because of the greater disparity of the mass–specific heat product for the two gaseous streams flowing in the heat exchanger.

A frequently used method of avoiding carbon dioxide accumulations in reversing exchangers is illustrated by the flow diagram of Figure 1. A driven reversing valve A

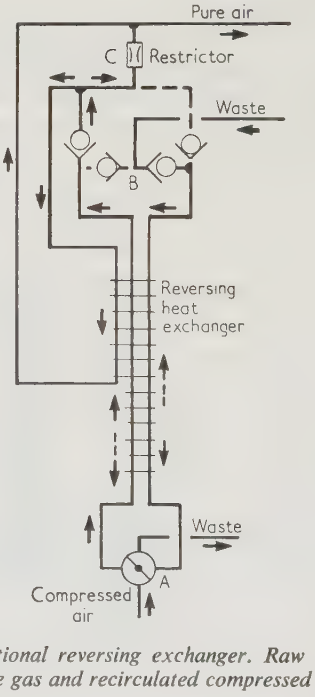

Figure 1. Conventional reversing exchanger. Raw air is cooled by waste gas and recirculated compressed air

switches the two streams of gas periodically. The duration of one cycle is generally about 5 min. Check valves B rectify the flow at the cold end automatically. An adjustable restrictor C forces a part of the compressed air to return part-way through the heat exchanger. Thereafter the two fractions are recombined. The effect of an additional cooling stream in the colder portion of the heat exchanger is to reduce substantially the temperature difference between the process air which is being freed of carbon dioxide and the waste gas which is absorbing carbon dioxide. Reversing exchangers operated in this manner have been industrially acceptable generally. Under certain circumstances, however, there is a distinct need for the ability to maintain temperatures at various points in the heat exchange system that are nearer the optimum than is possible with the simple procedure described above. A case in point is the relatively small, unattended nitrogen or oxygen generator.

The cycle indicated in Figure 2 was devised for use in liquid nitrogen plants. With minor changes it can be adapted to the production of oxygen. This cycle has been found to be particularly amenable to automatic control. A description follows.

A stream of compressed nitrogen is cooled to approximately 170° K. A large part of the stream is then expanded in an engine. The smaller fraction is liquefied while still at the higher pressure by heat exchange with the expanded nitrogen from the engine. The liquid so produced is drained into the top of the distilling column. An equivalent amount of nitrogen vapour is withdrawn from the column and returned to the nitrogen compressor. A stream of compressed air is purified by cooling to approximately 110° K and fed into the column for fractionation. The oxygen-containing fraction becomes the purge gas for the reversing exchanger.

There are four principal heat exchange elements in addition to the compressor, expansion machine, and distilling column. The compressor has four cylinders of which one is devoted to the compression of ambient air to 5 atm, one to the compression of nitrogen from 4·5 atm to 13 atm, and two to raising the nitrogen pressure from 13 to 37 atm.

Heat exchangers (1), (2), and (4) contain three channels each, exchanger (3) only two. The various channels are designated by the letters a, b, … k, respectively, Channels a and d constitute the reversing exchanger. Note that the two are not thermally connected.

Referring to Figure 2, the reversing valve is assumed to be directing the flow of compressed air through channel a while the waste gas finds its way through channel d. In order to cool the air stream a counter current of cold nitrogen consisting of the make-up nitrogen vapour from the column, combined with enough expanded nitrogen from the engine to secure the desired terminal temperature of the air, is set up in channel c. The magnitude of the total cooling stream can be controlled by external restrictors. Once set the restrictors rarely need to be changed.

The possibility of easily fixing the terminal temperature of the air stream in a set of reversing exchangers at a desirably low value is considered to be an advantage of great importance. The concentration of carbon dioxide can be reduced to an infinitesimal value.

During the half-cycle in which air is being purified in exchanger (1), channel d of exchanger (2) is being purged of impurities collected from the air stream during the preceding half-cycle. Although the pressure of the waste gas is low and the specific volume relatively large, the mass rate of flow is normally so low that complete elimination of condensed impurities would not occur unless the temperature is caused to rise for at least a part of the purging period. The desired change in temperature of the walls of channel d can be secured simply by adjusting the magnitude of a stream of high pressure nitrogen which flows from the compressor through channel e of exchanger (2). The possibility of promoting rapid evaporation of impurities by elevating the temperature is most useful and is the reason for placing the two reversing courses in separate heat exchangers.

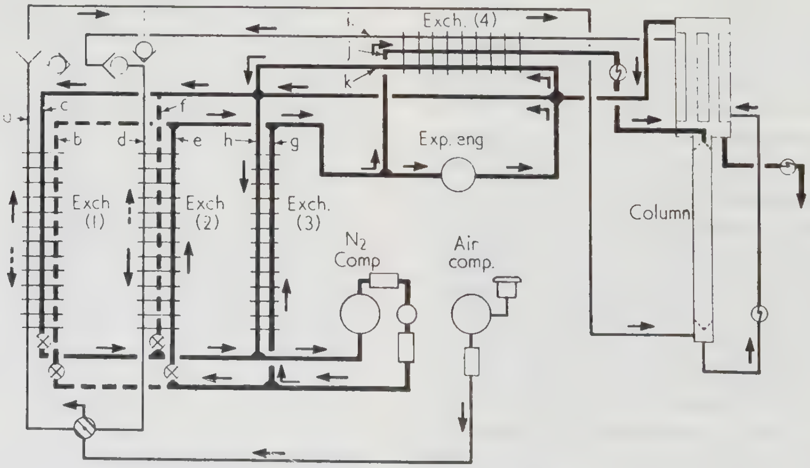

Figure 2. Flow diagram of new nitrogen cycle

If the temperature of a heat exchanger is to be increased to hasten the purging, it is obvious that the purging period must not continue for the entire half-cycle. Time must be left for cooling the exchanger before impure air is again admitted to the reversing channel. Experience with the new cycle has led to the following schedule:

Length of half-cycle 30 min
Duration of flow of warming stream 28 min
Duration of flow of cooling stream 32 min

Assuming that switching of streams occurred at time 0, a cycle would be completed in 60 min with channel assignments indicated in Table 1.

The principal part of the refrigerant nitrogen stream is cooled in exchanger (3) by a returning stream of expanded nitrogen. The remainder, of course, is cooled in the reversing exchanger by the outgoing waste. A small fraction of the cooled refrigerant stream is directed to exchanger (4) in which it is further cooled and mostly liquefied for delivery to the column. The function of this fraction of the high pressure nitrogen is two-fold. It provides liquid for the column and very cold gas for use in the reversing exchanger in amount required for adequate cooling of the air supply. Exchanger (4) is cooled partly by the waste gas from the column and mostly by expanded nitrogen from the expansion machine.

The larger fraction of the cooled high pressure nitrogen is expanded in the engine. The cold gas discharged by the engine provides nearly all of the available refrigeration. The Joule–Thomson effect in the other streams is useful but relatively small.

Table 1

Channel	*Fluid*	*Treatment*	*Time (min)*
a	Air	Cooling	0 to 30
a	Waste	Heating	30 to 60
b	—		−2 to 30
b	Nitrogen (37 atm)	Cooling	30 to 58
c	Nitrogen (4·5 atm)	Heating	−2 to 30
c	—		30 to 58
d	Waste	Heating	0 to 30
d	Air	Cooling	30 to 60
e	Nitrogen (37 atm)	Cooling	0 to 28
e	—		28 to 60
f	—		0 to 28
f	Nitrogen (4·5 atm)	Heating	28 to 60

The Joy Manufacturing Company of Pittsburg, Pa., has reduced the new cycle to practice. Capacities range from 12–200 litres per hour.

Messrs. A. Lee Barrett and Donald Wiebe of the Joy Manufacturing Company have given much valuable assistance in the development of the liquefiers. Their sustained interest is gratefully acknowledged.

The Thermosiphon as a Nitrogen Cryostat for Operation in the Horizontal Reactor Channel

L. Bewilogua and R. Knöner *Technische Hochschule, Dresden*

Received 8 June 1961

It is often necessary to maintain low temperatures at a large distance or at points where access is difficult even in cases of considerable heat supply. It has been found possible to apply the thermosiphon principle to this problem. Hitherto, the thermosiphon has been disregarded for low temperatures, though just as in this case large quantities of heat can be transferred very easily with small differences of temperature by means of a two-phase circuit.

The test model of a nitrogen thermosiphon which will be described here was developed particularly for operation in the horizontal reactor channel. For that purpose the thermosiphon shows special advantages because it is possible to operate with pure nitrogen in a closed circuit, and neither compressors[1] nor liquid pumps[2] are necessary. A suitable arrangement for operation in the vertical channel has been described.[3]

The scheme of the test model is shown in Figure 1. The outer Dewar vessel 1 contains the cooling liquid which effects a somewhat higher temperature in the closed cooling circuit. The system is filled with a sufficient quantity of gas of triple point temperature below and critical temperature above the temperature of the cooling liquid.

Heat contact between the circuit and the cooling liquid is made via the condenser 2. The surface and shape of the condenser are designed in such a manner that the heat transfer (cooling bath to metal and metal to condensate) will be as high as possible, and that in the case of high heat supply the quantity of liquid in the boiler 4 will not be decreased by any considerable amount.

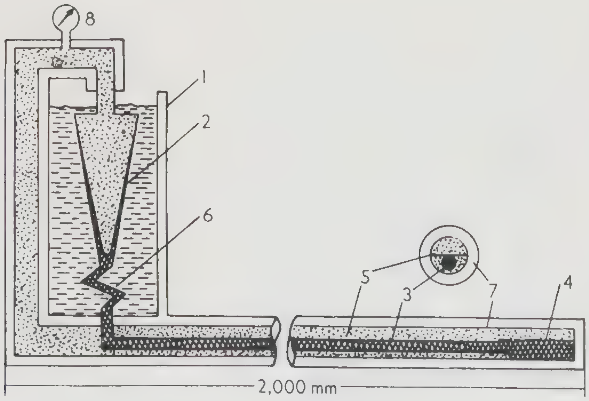

Figure 1. Schematic drawing of the test model cryostat for operation in the horizontal reactor channel

The liquid flows from the condenser through the double-walled liquid tube 3, placed in the interior of the vapour tube 5, into the boiler. The windings 6 supercool the condensate, thus preventing steam bubbles which may be formed on the way to the evaporator by the heat supply. The whole arrangement is insulated from its surroundings by means of a vacuum jacket 7.

A heater and a resistance thermometer are placed in the boiler and using these the efficiency of the circuit can be determined. The pressure in the system is characteristic of the condenser during equilibrium operation and allows a control when starting; it can be read at the manometer 8.

On starting the whole system is at room temperature. It is filled with nitrogen gas to a pressure p_1. The pressure p_1 is determined in such a manner that at 80° K a quantity of liquid is originated sufficient to fill the boiler, the liquid tube, and part of the condenser. In our model the filling pressure is 7 atm. For starting the thermosiphon the external Dewar vessel is filled with liquid nitrogen. At first the condenser cools off and the pressure in the system drops (Figure 2). As soon as the temperature of the condenser has decreased to the extent that the pressure in the system corresponds to the vapour pressure, the nitrogen starts condensing at the condenser walls. From this point onwards the temperature of the condenser can be determined at the manometer from the pressure, i.e. from the vapour pressure of the filling gas. The liquid originating in the condenser flows by gravity through the windings into the liquid tube and, after the latter has cooled off, into the boiler. About 15 min later steady state is attained (Figure 2). The equilibrium temperature depends on the heat supplied to the boiler and the insulating losses of the circuit. In the absence of heat supply and losses, the liquid levels in the boiler and in the condenser would be of equal height. When heat is supplied to the boiler, an equivalent quantity of liquid nitrogen will evaporate; at equilibrium this is replaced from the condenser. The circulation is maintained by the difference between the liquid level in the boiler and that in the condenser.

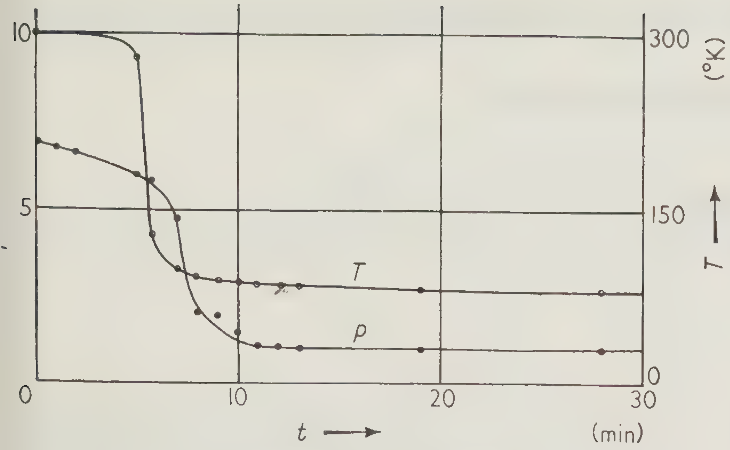

● Pressure in the closed circuit
○ Temperature in the boiler

Figure 2. Pressure and temperature as a function of time during the cooling process

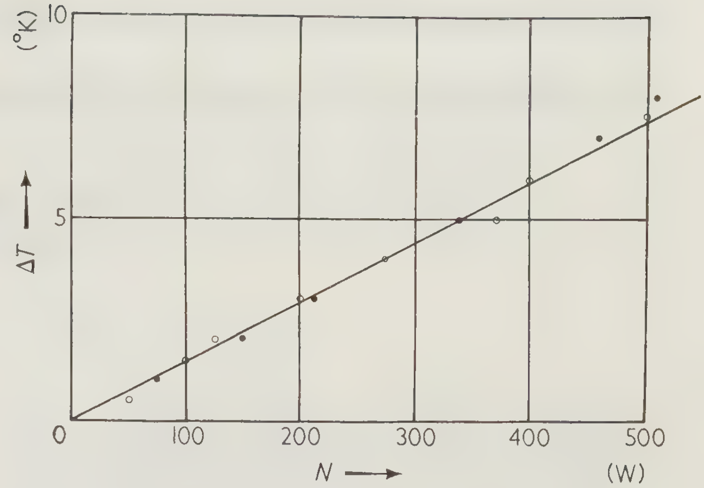

○ Experimental ● Calculated

Figure 3. Rise of temperature in the boiler as a function of heat supply

In our test model the distance between the condenser and the boiler is 2 m. Since radiation losses are high in the model (oxidized brass surfaces), the line can be extended to double or treble length without any increase of losses when using an appropriate arrangement. The tube sections have been dimensioned in such a manner that the flow resistances for the liquid in tube 3 and for the vapour in tube 5 are kept low up to a total supply of 500 W. In the test model the required pressure differences correspond to a difference of temperature of some 10^{-2} degrees (about 0·01°K at 200 W).

Applying the well known formula for heat transfer and our own results, an approximate formula was obtained for the dependence on the heat supply of the temperature difference ΔT between the condenser and the cooling bath. This difference rises about linearly with the supply from the boiler. For 200 W, a ΔT of about 3·2°K results; this means that the highest heat resistance within the system occurs in the condenser.

Figure 3 shows the dependence of temperature on supply. The fit of experimental and calculated dependences is satisfactory bearing in mind the rough approximation.

The temperature in the boiler increases by only 3·5°K when the vacuum in the insulation breaks down (i.e. when pressure rises to about 10^{-1} mm Hg). If the evaporated nitrogen in the cooling bath 1 is not replaced the temperature of the boiler rises by only about 5°K in 2 hr. The equipment may be easily controlled because regulation of temperature in the boiler can be replaced by regulation of the temperature in the cooling bath, where access is easier. The values mentioned above show clearly that the thermosiphon can transfer large quantities of heat and can operate reliably. They also show that it is capable of emergency operation and is suitable for continuous running.

REFERENCES

1. Coltman, R. R., Blewitt, T., and Noggle, T. S. *Rev. sci. Instrum.* **28,** 375 (1957)
2. Sartain, C. C., and Yockey, H. P. *Rev. sci. Instrum.* **29,** 118 (1958)
3. Bochirol, L., Doulat, J., and Weil, L. *Cryogenics* **1,** 44 (1960)

An Apparatus for Studying Ultrasonic Absorption in Metals at Low Temperatures

A. A. Galkin and A. P. Korolyuk

Institute of Radio-Physics and Electronics, Academy of Sciences, U.S.S.R.

Received 23 June 1961[†]

RECENTLY, there has been a considerable amount of work concerned with the study of ultrasonic absorption at low temperatures.[1–6] Most of this interest has been in the absorption in a magnetic field under conditions such that the mean free path of the conduction electrons l is considerably greater than the ultrasonic wavelength λ, while the Larmor radius of the electrons is of the order of λ. In this case the absorption coefficient varies periodically with the magnetic field.[1–3] From the period of oscillation of the absorption coefficient, the limiting electron momentum (and its size and shape) at the Fermi surface can be determined.[7] The establishment of the Fermi surface in metals requires a systematic study of the form of the angular dependence of the absorption coefficient as a function of magnetic field.

It would seem that satisfactory practical results can only be obtained in this field if the measuring of the absorption coefficient is made automatic.

This article describes an apparatus which enables the intensity of a signal transmitted through the specimen to be recorded automatically as a function of magnetic field. The ultrasonic absorption of a number of single crystals has been determined with such an apparatus. Experience with the apparatus has shown its reliability, and indicates that a programme of investigating the dependence of the period of oscillation on crystallographic orientation can be carried out in a comparatively short time. Such data enables the Fermi surface to be determined in most pure metals.

Block diagram of the measuring system

The dependence of absorption coefficient on magnetic field was measured by a pulse method. The block diagram of the measuring system is shown in Figure 1. The pulse generator 26I triggers both a modulator and a pulse delay system. The modulator in turn gates on a high frequency generator. The high frequency generator is connected to a transmitting quartz (a) by a variable length coaxial transmission line. Matching of the load (the quartz) to the generator is achieved by varying the length of the coaxial line. The quartz is excited at its harmonics for frequencies above 50 Mc/s.

Both the transmitting quartz (a) and the receiving quartz (b) are fixed to the specimen with vacuum grease. The receiving quartz is matched to the receiver by a variable length coaxial line. The signal from the receiver is fed to a pulse selector which simultaneously receives a strobe pulse derived from the 26I generator on a second channel. The strobe pulse goes through the delay system and triggers the strobe pulse generator (26I). The delay system introduces a variable pulse delay so that any of the pulses passing through the specimen, either by the shortest path or after many reflections, can be fed to the peak detector. After detection the signal falls on the recorder EPP09 through a cathode follower. The recording potentiometer EPP09 is converted into a two-dimensional plotter so that it registers the intensity of the signal transmitted through the specimen as a function of magnetic field.

A germanium probe is used to measure the magnetic field. The Hall potential difference, which is proportional to the field intensity is fed to the input of the two-dimensional plotter. The current through the germanium probe is stabilized; the limits of measuring the magnetic field are determined by its variation.

The arrangement of the magnet supply makes it possible to vary the magnet current from zero to its maximum value with the required speed.

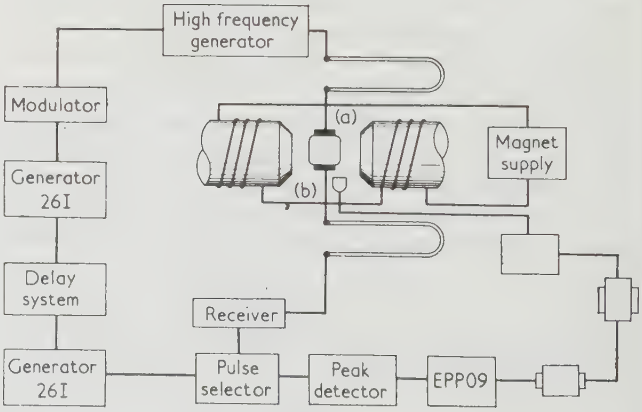

Figure 1

[†] Received by PTÉ Editor 13 October 1959: *Pribory i Tekhnika Éksperimenta* No. 6, p. 99 (1960).

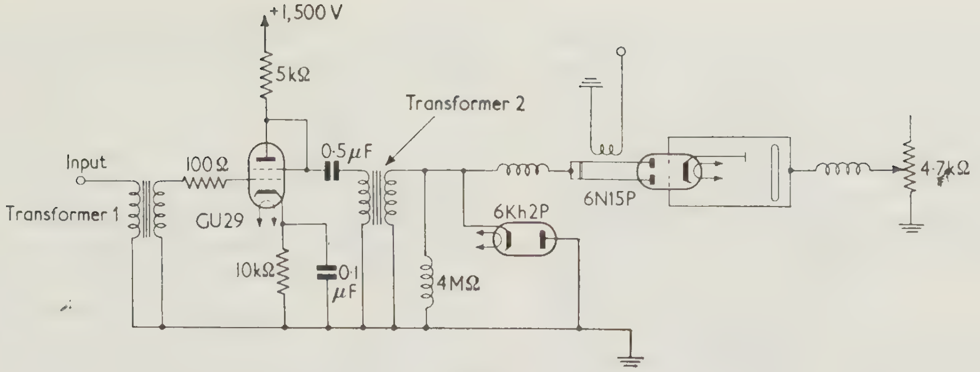

Figure 2

Description of the circuits

The modulator has a reservoir capacity in the anode circuit of valve GU29 (one tetrode is used in this valve). The circuit is shown in Figure 2. The negative voltage biasing off the valve (– 150 V) is taken off by a cathode resistance. The input stage is controlled by a 26I pulse generator. The voltage obtained from the 26I is insufficient for normal working of the modulator, so that there is a 1 : 2 step-up pulse transformer at the input. The pulse duration and the frequency of pulses is determined by the master generator 26I. The amplitude of the output signal is controlled by the anode voltage of the modulator (1–1·5 kV). There is a compensating inductance of 4 mF and a damping diode 6Kh2P in the anode circuit to improve the shape of the trailing edge of the pulse.

The modulator and high frequency generator are connected by the pulse transformer 2 (1 : 1). The generator is arranged on a push–pull system with two wire lines in the grid and anode circuits and is tunable by adjusting shorting links in the anode and grid lines. A miniature double triode 6NI5P is used as generator valve, working satisfactorily in the frequency range 50–250 Mc/s. The load (quartz) is coupled inductively by a single turn of wire placed in the magnetic field of the anode circuit. The change of coupling is achieved by rotating the turn from 0 to 180 degrees. The voltage applied to the quartz crystal from the generator is a pulse of 200–300 V.

The coaxial line connecting the receiver and generator to the quartz is made of RK cable. Part of the line is of variable length for matching the quartz. This U-shaped variable length is made of silvered brass tubes 15 and 10 mm in diameter. The inner lead is kept in place with polystyrene washers. The length of line can be varied from 85 to 150 cm.

The receiver consists of two units (Figure 3)—the high frequency and intermediate sections. A standard television programme selector PTK12 is used for the high frequency section, so that one can work in the ranges 50–100 and 160–230 Mc/s without any alteration. For using other frequencies the input and heterodyne circuits of the PTK12 have to be altered. The intermediate frequency of the

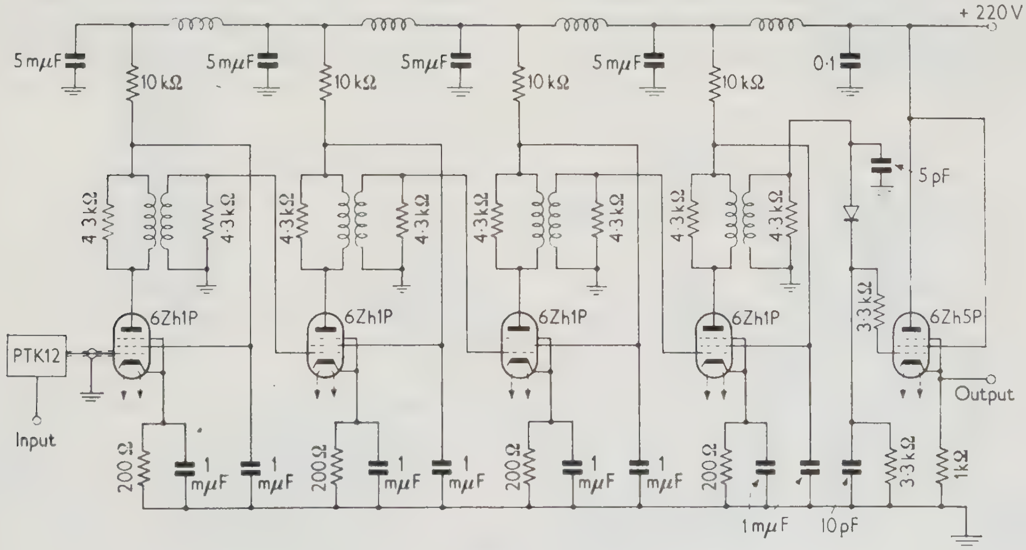

Figure 3

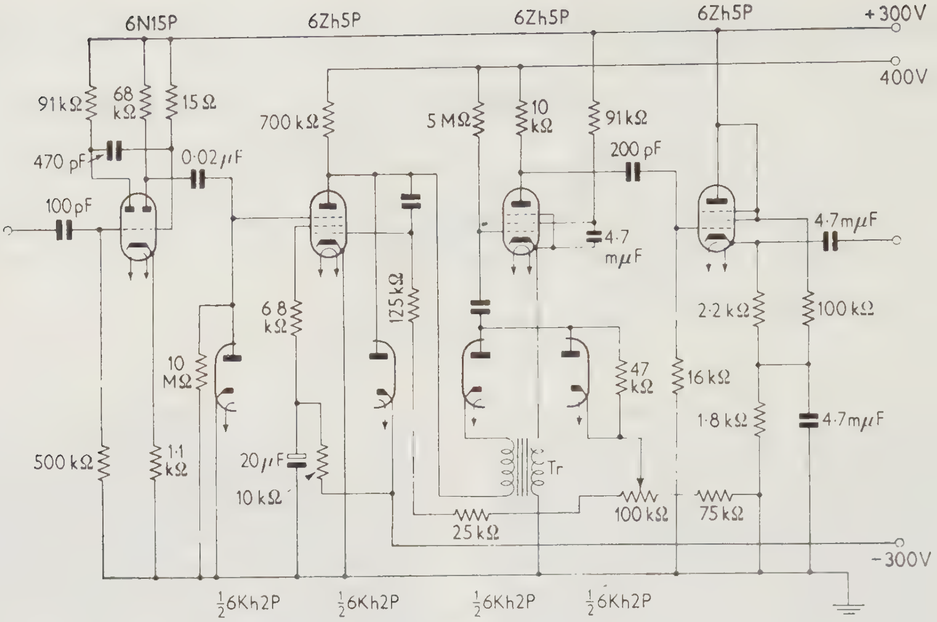

Figure 4

receiver was chosen to correspond to that of the television programme selector and was 32 Mc/s. The band width of the amplifier was ~ 3 Mc/s, the amplification coefficient 10^5, and the sensitivity varied from 5 to 10 μW.

The synchronization system consists of a variable pulse delay circuit described by Meerovich and Zelichenko.[8] The circuit with the components shown in Figure 4 allows the delay to be varied between 0 and 250 μsec, which is quite sufficient for specimens of great length and pulses undergoing several reflections. The pulse selector is based on a 6Zh4 pentode (Figure 5). The 6Zh4 valve is biased off by feeding 150 V negative voltage to a suppressor grid. When there is coincidence between the pulses arriving from the receiver at the control grid and from the pulse selector at the suppressor grid, pulses of negative polarity appear in the anode circuit of the 6Zh4. These pulses are fed to the diode detector with shunt load. A d.c. voltage appears across the 50 MΩ load resistance, proportional to the amplitude of the input pulse. This voltage is applied to the input of the EPP09 recorder through the cathode follower and balancing circuit.

The two-dimensional plotter is made from two automatic potentiometers (EPP09 and MS01) in which the synchronous motors of the chart winders are removed. The MS01 potentiometer is used to record the magnetic field. A selsyn connected to a slide wire is used to transmit indications of the angle of rotation of its moving system. The selsyn is connected directly with a reversible motor in order to increase its turning moment, and between the reversible motor and the slide wire there is an additional reduction of 1 : 12·8 made of a set of gear wheels, attached to the potentiometer. In this way 12·8 turns of the pick-up

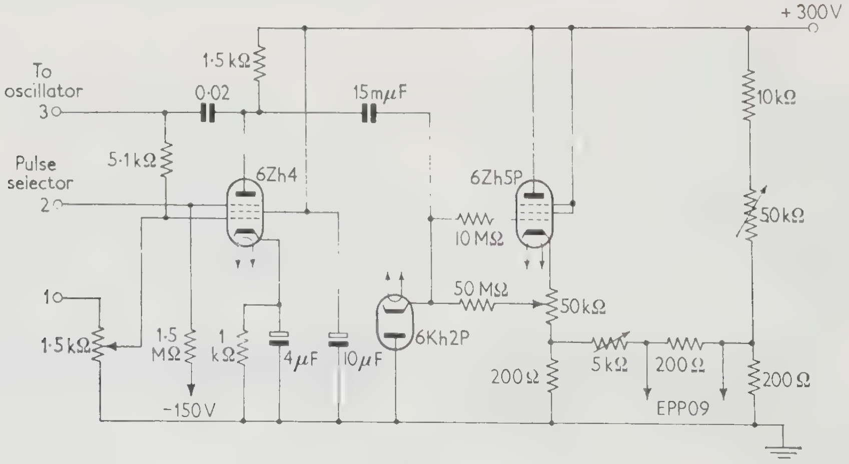

Figure 5

selsyn corresponds to one turn of the slide wire of the potentiometer. An additional selsyn, connected to the pick-up selsyn transmits the rotation directly to the chart winding drum of the EPP09 potentiometer. There is a gear reduction of 1:10 between the selsyn and the drum of the chart winder in order to change the velocity of motion of the chart. The angle of rotation of the chart drum of the EPP09 is thus proportional to the angle of rotation of the measuring recorder MS01, which in turn rotates with an angle proportional to H.

The cryostat for studying the absorption of sound is shown in Figure 6, and the means of attaching the specimen is shown in Figure 7. The specimen is fixed in a special holder to the bottom of a polished metal bung (10). The holder consists of two parts: the upper (fixed) part is connected to the central coaxial line, and the lower is soldered to the brass plate (13) which moves vertically on four guides. The specimen is cut by electropolishing so that it has two parallel faces to which the radiating and receiving quartz crystals are stuck. The specimen acts as one lead for the quartz (the specimen is earthed) and the second is a polished brass disk, completely covering the quartz face.

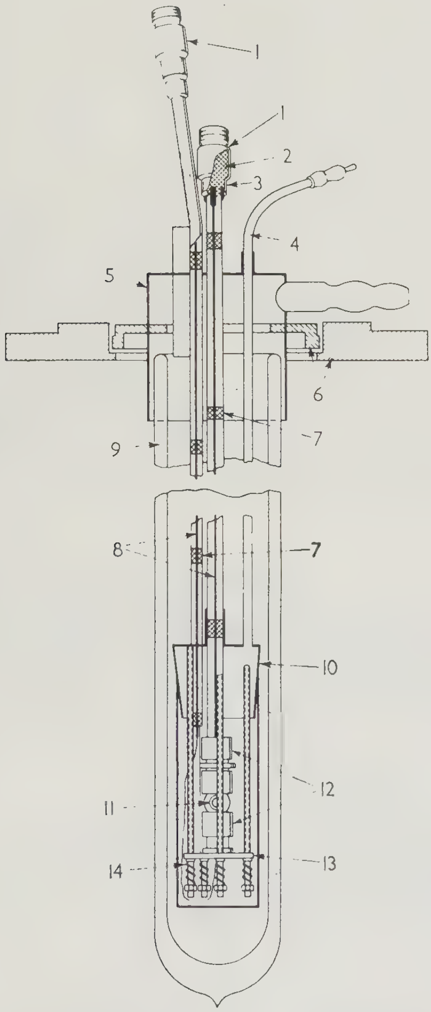

1: Coaxial plugs with vacuum seals
2: Polystyrene washers
3: Rubber gasket
4: German silver tube
5: Cap
6: Disk and ring with 1 degree divisions
7: Polystyrene spacers
8: Coaxial tubes
9: Dewar vessel
10: Polished metal bung
11: Specimen
12: Specimen holder
13: Brass plate
14: Beryllium bronze springs

Figure 6. The cryostat

The brass electrode is pressed on to the quartz with a beryllium bronze spring; the spring also serves as the electrical contact between the inner lead of the coaxial line and the brass disk. The electrodes of the receiver quartz are attached in the same way. The lower part of the holder presses the specimen against the upper by means of springs attached to the guide rods (14). German silver coaxial cables are used to lead in and out the high frequency electromagnetic waves from the cryostat. These cables are terminated outside the cryostat by standard plugs with vacuum seals (1).

A brass vessel is attached to the polished metal bung (10) and gaseous helium is let into it through the German silver tube (4) (this tube also serves for pumping air out of the vessel) to achieve thermal contact between the specimen and the liquid helium. The vessel with the specimen is inside a helium Dewar (9).

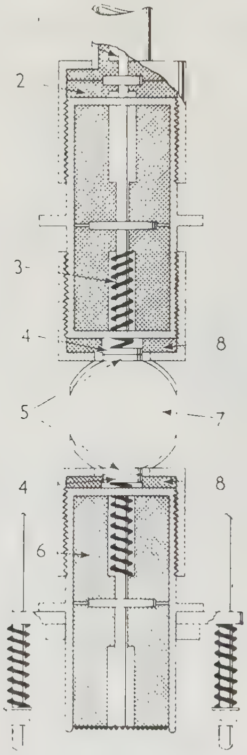

1: Central lead of the coaxial line
2: Polystyrene washer
3: Beryllium bronze spring
4: Brass disk
5: Quartz plate
6: Polystyrene insulator
7: Specimen
8: Insulating washer

Figure 7. Arrangement for fixing the specimen

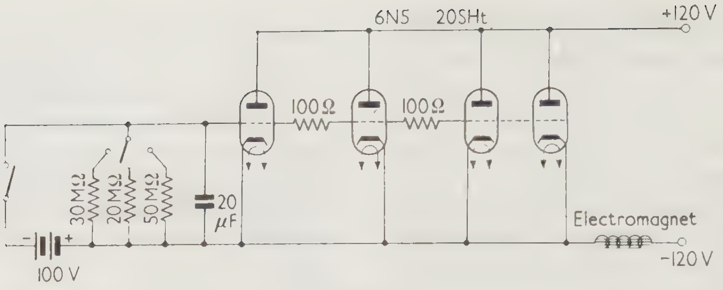

Figure 8

To obtain a rotation diagram (the dependence of the ultrasonic attenuation on the azimuthal angle between the direction of the magnetic field vector and the crystallographic axis) the magnet was rotated relative to the axes of the apparatus and the apparatus was rotated in the magnetic field. If the disk (6) and the divided ring are properly coaxial, and if also the cryostat is set up so that its axis is perpendicular to the magnetic field, beats can be obtained in the specimen for a rotation of the apparatus by an amount less than 0·2 degree.

The current in the magnet circuit from a 120 V network is varied from 0 to 8 A by the system shown in Figure 8 for a load of 2Ω.

Figure 9 shows as an example part of a recorder chart showing the intensity of sound passing through a single crystal of tin as a function of magnetic field. The wave vector of the sound ($\nu = 220$ Mc/s) was directed along the (101) axis and the vector **H** lay in the perpendicular plane, making an angle of about 36 degrees with the (100) axis. Two curves are shown in the drawing which show the reproducibility of the traces for the same orientation of the **K** and **H** vectors relative to the crystallographic axes; the oscillation curve is taken in 3–4 min. We should remark that using the same apparatus, but without the recorder, the measuring process takes 15–20 times longer.

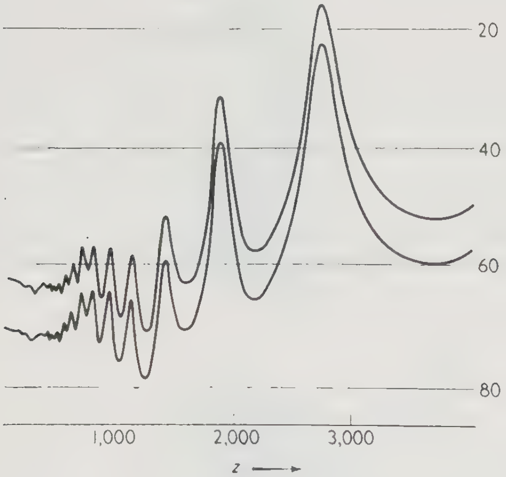

Figure 9

The apparatus described makes it possible to make relative measurements of absorption coefficient, i.e. to measure $\alpha(H)-\alpha(0)$, where $\alpha(H)$ is the value of the coefficient in a field and $\alpha(0)$ is the value without a field. It is easy to see that in such measurements the extent of the weakening of the signal in the cement layer does not affect the result, regardless of whether the first pulse passing through is registered or a pulse undergoing many reflections.

The total estimated error in determining the field and the sound intensity does not exceed a few per cent, and is mainly determined by errors in the measuring circuits and in the additional mechanical registering of the automatic potentiometers.

REFERENCES

1. Galkin, A. A., and Korolyuk, A. P. *J. exp. theor. Phys.* **36,** 1307 (1959), *Soviet Phys. JETP* **9,** 925 (1959)
2. Galkin, A. A., and Korolyuk, A. P. *J. exp. theor. Phys.* **37,** 310 (1959), *Soviet Phys. JETP* **10,** 219 (1960)
3. Morse, R. W., Bohm, H. V., and Gavenda, J. D. *Phys. Rev.* **109,** 1394 (1958)
4. Bömmel, H. E. *Phys. Rev.* **100,** 758 (1955)
5. Pippard, A. B. *Phil. Mag.* **2,** 1147 (1955)
6. Reneker, D. H. *Phys. Rev. Lett.* **1,** 440 (1958)
7. Gurevich, V. L. *J. exp. theor. Phys.* **37,** 71 (1959), *Soviet Phys. JETP* **10,** 51 (1960)
8. Meerovich, L. A., and Zelichenko, D. G. *Pulse Technique* (Published by 'Soviet Radio', 1953)

Letter to the Editors

A Cryogenic Pump for Carbon Dioxide

A CRYOGENIC pump offers a simple and cheap method of obtaining sub-atmospheric pressures. The operation of such a pump depends on the effective removal of gas by solidification on a cooled surface. Lazaryev et al.[1] have constructed pumps with capacities of 13,000 and 4,000 l./sec using a surface cooled with liquid hydrogen. Bailey and Chuan[2] describe a large 'cryopump' which condenses nitrogen on a surface held at about 20° K by a helium gas refrigerator. These pumps were constructed to deal with small mass flows at pressures below 1 mm Hg—Lazaryev et al. achieved 10^{-9} mm Hg. In this pressure range pumping capacity is often governed by gas flow considerations.

This letter describes a laboratory cryogenic pump used in a higher pressure range. It removes carbon dioxide from a small wind tunnel at 1 g/sec and is capable of maintaining pressures between 1 and 10^2 mm Hg in the tunnel, while the pump pressure varies between 10^{-2} and 50 mm Hg. In this region the pump performance is governed only by the transfer of heat across the layer of solidified gas. The condensing surface is maintained at 77° K by liquid nitrogen, while the temperature and, therefore, the vapour pressure of the free surface of the condensed layer rise as its thickness increases. The time t_p for which the pump can be maintained below a given pressure p is therefore limited, and may be shown by simple heat transfer theory to be given by

$$t_p = B_p \frac{A^2}{\dot{M}^2}$$

where A is the condensing area, $\dot{M}$ the gas mass flow rate, and B_p a constant for the given pressure.

Figure 1 shows a section of the cylindrical pump, in which high purity carbon dioxide passes through the control valve, down a central tube, into a cylinder which forms a condensing surface of 800 cm^2 when immersed in liquid nitrogen. Uncondensed impurities are removed by a diffusion pump.

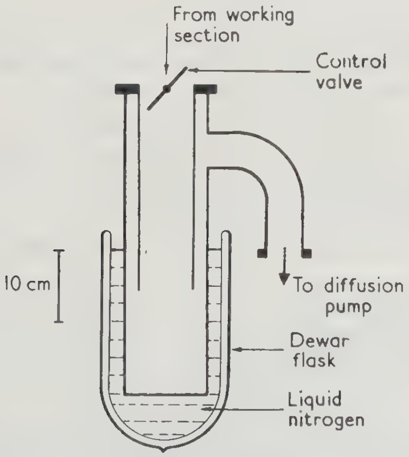

Figure 1. Section of cryogenic pump

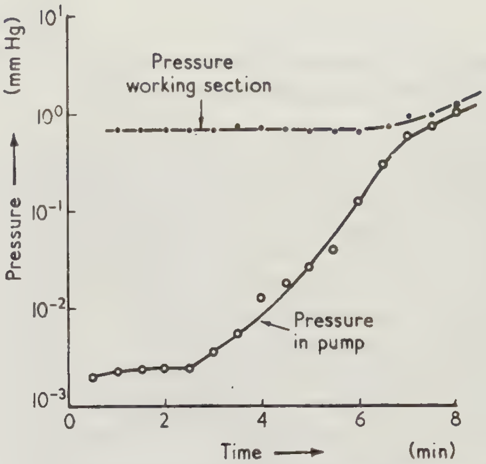

Figure 2. Variation of pressure in the working section and pump

The equation was verified for flow rates between 0·2 and 1·0 g/sec. Experimental values obtained for B_p ranged from $10{\cdot}0 \times 10^{-4}$ g^2 cm^{-4} sec^{-1} at 7·6 mm Hg to $6{\cdot}1 \times 10^{-4}$ at 0·38 mm Hg.

In Figure 2 an example is shown of the pressure history in the working section and in the pump for a gas flow rate of 0·93 g/sec. For about six minutes gas is at sonic velocity at the control valve and the pressure in the working section is independent of that in the pump. The pressure in the pump is constant for the first two minutes. This initial constant pump pressure is believed to be gas dynamic in origin, the pressure being that which is necessary to pass the gas at sonic velocity through an orifice with the same area as the condensing surface. If the gas is assumed to flow supersonically towards the pump wall and to pass through a plane shock before solidification, it can be shown theoretically that the minimum pressure in this pump is $1{\cdot}8 \times 10^{-3}$ mm Hg for a flow rate of 0·93 g/sec. This pressure agrees closely with the observed value.

Considerable experience has been gained in operating the pump over the last six months. A pump capable of handling 50 g/sec. for one hour at 7·6 mm Hg is under construction. It is hoped to report more fully when experience has been gained with the larger size.

Rocket Propulsion Establishment, J. D. C. COY
Ministry of Aviation, B. W. A. RICKETSON
Westcott, Bucks.
(12 May 1961)

REFERENCES

1. LAZARYEV, B. H., BOROVÝK, Y. S., FEDEROVA, M. F., and TSÝN, N. M. *Ukr. Phys. J.* **2**, 175 (1957)
2. BAILEY, B. M., and CHUAN, R. L. *Fifth National Symposium on Vacuum Technology Transactions* (Pergamon Press, London, 1959)

Book Review

Advances in Cryogenic Engineering. Vol. 6 *Edited by K. D. Timmerhaus*. (*Plenum Press*, 1961)

Volume 6 of *Advances in Cryogenic Engineering*—the Proceedings of the 1960 Cryogenic Engineering Conference held at Boulder, Colorado—establishes even more clearly than its predecessors the position of Cryogenics as an independent field of applied science. Sixty-seven papers attractively printed on 649 pages cover an immense range of research and development primarily on the practical application of temperatures which, a few years ago, were the exclusive preserve of laboratories experimenting in pure physics. The impression is gained that we are witnessing the birth of a whole series of new industries the development of which will be based on the efforts of a new type of specialist—the cryogenic engineer. Just as the chemical engineer emerged as a synthesis of the mechanical engineer and the chemist, so the cryogenic engineer is being moulded from the mechanical engineer and the low temperature physicist. Just as the chemical engineer of today is more than just a combination of an engineer and a chemist, so the cryogenic engineer of tomorrow will be more than the sum of his two component parts.

Until very recently all attempts to bring together technologists and low temperature physicists in conferences and research establishments have been singularly abortive. For many years the two species have refused to interbreed. Whereas science was advancing rapidly down the logarithmic temperature scale and discovering a wealth of new and fascinating phenomena, industry had stopped short at the 80° K level which it had reached with the creation of the oxygen industry over half a century ago. The volume under review may help us to understand why, in the U.S.A. at least, this position has suddenly changed.

The Proceedings are grouped, rather lamely, under a variety of headings, of which Space Technology is the first, and this endorses the fact that it was rocketry and its use of cryogenic fluids as propellants and oxidants which gave the initial impulse to cryogenic development. A number of technical problems have to be solved before liquid hydrogen and liquid oxygen can be combined in a successful rocket, problems of large scale liquefaction, storage, insulation, etc., all of which are treated in the volume under review and in its predecessors. It was the importance of these developments in the military sphere which provided the initial capital to launch cryogenic engineering, coupled with considerations of national prestige in space exploration. But once it was established that refrigeration at very low temperatures could be made available on a large scale, the industrial application of the low temperature properties of matter became a practical possibility. Thus a number of papers are devoted to various applications of superconductivity (motors, rectifiers, magnets, etc.), which all require refrigeration to liquid helium temperatures; one contribution describes a completely new cycle for producing refrigeration in this temperature range and another deals with a refrigerator using helium-3 as the working substance for temperatures around 0·5° K.

From the general tenor of the contributions it is easy to forecast for a growing demand for bulk quantities of liquid hydrogen for direct consumption. Liquid helium, on the other hand, will be required primarily as a source of low temperature, localized in many cases to appliances of very restricted volume. There is a need here not only for an easily available supply of bulk cold liquid, but also for an independent low output unit for 'point refrigeration'.

M. RUHEMANN

Bibliography

The following list of papers and letters concerning low temperature physics and engineering has been compiled from a wide range of periodicals and covers the period April–June 1961.

ALIKHANOV, R. A. 'Antiferromagnetism of CoCO$_3$.' *J. exp. theor. Phys.* **39**, 1481 (1960), *Soviet Phys. JETP* **12**, 1029 (1961)

ANDERSON, A. C., SALINGER, G. L., STEYERT, W. A., and WHEATLEY, J. C. 'Specific Heat and Thermal Boundary Resistance of Liquid He^3.' *Phys. Rev. Lett.* **6**, 331 (1961)

ANDERSON, A. C., SALINGER, G. L., and WHEATLEY, J. C. 'Thermal Conductivity of Liquid He^3.' *Phys. Rev. Lett.* **6**, 443 (1961)

ANON. 'Low-Temperature Reaction in Copper–Oxygen Systems.' *Nat. Bur. Stand. tech. News. Bull.* **45**, 61 (1961)

ANON. 'Seventh International Conference of Low Temperature Physics.' *J. sci. industr. Res.* **20A**, 65 (1961)

ANON. 'Thermocouple Calibration.' *Instrum. Pract.* **15**, 428 (1961)

ARP, V. D., KROPSCHOT, R. H., WILSON, J. H., LOVE, W. F., and PHELAN, R. 'Superconductivity of Nb$_3$Sn in Pulsed Fields of 185 Kilogauss.' *Phys. Rev. Lett.* **6**, 452 (1961)

BENDT, P. J., and OLIPHANT, T. A. 'Hydrodynamics of Helium II in Annular Geometry.' *Phys. Rev. Lett.* **6**, 213 (1961)

BETTERTON, J. O., BOOM, R. W., KNEIP, G. D., and WORSHAM, R. E. 'Superconductivity of Nb$_3$Sn in a Pulsed Magnetic Field.' *Phys. Rev. Lett.* **6**, 532 (1961)

BEWILOGUA, L. L., and LANGE, F. K. 'Level Gauge for Liquefied Gases.' *Prib. i Tekh. Eksper.* No. 5, 144 (1960), *Instrum. Exper. Tech.* No. 5, 836 (1961)

BOATO, G., CASANOVA, G., SCOLES, G., and VALLAURI, M. E. 'Vapour Pressure of Isotopic Liquids.' *Nuovo Cim.* **XX**, 87 (1961)

BOKOV, V. A. 'Vacuum Stage for Use in Optical Studies at Low Temperatures.' *Prib. i Tekh. Eksper.* No. 4, 143 (1960), *Instrum. Exper. Tech.* No. 4, 667 (1961)

BOLGER, B., NOOTHOVEN VAN GOOR, J. M., and GORTER, C. J. 'On the Power Transfer between Paramagnetic Spins and the Crystal Lattice III.' *Physica* **27**, 277 (1961)

BOLGER, B., NOOTHOVEN VAN GOOR, J. M., and VAN DAMME, K. J. 'On the Power Transfer between Paramagnetic Spins and Crystal Lattice II.' *Physica* **27**, 18 (1961)

BOLLING, G. F., MASSALSKI, T. B., and MCHARGUE, C. J. 'An X-ray Study of Deformation Stacking Faults at Low Temperatures in Lead, Some Lead Alloys, and Aluminium.' *Phil Mag.* **6**, 212 (1961)

BORDONI, P. G., NUOVO, M., and VERDINI, L. 'Dynamic Behaviour of Polymethyl Methacrylate between 60 and 300° K.' *Nuovo Cim.* **XX**, 667 (1961)

BRACKMANN, R. T., and FITE, W. L. 'Condensation of Atomic and Molecular Hydrogen at Low Temperatures.' *J. chem. Phys.* **34**, 1572 (1961)

BRODY, M., and LINSCHITZ, H. 'Fluorescence of Photosynthetic Organisms at Room and Liquid Nitrogen Temperatures.' *Science* **133**, 705 (1961)

BROOM, R. F. 'An Upper Limit for the Resistivity of a Superconducting Film.' *Nature, Lond.* **190**, 992 (1961)

BROWN, F. C., and INCHAUSPÉ, N. 'Photoelectric Hall Effect in KCl at Low Temperatures.' *Phys. Rev.* **121**, 1303 (1961)

BUISSON, R., CHICAULT, R., DESCAMPS, D., GALLAND, J., and SOUTIF, M. 'Réalisation d'un Maser à Rubis Utilisant un Pompage par Transrelaxation.' *C.R. Acad. Sci., Paris* **252**, 2197 (1961)

CALLAWAY, J. 'Low Temperature Lattice Thermal Conductivity.' *Phys. Rev.* **122**, 787 (1961)

CARERI, G., and GAETA, F. 'Ionic Recombination in Liquid Helium.' *Nuovo Cim.* **XX**, 152 (1961)

CASSUTO, A. 'Variations des Spectres de Masse avec la Temperature entre – 195 and 200° C.' *C.R. Acad. Sci., Paris* **252**, 1311 (1961)

CHARI, M. S. R. 'Inelastic Scattering of Conduction Electrons in Dilute Silver–Manganese Alloys at Low Temperatures.' *Nature, Lond.* **190**, 994 (1961)

COCHRAN, J. F., and MAPOTHER, D. E. 'Superconducting Transition in Zinc and Gallium.' *Phys. Rev.* **121**, 1688 (1961)

CONRAD, H., ARMSTRONG, R., WEIDERSICH, H., and SCHOEK, G. 'Thermally-activated Glide in Magnesium Crystals from 4·2° to 420° K.' *Phil. Mag.* **6**, 177 (1961)

CONRAD, H., HAYS, L., SCHOEK, G., and WIEDERSICH, H. 'On the Rate-controlling Mechanism for Plastic Flow of Mg Crystals at Low Temperatures.' *Acta Metall.* **9**, 367 (1961)

CROFT, A. J., and EXELL, R. H. B. 'The Direct Measurement of the Magnetization Entropy of a Paramagnetic Substance: Thermal and Magnetic Properties of a Ferric Methylammonium Alum at Low Temperatures.' *Proc. roy. Soc.* **A262**, 110 (1961)

DAUNT, J. G., and OLSEN, J. L. 'Compressibility, zero-point energy, and Specific Heat in Superconductors.' *Phys. Rev. Lett.* **6**, 267 (1961)

DEB, K. K. 'Raman Spectra of Para Fluorotoluene and Phenyl Acetonitrile in the Solid State at —180° C.' *Indian J. Phys.* **35**, 16 (1961)

DOUGLASS, D. H., JR. 'Magnetic Field Dependence of the Superconducting Energy Gap.' *Phys. Rev. Lett.* **6**, 346 (1961)

Douglass, D. H., Jr., and Strandberg, M. W. P. 'Antiferromagnetic Resonance in Manganous Chloride.' *Physica* **27,** 1 (1961)

Douthett, D., and Friedberg, S. A. 'Effects of a Magnetic Field on Heat Conduction in Some Ferrimagnetic Crystals.' *Phys. Rev.* **121,** 1662 (1961)

Dreyfus, B., Goodman, B. B., Trolliet, G., and Weil, L. 'Le Chaleur Specifique de Structure Hyperfine du Samarium.' *C.R. Acad. Sci., Paris* **252,** 1743 (1961)

Eatwell, A. J., and Smith, B. L. 'Density and Expansivity of Solid Xenon.' *Phil. Mag.* **6,** 461 (1961)

Eremenko, V. V. 'Investigation of the Photoconductivity-response Spectrum of CdSe Monocrystals at 77 and 20° K.' *Fiz. Tverd. Tela* **2,** 2596 (1960), *Soviet Phys. Solid State* **2,** 2315 (1961)

Eremenko, V. V. 'Investigation of the Photoconductivity-response Spectrum of Mixed $CdS_x{\cdot}CdSe_{1-x}$ Monocrystals at 77 and 20° K.' *Fiz. Tverd. Tela* **2,** 2602 (1960), *Soviet Phys. Solid State* **2,** 2324 (1961)

Feltham, P. 'Creep and Stress Relaxation in Alpha-brass at Low Temperatures.' *Phil. Mag.* **6,** 259 (1961)

Feltham, P. 'The Flow Stress of Metals at Low Temperatures.' *Phil. Mag.* **6,** 209 (1961)

Ferrell, R. A. 'Anomalous Lattice Specific Heat of Superconductors.' *Phys. Rev. Lett.* **6,** 541 (1961)

Flippen, R. B., and Friedberg, S. A. 'Low-Temperature Magnetic Susceptibilities of the Hydrated Acetates of Ni^{++}, Co^{++}, and Mn^{++}.' *Phys. Rev.* **121,** 1591 (1961)

Flotow, H. E., and Osborne, D. W., 'Heat Capacities and Thermodynamic Functions of ZrH_2 and ZrD_2 from 5 to 350° K and the Hydrogen Vibration Frequency in ZrH_2.' *J. chem. Phys.* **34,** 1418 (1961)

Forrester, J. D. 'X-ray Diffraction Data from Single Crystals at 20° K.' *J. sci. Instrum.* **38,** 153 (1961)

Fradkov, A. B. 'An Apparatus for Low-temperature Testing with Transport Liquid Helium.' *Prib. i Tekh. Eksper.* No. 4, 126 (1960), *Instrum. Exper. Tech.* No. 4, 650 (1961)

Galt, J. K., Merritt, F. R., and Schmidt, P. H. 'Cyclotron Resonance Observations in Cadmium.' *Phys. Rev. Lett.* **6,** 458 (1961)

Geballe, T. H., Matthias, B. T., Hull, G. W., and Corenzwit, E. 'Absence of an Isotope Effect in Superconducting Ruthenium.' *Phys. Rev. Lett.* **6,** 275 (1961)

Giaever, I., and Megerle, K. 'Study of Superconductors by Electron Tunneling.' *Phys. Rev.* **122,** 1101 (1961)

Gibbons, D. F. 'Observation of de Haas–van Alphen Type Oscillations in the Acoustomagnetic Attenuation of Zinc.' *Phil. Mag.* **6,** 445 (1961)

Gill, J. C. 'Spin–Lattice Relaxation of Pairs of Chromium Ions in Ruby.' *Nature, Lond.* **190,** 619 (1961)

Glassgold, A. E., and Sessler, A. M. 'Flow Properties of Superfluid Systems of Fermions.' *Nuovo Cim.* **XIX,** 723 (1961)

Goldstein, L. 'Theory of Solid He^4.' *Phys. Rev.* **122,** 726 (1961)

Golovashkin, A. I., Motulevich, G. P., and Shubin, A. A. 'Measurement of the Optical Constants of Metals at Low Temperatures.' *Prib. i Tekh. Eksper.* No. 5, 74 (1960), *Instrum. Exper. Tech.* No. 5, 762 (1961)

Gordon, J. E., and Silsbee, H. B. 'Theory for the Operation of a Magnetic Refrigerator at Temperatures below 1° K.' *Rev. sci. Instrum.* **32,** 572 (1961)

Hellwege, K. H., Küch, F., Niemann, K., and Pfeffer, W. 'Spezifische Wärme von $GdCl_3 . 6H_2O$ in Temperaturbereich zwischen 1,1° K und 260° K.' *Z. Phys.* **162,** 358 (1961)

Henshaw, D. G., and Woods, A. D. B. 'Modes of Atomic Motions in Liquid Helium by Inelastic Scattering of Neutrons.' *Phys. Rev.* **121,** 1266 (1961)

Hirabayashi, M., and Muto, Y. 'Electrical Resistance of Copper–Gold Alloys at Low Temperatures.' *Acta Metall.* **9,** 497 (1961)

Hoselitz, K. 'Some Methods and Results in the Study of Cubic Ferrites.' *Z. angew. Phys.* **13,** 182 (1961)

Hurd, C. M. 'Liquid Nitrogen Cryostat for Electrical Measurements on Crystal Samples in Magnetic and Light Fluxes.' *J. sci. Instrum.* **38,** 161 (1961)

Huzan, E., Abbis, C. P., and Jones, G. O. 'Thermal Expansion of Aluminium at Low Temperatures.' *Phil. Mag.* **6,** 277 (1961)

Jansen, H. G. 'Experimente zur Supraleitung in dem System Niob-Zinn und der Mischkristallreihe Nb_3Sn–Ta_3Sn.' *Z. Phys.* **162,** 275 (1961)

Kaushiva, B. S. 'Cryobiology.' *J. sci. industr. Res.* **20A,** 55 (1961)

Keyes, R. W. 'Low-Temperature Thermal Resistance on *n*-Type Germanium.' *Phys. Rev.* **122,** 1171 (1961)

Klein, R., and Scheer, M. D. 'Hydrogen Atom Reactions with Propene at 77° K. Disproportionation and Recombination.' *J. phys. Chem.* **65,** 324 (1961)

Knaap, H. F. P., Knoester, M., and Beenakker, J. J. M. 'The Volume Change on Mixing for Several Liquid Systems and the Difference between the Ortho and Para Modifications of the Hydrogenic Molecules.' *Physica* **27,** 309 (1961)

Knobler, C. M., van Heijningen, R. J. J., and Beenakker, J. J. M. 'Excess Thermodynamic Properties of the Liquid Systems O_2–A and O_2–N_2.' *Physica* **27,** 296 (1961)

Kume, K., and Hoshino, R. 'Proton Magnetic Resonance of Ice Single Crystal.' *J. phys. Soc. Japan* **16,** 290 (1961)

Kuper, C. G. 'Theory of Negative Ions in Liquid Helium.' *Phys. Rev.* **122,** 1007 (1961)

Lee, D. M., Fairbank, H. A., and Walker, E. J. 'Dielectric Constant, Density, Expansion Coefficient, and Entropy of Liquid He^3 under Pressure below 1° K.' *Phys. Rev.* **121,** 1258 (1961)

Litting, C. N. W. 'The Physics of Computer Elements.' *Brit. J. appl. Phys.* **12,** 207 (1961)

Makin, M. J., Whapman, A. D., and Minter, F. J. 'Dislocation Loops and Hardening in Neutron Irradiated Copper.' *Phil. Mag.* **6,** 465 (1961)

Mamaladze, Y. G. 'On Mutual Friction in Helium II.' *J. exp. theor. Phys.* **39,** 859 (1960), *Soviet Phys. JETP* **12,** 595 (1961)

Miller, D. 'A Level Controller for Liquid Nitrogen.' *J. sci. Instrum.* **38,** 162 (1961)

Mills, R. L., and Schuch, A. F. 'Crystal Structure of the β Form of He^4.' *Phys. Rev. Lett.* **6,** 263 (1961)

Mohling, F. 'Very Low-Temperature Fermi Gas.' *Phys. Rev.* **122,** 1062 (1961)

Mott, N. F. 'The Transition of the Metallic State.' *Phil. Mag.* **6,** 287 (1961)

Mutô, Y. 'Magnetoresistances of Dilute Alloys of Manganese in Copper, Manganese in Zinc and Chromium in Zinc at Liquid Helium Temperatures.' *Sci. Rep. Res. Insts Tôhoku Univ.* **13,** 1 (1961)

Neuringer, L. J., and Bernard, W. 'Generation–Recombination Noise in p-type Gold-doped Semiconductors.' *Phys. Rev. Lett.* **6,** 455 (1961)

Nigam, B. P. 'The Theory of Superconductivity in the Tamm–Dancoff Approximation.' *Progr. theor. Phys., Osaka* **25,** 436 (1961)

Okazaki, A., and Suemune, Y. 'The Crystal Structures of KMnF$_3$, KFeF$_3$, KCoF$_3$,NKiF$_3$ and KCuF$_3$ above and below their Néel Temperatures.' *J. phys. Soc. Japan* **16,** 671 (1961)

Ouboter, R, de B., and Beenakker, J. J. M. 'Some Thermodynamic Considerations on the Properties of Liquid ^{3}He-^{4}He Mixtures.' *Physica* **27,** 219 (1961)

Parks, R. D., and Little, W. A. 'Magnetic Cooling with Paramagnetic Metals.' *Phys. Rev. Lett.* **6,** 539 (1961)

Parsons, R. B., Wardzynski, W., and Yoffe, A. D. 'The Optical Properties of Single Crystals of Cadmium Selenide ' *Proc. roy. Soc.* **A262,** 120 (1961)

Pfeffer, W. 'Spezifische Wärmen von HoCl$_3$.6H$_2$O und ErCl$_3$.6H$_2$O in Temperaturbereich zwischen 1,2° K und 230° K.' *Z. Phys.* **162,** 413 (1961)

Pilkuhn, M. 'Schwankungserscheinungen bei der Ausbildung von Stossionisationslawinen in Ge-Einkristallen zwischen 5° und 10° K.' *Z. Naturf.* **16a,** 182 (1961)

Pistorius, C. A. 'Influence of Plastic Stretching on the Resistivity of Aluminium.' *Physica* **27,** 144 (1961)

Price, P. B. 'On Dislocation Loops Formed in Zinc Crystals during Low Temperature Pyramidal Glide.' *Phil. Mag.* **6,** 449 (1961)

Ptukha, T. P. 'The Determination of the Coefficients of Diffusion and of Heat Conductivity of Weak Solution of He^3 in Helium II.' *J. exp. theor. Phys.* **39,** 896 (1960), *Soviet Phys. JETP* **12,** 621 (1961)

Quéré, Y., and Doulat, J. 'Deformation sous Irradiation de l'Uranium à Basse Température.' *C.R. Acad. Sci., Paris* **252,** 1305 (1961)

Roberts, B. W. 'Ultrasonic Cyclotron Resonance in Gallium.' *Phys. Rev. Lett.* **6,** 453 (1961)

Rollin, B. V. 'Detection of Millimetre and Sub-millimetre Wave Radiation by Free Carrier Absorption in a Semiconductor.' *Proc. phys. Soc. Lond.* **77,** 1102 (1961)

Sawicki, J. 'The Green's Function Method and Superconductivity of Systems of Fermions.' *Ann. Phys. N.Y.* **13,** 237 (1961)

Scholz, W. 'Die technische Durchfürung der Wasserstoffrektifikation.' *Kältetech.* **13,** 185 (1961)

Seraphim, D. P., Novick, D. T., and Budnick, J. I. 'The Effects of Imperfections on the Superconducting Critical Temperature of Tantalum.' *Acta Metall.* **9,** 446 (1961)

Severne, G. 'Magneto-resistance in Superfluid Liquid Helium.' *Physica* **27,** 465 (1961)

Sharbaugh, A. H., and Lippitt, M. W., Jr. 'A Capacitance Densitometer for Determination of the Transient Densities of Cryogenic Liquids.' *J. Amer. Rocket Soc.* **31,** 294 (1961)

Sharvin, Y. V., and Gantmakher, V. F. 'Dependence of the Depth of Penetration of the Magnetic Field in a Superconductor on the Magnetic Field Strength.' *J. exp. theor. Phys.* **39,** 1242 (1960), *Soviet Phys. JETP* **12,** 866 (1961)

Sherril, M. D., and Edwards, H. H. 'Superconducting Tunneling on Bulk Niobium.' *Phys. Rev. Lett.* **6,** 460 (1961)

Siegel, S., Flournay, J. M., and Baum, L. H. 'Irradiation Yields of Radicals in Gamma-Irradiated Ice at 4·2° K and 77° K.' *J. chem. Phys.* **34,** 1782 (1961)

Sim, A. C. 'The Kinetics of Moving Phase Boundaries in Ferromagnetic, Ferroelectric and Superconducting Materials.' *J. Electron. Control* **10,** 97 (1961)

Smith, R. A. 'Amplification through Stimulated Emission —the MASER.' *Brit. J. appl. Phys.* **12,** 197 (1961)

Sparks, M., Loudon, R., and Kittel, C. 'Ferromagnetic Relaxation I. Theory of the Relaxation of the Uniform Precession and the Degenerate Spectrum in Insulators at Low Temperatures.' *Phys. Rev.* **122,** 791 (1961)

Strongin, M., Zimmerman, G. O., and Fairbank, H. A. 'Specific Heat of Liquid He^3 down to 0·054° K.' *Phys. Rev. Lett.* **6,** 404 (1961)

Swihart, J. C. 'Field Solution for a Thin-Film Superconducting Strip Transmission Line.' *J. appl. Phys.* **32,** 461 (1961)

Thouless, D. J., and Tilley, D. R. 'Collective Modes in the Theory of Superconductivity.' *Proc. phys. Soc. Lond.* **77,** 1175 (1961)

van Itterbeek, A., van Dael, W., and Cops, A. 'Velocity of Ultrasonic Waves in Liquid Normal and Para Hydrogen.' *Physica* **27,** 111 (1961)

Van den Meijdenberg, C. J. N., Taconis, K. W., and Ouboter, R. de B. 'The Entropy of Helium-II under Pressure from Measurements on the Fountain Effect.' *Physica* **27,** 197 (1961)

Van den Meijdenberg, C. J. N., Taconis, K. W., and le Pair, C. 'The Influence of He^3 on Film Flow.' *Physica* **27,** 117 (1961)

Vignos, J. H., and Fairbank, H. A. 'New Solid Phase in He^4.' *Phys. Rev. Lett.* **6,** 265 (1961)

Volger, J. 'Solid state Research at Low Temperatures. I. Introduction.' *Philips techn. Rev.* **22,** 190 (1961)

VOLGER, J. 'Solid State Research at Low Temperatures. II. Electron Conduction in Metals and Semiconductors.' *Philips techn. Rev.* **22,** 226 (1961)

VOLGER, J. 'Solid State Research at Low Temperatures. III. Thermal Conduction in Insulators; Paramagnetism; Dielectric Losses Related to Chemical Lattice Imperfections.' *Philips techn. Rev.* **22,** 268 (1961)

VUL, B. M., ZAVARITSKAYA, E. I., and KELDYSH, L. V. 'The Impurity Conductivity of Germanium at Low Temperatures.' *C.R. Acad. Sci. U.R.S.S.* **135,** 1361 (1960), *Soviet Phys. Doklady* **5,** 1303 (1961)

WILD, R. L., and BROWN, F. C. 'Low-Temperature Photoconductivity of Additively Colored KCl.' *Phys. Rev.* **121,** 1296 (1961)

WU, F. Y., and FEENBERG, E. 'Ground State of Liquid Helium (mass 4).' *Phys. Rev.* **122,** 739 (1961)

YAMASHITA, J. 'Low-Temperature Electrical Breakdown in Germanium.' *J. phys. Soc. Japan* **16,** 720 (1961)

ZAVARITSKAYA, E. I. 'Thermal Effects in the Study of the Electrical Conductivity of Germanium in Liquid Helium.' *Fiz. Tverd. Tela* **2,** 3009 (1960), *Soviet Phys. Solid State* **2,** 2673 (1961)

ZAVARITSKII, N. V. 'Measurement of the Anisotropy of Thermal Conductivity of Zinc and Cadmium in the Superconducting State.' *J. exp. theor. Phys.* **39,** 1193 (1960), *Soviet Phys. JETP* **12,** 831 (1961)

ZAVARITSKII, N. V., SVIRIDOV, V. A., and TOLSTOV, K. D. 'Sensitivity and Thermal Conductivity of Nuclear Photoemulsions at Low Temperatures.' *Prib. i Tekh. Eksper.* No. 5, 131 (1960), *Instrum. Exper. Tech.* No. 5, 822 (1961)

ZIMMERMAN, J. E. 'Measurement of Electrical Resistivity of Bulk Metals.' *Rev. sci. Instrum.* **32,** 402 (1961)

ZUCKER, I. J. 'The Reduced Equation of State of the Inert Gas Solids at the Absolute Zero.' *Proc. phys. Soc. Lond.* **77,** 889 (1961)

EDITORIAL NOTE

THE SIMON MEMORIAL PRIZE 1961: PROFESSOR I. M. LIFSHITZ

THE late Sir Francis Simon, F.R.S., was one of the founders of the Low Temperature Group of the Physical Society and its first Chairman. One of his outstanding achievements was to establish closer contact between low temperature scientists in the universities and their colleagues in industry. After his death in 1956 a number of industrial organizations subscribed generously to a fund opened by the Group with the object of establishing a memorial prize of £250 to be awarded every two or three years to a scientist of outstanding merit in the low temperature field.

The Committee of the Low Temperature Group have announced that the prize for 1961 has been awarded to Professor I. M. Lifshitz of the Ukrainian Academy of Sciences, Kharkov. Professor Lifshitz is well known for his many contributions to the understanding of the structure of the Fermi surface in metals and for his work on liquid helium.